COMPRESSION OF NEUROLOGICAL SIGNALS FROM THE POINT OF VIEW OF TELEMEDICINE

A DISSERTATION

Submitted in partial fulfillment of the
requirements for the award of the degree
of
MASTER OF TECHNOLOGY
in
ELECTRICAL ENGINEERING
(With Specialization in Measurement and Instrumentation)

By

A. KRISHNA

DEPARTMENT OF ELECTRICAL ENGINEERING
INDIAN INSTITUTE OF TECHNOLOGY ROORKEE
ROORKEE - 247 667 (INDIA)
JUNE, 2008

I.D. No.-M.T. 455/2008-39/ RSA
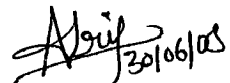
INDIAN INSTITUTE OF TECHNOLOGY ROORKEE

CANDIDATE'S DECLARATION

I hereby declare that the work which is being presented in this dissertation report entitled **"COMPRESSION OF NEUROLOGICAL SIGNALS FROM THE POINT OF VIEW OF TELEMEDICINE"** submitted in partial fulfillment of the requirements for the award of the degree of **Master of Technology** with specialization in **Measurement and Instrumentation,** to the Department of Electrical Engineering, Indian Institute of Technology Roorkee, INDIA, is an authentic record of my own work carried out from August 2007 to June 2008 under the guidance and supervision of **Dr. R.S. Anand,** Associate Professor, Department of Electrical Engineering, Indian Institute of Technology, Roorkee.

To the best of my knowledge the matter embodied in this dissertation report has not been submitted for the award of any other degree or diploma.

Date: 30th June 2008

Place: Roorkee

(A.Krishna)

CERTIFICATE

This is to certify that the above statement made by the candidate is correct to the best of my knowledge.

Date: 30th June 2008

Place: Roorkee

(Dr. R. S. ANAND)

Associate Professor,

Department of Electrical Engineering

IIT Roorkee, Roorkee-247667 India

ACKNOWLEDGEMENTS

ABSTRACT

Neurological signal compression is an area of digital signal processing that can be used to convert neurological signals into an efficient encoded representation which again can be decoded to produce a close approximation. In the field of neurology, common signals of interest are electrical potentials caused by firings of millions of neurons in the human brain during various mental activities. Many applications require acquisition, storage and automatic processing of Electroencephalogram (EEG) during an extended period of time. Our main aim of this work is to compress the recorded EEG. Efficient compression techniques are desired in order to effectively store or transmit the huge amount of EEG data.

In this dissertation work, three compression techniques have been implemented for the purpose of compressing the EEG. These are Discrete Cosine Transform (DCT), Wavelet Transform and Linear Predictive Coding (LPC). Out of these three, Wavelet Transform based EEG compression is a new technique. Wavelets have been successfully used in myoelectric signals compression applications, but less attention has been paid towards its application in the field of the EEG compression. The aim of this dissertation work has been centered on the implementation and comparison of EEG compression techniques. Our comparative evaluation was based on the following parameters.

1. Compression Ratio (CR)
2. Compression Factor (CF)
3. Signal to noise ratio (SNR)
4. Percent Residual Difference (PRD)

In this work, it is found that compression ratio in the case of LPC is not variable where as in the case of DCT and Wavelet transform based EEG compression, compression ratio is variable and quality is also good with respect to LPC. In the case of LPC expected results are not obtained and this coding is working only for few signals. It is also concluded that quality decreases by increasing the compression ratio. Quality and compression ratio is moderate in the case of DCT and Wavelet transform based EEG compression. Out of three techniques Wavelets have shown better results in all aspects of data compression.

LIST OF FIGURES

LIST OF TABLES

LIST OF ABBREVIATIONS

EEG	Electro Encephalo Gram
VLSI	Very Large Scale Integration
ECG	Electro Cardio Gram
REM	Rapid Eye Movement
ERG	Electro Retino Gram
EOG	Electro Oculo Gram
EGG	Electro Gustro Gram
KLT	Karhunenloeve Transform
NLEO	Non Linear Energy Operator
QSS	Quasi Stationary Segments
PCM	Pulse Code Modulation
DPCM	Differential Pulse Code Modulation
ADPCM	Adaptive Differential Pulse Code Modulation
QMF	Quadrature Mirror Filter
FC	Formant Coder
RPELPC	Regular Pulse Excited Linear Predictive Coding
MPLPC	Multi Pulse Excited Linear Predictive Coding
CELP	Code Excited Linear Predictive Coding
SELP	Self Excited Linear Predictive Coding
MBE	Multi Excited Linear Predictive Coding
STFT	Short Time Fourier Transform
WT	Wavelet Transform
DCT	Discrete Cosine Transform
LPC	Linear Predictive Coding
DWT	Discrete Wavelet Transform

CONTENTS

Chapter - 1

INTRODUCTION

1.1 General Description

Medical signal processing is a fast growing field of research that is producing increasingly sophisticated applications in today's high-tech medicine. Many applications in signal processing require the efficient representation and processing of data. The traditional approach to efficient signal representation is compression. Advances in digital signal processing; compression of biomedical signals has received great attentions for use in telemedicine applications. These studies were mainly focused on the applications of predictive coding or wavelet transforms for compression of ECG signals, EMG signals and of an integrated respiratory and swallowing sounds remote assessment tool, in which the sounds with a bandwidth of over 5 kHz have to be transferred online. Hence, compression of such data is of interest for a fast and reliable transmission. These compression techniques are capable of recording and processing long records of biomedical signals.

Neurological signal compression is the technology of converting neurological signals into an efficiently encoded representation that can be later decoded to produce a close approximation of the original signal. The present dissertation is compression of neurological signals for telemedicine point of view means, higher compressions of the signals is the main goal of this dissertation. How it was achieved in this dissertaion is explained in this report.

1.2 Motivation and Statement of Problem

The motivation behind neurological signal compression is the fact that access to unlimited amount of bandwidth is not possible. Compression reduces the amount of data to be transmitted, thereby more efficiently utilizing the available communication bandwidth signals for better diagnosis of diseases and telemedicine purposes and also developing good communication between doctors and patients and hospital staff for better healthcare.

Minimizing the storage space without loosing any clinically significant information characterizes the goal of a biomedical signal compression scheme. The storage problem can be overcome by properly modifying digital speech coding techniques which have been successfully utilized in speech.

1

Neurological compression is the act of transforming the neurological signals to a more compact form, which can then be stored with a considerably smaller memory. The main aim of the neurological compression in this dissertation work is to encode and decode the neurological signals.

As part of this dissertation work DCT, Wavelet, LPC compression techniques were implemented on four varieties of EEG signals. These neurological signals are taken from the forty-five patients from standard website [26] and biomedical instrumentation laboratory of Electrical Engineering department, IIT Roorkee.

1.3 A Brief History of Biomedical Signal Processing

The field of medical instrumentation occurred primarily during the 1950's [11] and the results were often disappointing, for the experimenters soon learned that physiological parameters are not measured in the same way as physical parameters. During the next decade many instrument manufacturers entered the field of medical instrumentation, but development costs were high. Then a large measure of help was provided by the U.S. government, in particular by NASA (National Aeronautics and Space Administration). The Mercury, Gemini, and Apollo programs needed accurate physiological monitoring for the astronauts; consequently, much research and development money went into this area. The aerospace medicine programs were expanded considerably, both within NASA facilities, and through grants to universities and hospital research units. Some of the concepts and features of patient-monitoring systems presently used in hospitals throughout the world evolved from the base of astronaut monitoring. The use of adjunct fields, such as biotelemetry, also finds some basis in the NASA programs.

Coming to neurological signal compression, In 1997 Zlatko sijercis invented the ADPCM (adaptive differential pulse code modulation) subband coding [5] in the EEG compression in his work he proved by using filter banks decomposing the EEG signals into time-frequency approach into different bands and coded each bank with different bit resolutions. Then after many researchers enter into this area and started working. In 2003 perceptron predictors [6] for lossless EEG signal compression using neural networks was done by N.sriram, this is the area of lossless compression. Then after many works has carried out in [1] to [5] in the areas such as lossy and lossless. Now a days there are many working on this area because of interest of neurological signals, how it generates when man is doing

2

different tasks in his daily life, can we be able to control or process it for some other purposes?

1.4 Applications of Biomedical Signals Compression

Digital recording and compression of neurological signals

(i)   Enables the construction of large signal databases for subsequent evaluation and comparison.

(ii)   Makes the transmission of biomedical information feasible over telecommunication networks in real time or off line.

(iii) Increases the capabilities of ambulatory recording systems such as the Holter recorders for ECG signals. In spite of the great advances in VLSI [5] memory technology the amount of data generated by digital systems may become excessive. For example, a Holter recorder needs more than 200 Mbits/day of memory space to store 2-channel ECG signal sampled at a rate of 200 samples/second with 10 bit/sample resolution.

(iv)   Patient monitoring.

(v)   Packet network transmission (internet).

(vi)   Another application where biomedical signal compression is need is in digital storage. For a fixed amount of available memory, compression makes it possible to store longer datasets.

1.5 Organization of the Dissertation

The dissertation has been composed of seven chapters. The organization of this dissertation report is as follows.

Chapter 1: In this chapter, introduction of the dissertation, statement of problem, history and applications of neurological signal compression have been explained.

Chapter 2: In this chapter, physiological systems of the body such cardio vascular system respiratory system are explained. Then after origin of neurological signals, nervous system was explained. Then the main neurological signals are explained such EEG and EMG. At last other neurological signals EOG, EGG are briefly explained.

Chapter 3: In this chapter, variety of signal compression techniques including lossless and lossy techniques is explained. Efficient coding techniques such that speech coders which are suitable for neurological signal compression has been explained. It has also been

explained briefly about the different coding methods based on neural networks based signal compression techniques such as perceptron predictors, TNLEO (teagers non linear energy operator), k-means clustering algorithm, compressed sensing frame works has also explained in this chapter.

Chapter 4: In this chapter, implemented compression techniques in this dissertation work are given. DCT, Wavelet (basics wavelets, wavelet transform, about continuous wavelet transform, discrete wavelet transform and different steps involved in the implementation of wavelet transform based EEG compression are explained one by one) and LPC coding methods are elaborately described. Quantization and Huffman coding has also been explained in this chapter.

Chapter 5: In this chapter, signal acquisition and instruments used in the laboratory are explained and the databases from different physiological signal banks are explained and variety of diseases conditions also explained.

Chapter 6: In this chapter, what ever the algorithms that are proposed in the present work, DCT, WT technique and LPC coding simulation results are tabulated. For the analysis purpose different neurological signals are taken form different persons. Comparative evaluation has been done on the basis of C.R, C.F, SNR and PRD.

Chapter 7: In this chapter, conclusion of present work and some suggestions for future work have been given.

Chapter - 2

NEUROLOGICAL SIGNALS AND CLASSIFICATION

2.1 Overview

There is one vital advantage that biomedical engineering has over many of the other fields that preceded it. The fact that aimed keeping people healthy and helping to cure them when they are ill. The prefix *bio-*, of course, denotes something connected with life. One school of thought subdivides bioengineering into different engineering areas—for example, bio-mechanics and bioelectronics. These categories usually indicate the use of that area of engineering applied to living rather than to physical components. *Bioinstrumentation* [11] implies measurement of biological variables, and this field of measurement is often referred to as *biometrics,* accurate instrumentation to measure vital physiological parameters, and the development of interdisciplinary tools to help fight the effects of body malfunctions and diseases are all a part of this new field.

Neurological signals are the major part of human system, these signals are vital role in man functionality in every aspect, and without brain man doesn't exist similarly without neurons brain doesn't exist. The ongoing chapter explains complete knowledge about human system and functionality of neurological signals.

2.2 Physiological Systems of the Body

To obtain valid measurements from a living human being, it is necessary to have some understanding of the subject on which the measurements are being made. Within the human body can be found electrical, mechanical, thermal, hydraulic, pneumatic and chemical and various other types of systems, each of which communicates with an external environment and internally with the other systems of the body. By means of a multilevel control system and communications network, these individual systems are organized to perform many complex functions. Through the integrated operation of all these systems, and their various subsystems, man is able to sustain life, learn to perform useful tasks, acquire personality and behavioral traits, and even reproduce himself.

5

The human being as a whole (the highest level of organization) communicates with his environment in many ways. These methods of communicating could be regarded as the inputs and outputs of the black box and are illustrated in figure 2.1.
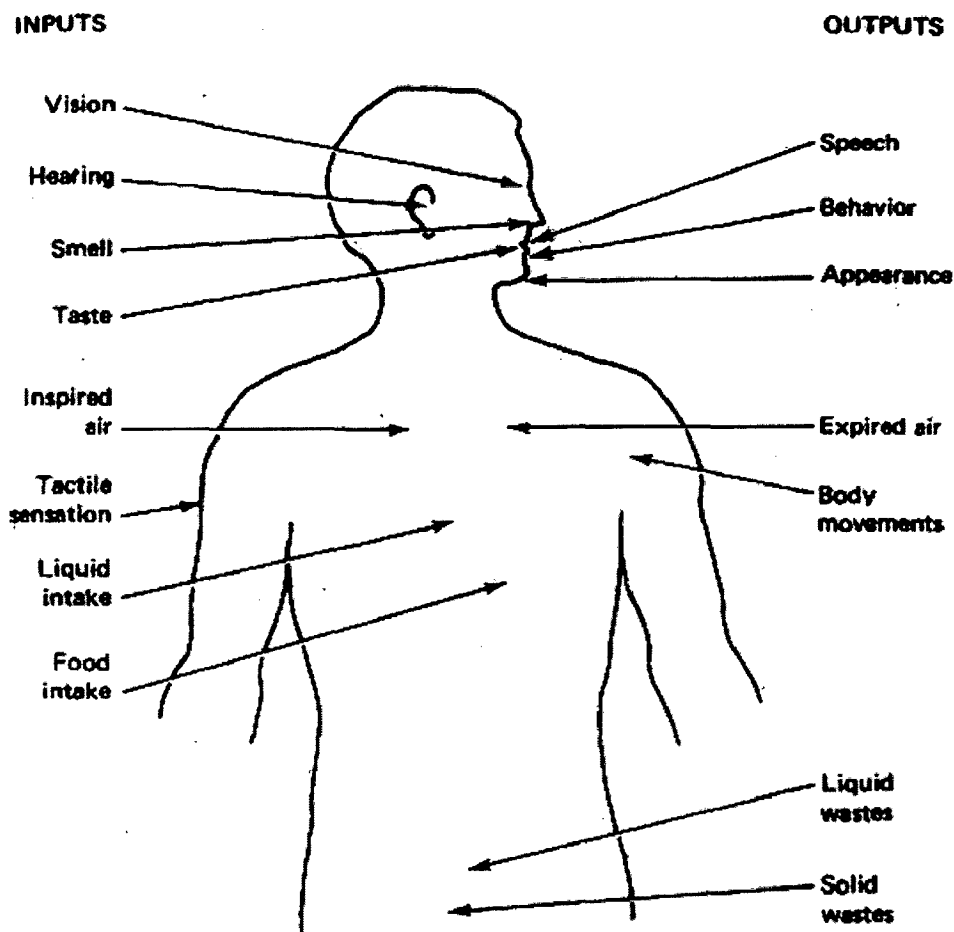
INPUTS   OUTPUTS

Figure 2.1 Communication of man with his environment [11]

In addition, these various inputs and outputs can be measured and analyzed in a variety of ways. Most are readily accessible for measurement, but some, such as speech, behavior and appearance, are difficult to analyze and interpret. Next to the whole being in the hierarchy of organization are the major *functional systems* [11] of the body, including the nervous system, the cardiovascular system, the pulmonary system, and so on.

Just as the whole person communicates with his environment, these major systems communicate with each other as well as with the external environment. These *functional systems* can be broken down into subsystems and organs, which can be further subdivided into smaller and smaller units. The process can continue down to the cellular level and perhaps even to the molecular level.

A brief engineering-oriented description of the major physiological systems is given as [11]:

1. Biochemical System

2. The Cardiovascular System

3. The Respiratory System

4. The Nervous System

2.3 Nervous System

The nervous system is the communication network for the body. Its center is a self-adapting central information processor or computer (the brain) with memory computational power, decision-making capability and a myriad of input-output channels. This computer is self adapting in that if a certain section is damaged; other sections can adapt and eventually take over (at least in part) the function of the damaged section. By use of this computer [11], a person is able to make decisions, solve complex problems, create art, poetry, music, feel emotions and integrate input information from all parts of the body and coordinate output signals to produce meaningful behavior.

Almost as fascinating as the central computer are the millions of communication lines (afferent and efferent nerves) that bring sensory information into and transmit control information out of the brain. In general, these lines are not single long lines but often complicated networks with many interconnections that are continually changing to meet the needs of the system. By means of the interconnection patterns, signals from a large number of sensory devices, which detect light, sound, pressure, heat, cold, and certain chemicals, are channeled to the appropriate parts of the computer, where they can be acted upon. Similarly, output control signals are channeled to specific motor devices (motor units of the muscles), which respond to the signals with some type of motion or force.

Feedback regarding every action controlled by the system is provided to the computer through appropriate sensors. Information is usually coded in the system by means of electrochemical pulses (nerve action potentials) that travel along the signal lines (nerves). The pulses can be transferred from one element of a network to another in one direction only, and frequently the transfer takes place only when there is the proper combination of elements acting on the next element in the chain. Action by some elements tends to inhibit transfer by

7

making the next element less sensitive to other elements that are attempting to actuate it. Both serial and parallel coding are used, sometimes together in the same system. In addition to the central computer, a large number of simple decision-making devices (spinal reflexes) are present to control directly certain motor devices from certain sensory inputs. A number of feedback loops are accomplished by this method. In many cases, only situations where important decision making is involved require that the central computer be utilized.

2.4 Neurological Signals

2.4.1 Sources of bioelectric potentials

In carrying out their various functions, certain systems of the body generate their own monitoring signals, which convey useful information about the functions they represent. These signals are the bioelectric potentials associated with nerve conduction, brain activity, heartbeat, muscle activity, and so on. Bioelectric potentials are actually ionic voltages produced as a result of the electrochemical activity of certain special types of cells. Although measurement of individual action potentials can be made in cells, such measurements are difficult because they require precise placement of an electrode inside a cell. To measure bioelectric potentials, a transducer [11] capable of converting ionic potentials and currents into electric potentials and currents is required. Such a transducer consists of two *electrodes,* which measure the ionic potential difference between their respective points of application. The more common form of measured biopotentials is the combined effect of a large number of action potentials as they appear at the surface of the body, or at one or more electrodes inserted into a muscle, nerve, or some part of the brain potentials, instead of the potentials themselves. Part of the difficulty arises from the numerous assumptions that must be made concerning the ionic current and electric field patterns throughout the body. The validity of some of these assumptions is considered somewhat questionable. Regardless of the method by which these patterns of potentials reach the surface of the body or implanted measuring electrodes, they can be measured as specific bioelectric signal patterns that have been studied extensively and can be defined quite well. Through, the use of transducers capable of converting ionic potentials into electrical voltages, these natural monitoring signals can be measured and results displayed in a meaningful way to aid the physician in his diagnosis and treatment of various diseases such as epileptic seizures, paralysis.

2.4.2 Electroencephalogram (EEG)

Now we will discuss about significant bioelectric potentials related to neurological signals. The designation of the waveform itself generally ends in the suffix gram, whereas the name of the instrument used to measure the potentials and graphically reproduce the waveform ends in the suffix graph. For example, the electrocardiogram (the name of the waveform resulting from the heart's electrical activity) (ECG) is measured on an electrocardiograph (the instrument).

The recorded representation of bioelectric potentials generated by the neuronal activity of the brain is called the *electroencephalogram* [11], abbreviated as EEG. The EEG has a very complex pattern, which is much more difficult to recognize than the ECG. A typical sample of the EEG is shown in figure 2.2.
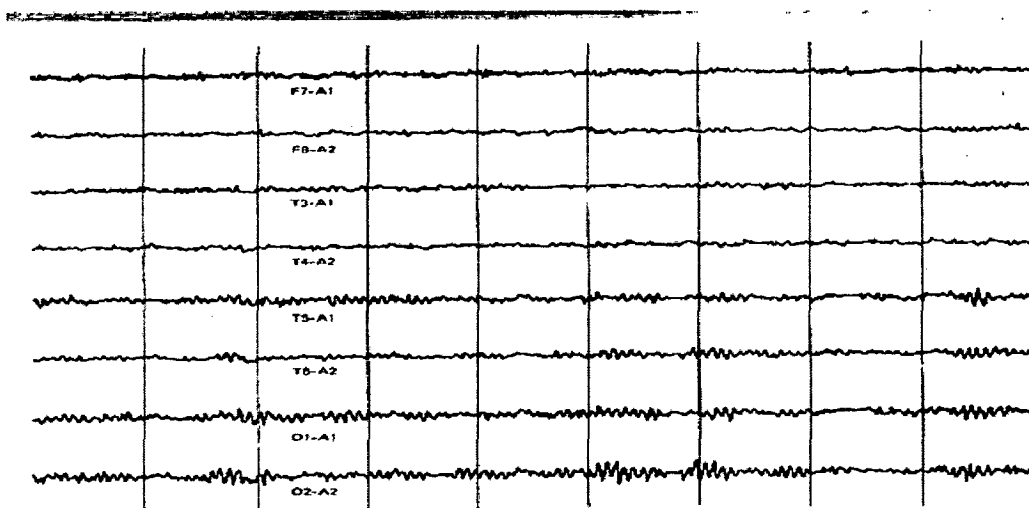
Figure 2.2 Typical human electroencephalograms. The eight tracings indicate regions of the scalp from which each channel of EEG was measured with respect to one of two reference ear electrodes (A1 and A2) [11].

As it can be seen, the waveform varies greatly with the location of the measuring electrodes on the surface of the scalp. EEG potentials, measured at the surface of the scalp, actually represent the combined effect of potentials from a fairly wide region of the cerebral cortex and from various points beneath. Experiments have shown that the frequency of the EEG seems to be affected by the mental activity of a person.

The wide variation among individuals and the lack of repeatability in a given person from one occasion to another make the establishment of specific relationships difficult. There are, however, certain characteristic EEG waveforms that can be related to epileptic seizures

9

and sleep. The waveforms associated with the different stages of sleep are shown in the following figure 2.3.
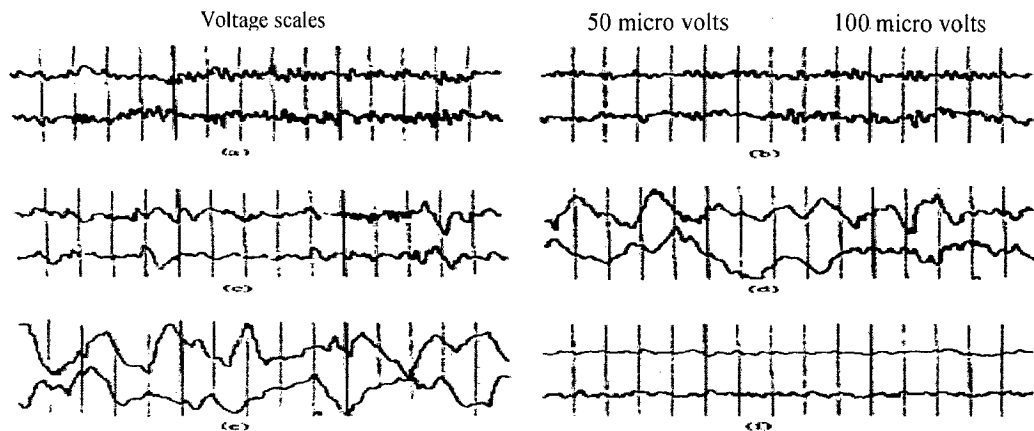
Figure 2.3Typical human EEG patterns for different stages of sleep. In each case the upper record is from the left frontal regions of the brain and the lower tracing is from the right occipital region. (a) Awake and alert-mixed frequencies; (b) Stage1- subject is drowsy and producing large amount of alpha waves: (c) Stage 2-light sleep; (e) stage 4 deeper slow eave sleep; (f) paradoxical or rapid eye movement (REM) sleep [11].

a) Characteristics of EEG

An alert, wide-awake person usually displays an unsynchronized high-frequency EEG, A drowsy person, particularly one whose eyes are closed, often produces a large amount of rhythmic activity in the range 8 to 13 Hz. As the person begins to fall asleep, the amplitude and frequency of the waveform decrease; and in light sleep, a large-amplitude, low-frequency waveform emerges; deeper sleep generally results in even slower and higher-amplitude waves. At certain times, however, a person, still sound asleep, breaks into an unsynchronized high-frequency EEG pattern for a time and then returns to the low-frequency sleep pattern.

The period of high-frequency EEG that occurs during sleep is called *paradoxical sleep*, because the EEG is more like that of an awake, alert person than of one who is asleep. Another name is *rapid eye movement* (REM) [11] sleep, because associated with the high-frequency EEG is a large amount of rapid eye movement beneath the closed eyelids. This phenomenon is often associated with dreaming, although it has not been shown conclusively that dreaming is related to REM sleep.

The various frequency ranges of the EEG have arbitrarily been given Greek letter designations because frequency seems to be the most prominent feature of an EEG pattern. Electroencephalographers do not agree on the exact ranges, but most classify the EEG frequency bands or rhythms approximately as follows:

Below 3 & 1/2 Hz   delta

From 3 & 1/2 Hz to about 8 Hz   theta

From about 8 Hz to about 13 Hz alpha

From about 13 Hz to about 22 Hz beta

Above 22 Hz   gamma
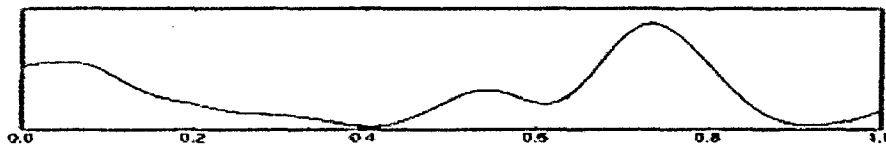
Figure 2.4 Typical delta waveform of EEG
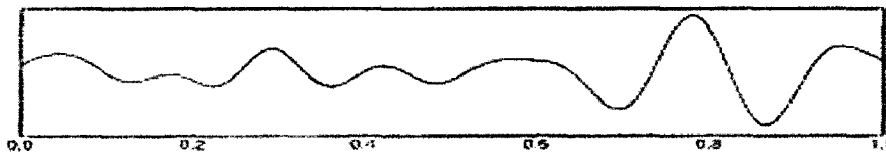
Figure 2.5 Typical theta waveform of EEG
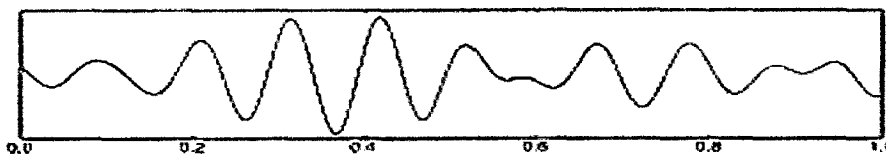
Figure 2.6 Typical alpha waveform of EEG
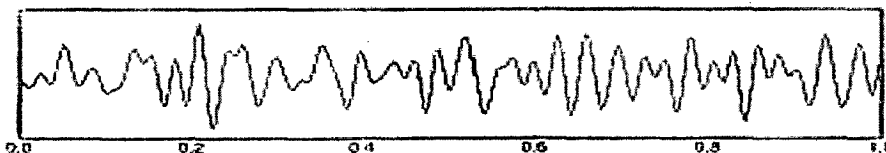
Figure 2.7 Typical beta waveform of EEG

Portions of some of these ranges have been given special designations, as they have certain sub bands that fall on or near the stated boundaries. Most humans seem to develop EEG patterns in the alpha range when they are relaxed with their eyes closed. This condition seems to represent a form of synchronization, almost like a "natural" or "idling" frequency of the brain. As soon as the person becomes alert or begins "thinking" the alpha rhythm disappears and is replaced with a "desynchronized" pattern, generally in the beta range. Much research is presently devoted to attempts to learn the physiological sources in the brain responsible for these phenomena, but so far nothing conclusive has resulted in this area.

11

Experiments in biofeedback have shown that under certain conditions, people can learn to control their EEG patterns to some extent when information concerning their EEG is fed back to them either visibly or audibly. As indicated, the frequency content of the EEG pattern seems to be extremely important. In addition, phase relationships between similar EEG patterns from different parts of the brain are also of great interest. Information of this type may lead to discoveries of EEG sources and will, hopefully, provide additional knowledge regarding the functioning of the brain.

Another form of EEG measurement is the *evoked response* [11]. This is a measure of the 'disturbance' in the EEG pattern that results from external stimuli, such as a flash of light or a click of sound. Since these 'disturbance' responses are quite repeatable from one flash or click to the next, the evoked response can be distinguished from the remainder of EEG activity.

2.4.3 Electromyogram (EMG)

The bioelectric potentials associated with muscle activity constitute the *electromyogram*, abbreviated EMG. These potentials may be measured at the surface of the body near a muscle of interest or directly from the muscle by penetrating the skin with needle electrodes. Since most EMG measurements are intended to obtain an indication of the amount of activity of a given muscle, or group of muscles, rather than of an individual muscle fiber, the pattern is usually a summation of the individual action potentials from the fibers constituting the muscle or muscles being measured.

As with the EEG, EMG electrodes pick up potentials from all muscles within the range of the electrodes. This means that potentials from nearby large muscles may interfere with attempts to measure the EMG from smaller muscles, even though the electrodes are placed directly over the small muscles. Where this is a problem, needle electrodes inserted directly into the muscle are required. As stated earlier, the action potential of a given muscle (or nerve fiber) has a fixed magnitude, regardless of the intensity of the stimulus that generates the response. Thus, in a muscle, the intensity with which the muscle acts does not increase the net height of the action potential pulse but does increase the rate with which each muscle fiber fires and the number of fibers that are activated at any given time. The amplitude of the measured EMG waveform is the instantaneous sum of all the action potentials generated at any given time. Because these action potentials occur in both positive and negative polarities at a given pair of electrodes, they sometimes add and sometimes

cancel. Thus, the EMG waveform appears very much like a random-noise waveform, with the energy of the signal a function of the amount of muscle activity and electrode placement. Typical EMG waveforms are shown in figure 2.8.
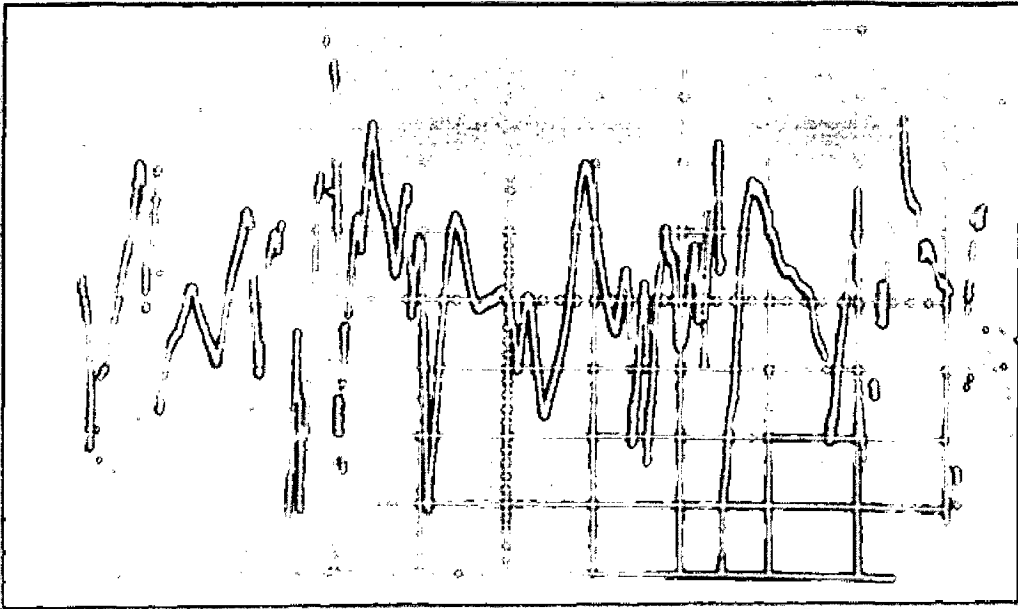
Figure 2.8 Typical electromyogram (EMG) waveform of normal "interference pattern" with full strength muscle contraction producing obliteration of the baseline. Sweep speed is 10 milliseconds per cm; amplitude is 1 millivolt per cm. (Courtesy of the Veterans Administration Hospital, Portland) [11].

2.4.4 Other neurological signals

In addition to the three most significant bioelectric potentials (ECG, EEG, and EMG), several other electric signals can be obtained from the body, although most of them are special variations of EEG, EMG, or nerve-firing patterns. Some of the more prominent ones as the following:

1. Electroretinogram (ERG): A record of the complex pattern of bioelectric potentials obtained from the retina of the eye. This is usually a response to a visual stimulus.

2. Electrooculogram (EOG): A measure of the variations in the corneal-retinal potential as affected by the position and movement of the eye.

3. Electrogustrogram (EGG): The EMG patterns associated with the peristaltic movements of the gastrointestinal tract.

13

Chapter - 3

SIGNAL COMPRESSION TECHNIQUES

3.1 Introduction

There are no separate special techniques existing for biomedical signal compression. The techniques adapted for biomedical signal compression are well defined speech compression techniques or neural network based compression techniques. Recently some of sensor based compression algorithms are also emerging in this field. This chapter will be going to explain some of fundamentals how the signals were compressed in these techniques based on time domain or frequency domain. Some of EEG compression algorithms are also explaining related to neural networks.

3.1.2 Types of compression techniques

Compression techniques are mainly classified into Lossless and lossy. Lossless compression techniques works on arithmetic or entropy coders which mainly focuses, coding the given signal in some encrypted format, but lossy techniques focuses the processing of the given signals, means by using the bit assigning per samples or redundancy removal of the signal and so on. These are elaborated as follows:

3.2 Lossless Compression Techniques

3.2.1 Recurrent neural network predictors

Classical compression techniques which are available are mostly suitable for compressing images and speech signals where a slight loss of information may not pose a significant problem. In the case of EEG, however a small discrepancy between the original and recovered signals can be problematic. In the spectral analysis, for example, the low-amplitude high frequency components of the signal can be easily altered by using losssy compression leading to erroneous results. Lossy compression techniques are therefore unsuitable for EEG data. It is known that neural networks can be used as predictors [3] in a two-stage lossless compression scheme. A predictor is used in the first stage to decorrelate the source data, thus reducing the amplitude range of the data to almost white Gaussian. In the second stage, an

entropy encoder such as Huffman or arithmetic encoder is employed to decorrelate the residue stream produced by the predictor.

3.2.2 Compressed sensing frameworks

In recent years, there has been a new approach to compression at the sensing level. *Compressed Sensing* (CS) [1] can be used for signal sensing and compression. Compressed sensing (CS) is an emerging field which is based on the revelation that a small collection of linear projections of a sparse signal contains enough information for reconstruction. An application of compressed sensing in the field of biomedical signal processing is particularly electroencephalogram (EEG) collection and storage and efficient representation of multichannel, multiple trial EEG data. The proposed framework is based on the revelation that EEG signals are sparse in a Gabor frame. The sparsity of EEG signals in a Gabor frame is utilized for compressed sensing of these signals. A simultaneous orthogonal matching pursuit algorithm is shown to be effective in the joint recovery of the original multiple trail EEG signals from a small number of projections. CS builds on the revelation that a signal having a sparse representation in one basis can be recovered from a small number of projections onto a second basis that is incoherent with the first. This revelation has a promising implication for applications for signal acquisition and compression. With no a priori knowledge of a signal's structure, a sensor node could simultaneously acquire and compress the signal, preserving the critical information. Some recent applications of this theory include the single pixel camera and compressed sensing for rapid MR (Magnetic resoning) imaging. This algorithm is as follows; they first show that EEG signals are sparse in a Gabor frame based on an empirical study using a large set of EEG data. Next, they apply the CS framework to compress single-trial EEG recordings using a few numbers of projections onto Gaussian basis. The reconstruction of the actual EEG signal from these projections is achieved using orthogonal matching pursuit algorithm. After the sparsity of individual EEG signals is established, they extend the CS framework to joint recovery of multiple signals using recent results in distributed compressed sensing. The joint sparsity of multiple EEG signals is shown and a simultaneous orthogonal matching pursuit algorithm is used to reconstruct multiple recordings simultaneously.

3.2.3 Karhunenloeve transform (KLT)

EEG signals are simply measured from different electrode positions on human scalp as shown in fig3.1. In order to compress EEG signals, several types of redundancies must be

taken into account. The temporal redundancy is successfully removed in many works. Antoiol et al [2] presented the survey on EEG lossless compression algorithms using predictive coding, transform coding vector quantization together with the entropy coding and compared with some well known lossless compression algorithms. Coming to next redundancy the neighboring channels of EEG signals usually have a high degree of similarity in their structures. In order to efficiently compress the multi-channel data, this inter-channel redundancy must be exploited. Although, these multi-channel signals are visually correlated, the correlation models of the signals are unpredictable. Hence data independent transforms such as DCT, or DFT usually fail to efficiently decorrelate them. This problem can be solved by employing an optimal transform that can decorrelate the signals by finding the eigenvectors of their correlation matrix. This optimal transform is known as karhuen Loeve transform (KLT). An efficient algorithm employing KLT to decorrelate the inter-channel redundancy of multi-channel signals has been applied to audio coding. In practice, the KLT is simply truncated yielding a non-reversible process.
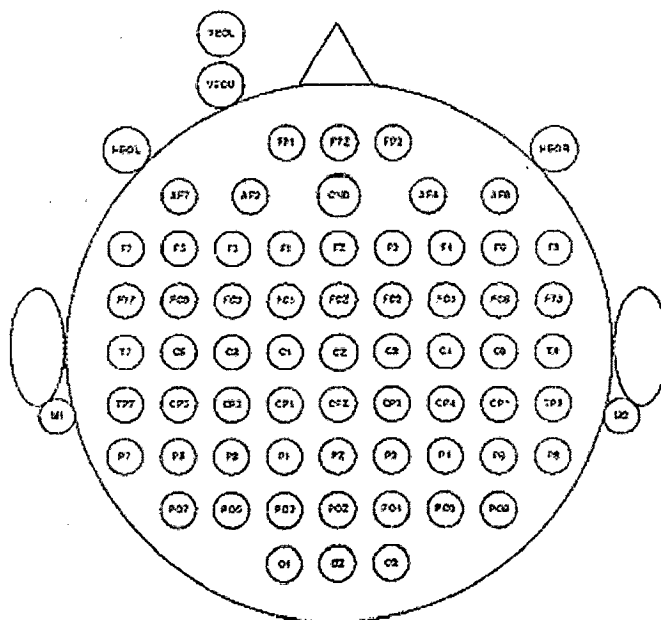
Fig 3.1 N-channel EEG [2]

In this algorithm, a lossless compression algorithm for multi-channel EEG signals exploiting an integer-to-integer mapping approximation of KLT is presented. Using the factorization, KLT is further parameterized by a ladder factorization, rendering a reversible structure under quantization of coefficients called IntKLT. It should be noted that the choice of selecting the permutation matrices for the factorization is important to the lossless coding application. Since the factorization of the KLT is not unique, each solution results in a different permutation and dynamic range of coefficient. Thus finding the best solution in the

sense of minimum dynamic range of coefficients is very difficult. An obvious approach is to compare all the possible factorization which minimizes the ladder coefficients. This however is impractical for a large scale $N \times N$ matrix since the number of solution is of order $O\ (N!)$ (N factorial). In order to minimize the ladder coefficients while maintaining the acceptable complexity, pivoting is also suggested.

3.2.4 K-means clustering algorithm

The automatic EEG analysis method presented in this algorithm involves 4 basic steps: 1) Segmentation – where the non- stationary multi-channel EEG data is broken into quasi-stationary segments. The methodology as proposed uses adaptive segmentation of non-stationary EEG into quasi-stationary segments (QSS) using the *Teagers' non linear energy operator* (NLEO) [4]. 2) Feature Extraction – segments are characterized with different features. The features to characterize the different QSS are extracted from the EEG. The QSS with similar features are grouped into eight clusters, using an iterative method based on the k-means clustering algorithm [6]. To improve the performance, the artifact contaminated QSS were removed prior to clustering. The artifact or outlier removal method is a multilayered one that is applied at several stages of segmentation. 3) Self-organization –segments with similar features are grouped together. 4) Presentation – the compressed data is presented to assist the review of long-term EEG.

In the literature many different features have been proposed to characterize the EEG. Some examples are amplitude, first and second order derivatives and amplitudes in different spectral bands. In some other work amplitude, dominant rhythm, and frequency-weighted energy (referred to as generic features) have been used. The absolute average amplitude of a channel in quasi-stationary segments (QSS) was used to describe the amplitude of the signal. The dominant rhythm was estimated using a second order auto regressive model. The frequency-weighted energy was based on the idea of non linear energy operator (NLEO). It was suggested that the resulting energy provides a combined frequency and amplitude measure of the EEG. The expectation is that if we could use more direct measures of the spectral content, such as power in the different spectral bands, then the performance of the system may improve. This is further exemplified by the work of Johnson *et al* [5]. They used spectral analysis to characterize the visually selected epochs from different sleep stages. Larson *et al* [7] evaluated these features with multiple regression and multiple discriminant analysis and concluded that spectral analysis can be used effectively to classify sleep EEG.

To calculate the proposed spectral features the EEG spectrum is divided into different spectral bands. Each epoch is described by the power in these bands. The classical band definitions in EEG are used - delta (0-4 Hz), theta (4-8 Hz), alpha (8-12 Hz), sigma (12-15 Hz), beta1 (15-24 Hz), beta2 (24-36 Hz). The power spectral density (PSD) for each QSS is calculated using the Fast Fourier transform (FFT) with mean removed. For each QSS, the power in each band is normalized by the total segment power. Each QSS has one frontal and one occipital channel with each channel described by six spectral features. Thus, twelve features are needed to describe each QSS. The generic features and the spectral features are evaluated in terms of their ability to classify and create homogenous clusters of the different pattern that may exist in the EEG. In this algorithm, they use the sleep EEG data, since the recurring sleep stages are example of the repetitive patterns occurring in the background EEG. The manually-scored Hypnogram gives information about the different homogeneous patterns (sleep stages) and their temporal profile. Most sleep laboratories divide the EEG into epochs of 20 or 30 seconds for stage scoring. They translate the clustering information based on QSS into clusters of 20 second epochs. This provides a Hypnogram-like temporal distribution of clusters of epochs. It is done by assigning to each epoch the number of the QSS clusters that occupies majority of the epoch. Each newly formed cluster of epochs represents a particular pattern occurring in the data set. The compressed data, thus obtained, can be assessed against the manually-scored Hypnogram.

3.3 Lossy Compression Techniques

Lossy compression techniques discussed hear are mostly speech compression techniques. Speech compression techniques described here are as it is related to speech only. How we will use these techniques for our work, we will discuss in next chapter.

The objective of speech is communication whether face to face or cell phone to cell phone. To fit a transmission channel or storage space, speech signals are converted to formats using various techniques. This is called speech coding or compression. Theoretically speaking, speech coding can be achieved based on two facts. One is redundancy in speech signals, and another one is perception properties of human ears. In this we will discuss about classification of speech compression techniques.

Properties of speech coding techniques are discussed briefly one by one. Speech quality of compressed speech signal depends on compression ratio, complexity, delay, and bandwidth. These are nothing but the attributes of speech coders. So, there is an interaction

between all these attributes and that they can be traded off against each other. For example, in the case of low bit rate coders delay is more with respect to high bit rate coders and also complexity is more in the case of low bit rate coders and also quality is low in the case of low bit rate coders.

Speech coding methods are classified into three categories.

3.3.1 Waveform coding

The most basic waveform coders do not attempt to exploit any knowledge of the signal production process in the encoding of the input signal. Their aim, as the name implies, is to reproduce the original waveform as accurately as possible. As these coders are not speech specific they can cater for many non-speech signals, background noise and multiple speakers without difficulty. The penalty of a relatively high bit-rate, however, must be paid for this 'acoustic robustness'.

In general, waveform coding techniques are designed to be signal independent. That means waveform coding techniques treats any signals as normal signal waveform. They are designed to map the waveform of the encoder into a facsimile-like replica of it at the output of the decoder. Because of this advantage, the waveform coding methods can also be used to encode secondary type of information such as signaling tones, voice band data, or even music. Because of the signal reproduction as accurately as possible the compression ratio is not good with respect to other coding methods. The coding efficiency can be improved by exploiting some statistical signal properties, if the codec parameters are optimized for the most likely categories of input signals, while still maintaining good quality for other types of signals as well. The waveform codec's can be further subdivided into time-domain waveform codec's and frequency-domain waveform codec's.

a) **Time domain waveform coding:** The most well known representative of signal independent time domain waveform coding [12] is the A-law companded pulse code modulation (PCM) scheme. A-law is a nonlinear type of companding. This results in near constant signal to noise ratio (SNR) over the total input dynamic range. The simplest and best known waveform encoding technique is pulse code modulation (PCM). When PCM employs non-uniform 8-bit quantization (A-law or μ-law) with 8 KHz sampling, very good quality speech is achieved at 64 kbps. The bit-rate required by waveform coders for speech encoding can be reduced by exploiting the correlation between adjacent samples, for example by

encoding the difference between successive samples rather than the samples themselves. One such scheme is known as differential pulse code modulation (DPCM). By adapting the quantizer step-size of a DPCM coder according to the short-term signal power, the signal coding technique known as adaptive differential pulse code modulation (ADPCM).

b) Frequency domain waveform coding: In frequency domain waveform codec's, the input signal undergoes a more or less accurate short time spectral analysis. The signal is split into a number of sub bands, and the individual sub band signals are then encoded by using different numbers of bits in order to obey rate distortion theory on the basis of their prominence. Two well known representations of this class are sub band coding (SBC) and adaptive transform coding (ATC). Wavelet transform based signal compression comes under the waveform coding method and it is similar to subband coding [13].

c) Subband coding: The process of breaking the input signal into subbands via band pass filters and coding each band separately is called sub band coding. To keep the number of samples to be coded at a minimum, the sampling rate for the signals in each band is reduced by decimation. Since the band pass filters are not ideal, there is some overlap between adjacent bands and aliasing occurs during decimation. Ignoring the distortion or noise due to compression, Quadrature Mirror Filter (QMF) banks allow the aliasing that occurs during filtering and sub sampling at the encoder to be cancelled at the decoder. The codec's used in each band can be PCM, ADPCM, or even an analysis-by-synthesis method. The advantage of subband coding is that each band can be coded differently and that the coding error in each band can be controlled in relation to human perceptual characteristics.

d) Transform coding: This method was first applied to still images but later investigated for signals. The basic principle is that a block of speech samples is operated on by a discrete unitary transform and the resulting transform coefficients are quantized and coded for transmission to the receiver. Low bit rates and good performance can be obtained because more bits can be allocated to the perceptually important coefficients, and for well-designed transforms, many coefficients need not be coded at all, but are simply discarded, and acceptable performance is still achieved. Although classical transform coding has not had a major impact on narrowband signal coding and subband coding has fallen out of favor in recent years, filter bank and transform methods play a critical role in high quality audio coding, and at least one important standard for wideband speech coding (G.722.1) is based upon filter bank and transform methods. The distinction between transforms and filter bank

methods is somewhat blurred, and the choice between a filter bank implementation and a transform method may simply be a design choice.

3.3.2 Vocoding

Vocoders are nothing but voice coders. These use the properties of the speech production model. Vocoders make no attempt to reproduce the original waveform as like waveform coding. Vocoders derive a set of parameters at the encoder which can be used to control a signal production model at the decoder. The parameter set for the signal production model is relatively small and can be efficiently quantized for transmission. These give less quality output but compression is more.

3.3.3 Hybrid coding

Waveform coding methods are good with respect to signal quality and vocoding methods are good with respect to compression. By taking advantages in both waveform and vocoding techniques hybrid coding methods are formed. But hybrid coding methods have higher complexity. So every coding method formed by combining waveform coding and source coding methods falls under this category. Hybrid coding improves the signal quality and reduces the compression. Hybrid coding methods are often referred to as analysis by synthesis coding methods. In the following figure 3.2 classifications of signal (speech) compression techniques has been given.
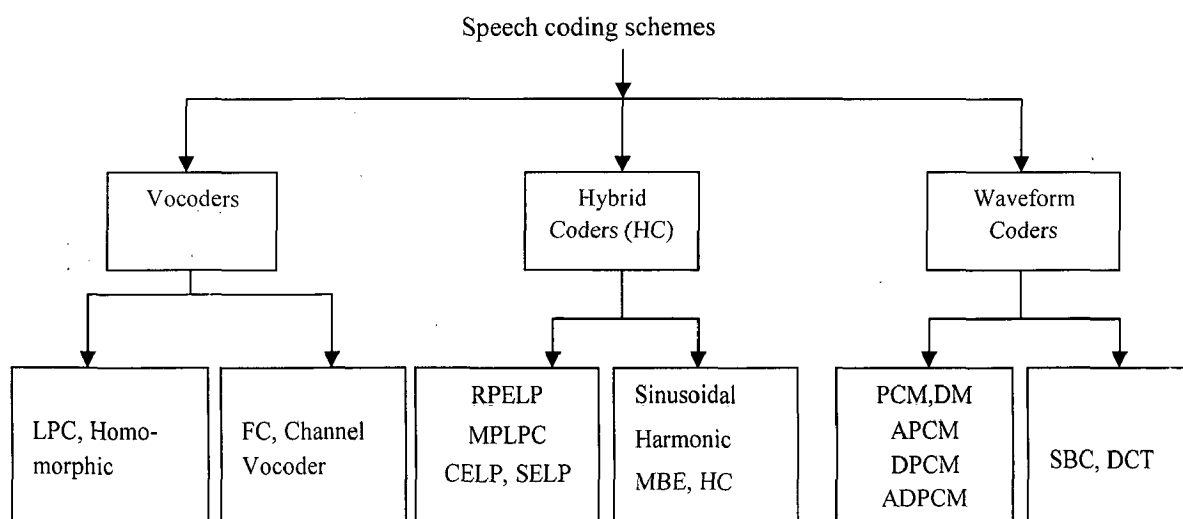
Figure 3.2 Classification of speech coding schemes [12].

21

IMPLEMENTED COMPRESSION TECHNIQUES

4.1 Motivation

The neurological signals selected in this dissertation work are Electroencephalogram (EEG) because of less work done on this area compared to other physiological variables such as ECG and EMG, and the work going in this area is amazing, for example the brain computer interface, controlling the EEG signals for various purposes mouse moment on computer monitor, teeth clinching, motor control and variety of activities. The compression techniques selected are easy to implement and better compression ratios with good signal quality. We will discuss about these techniques in this chapter.

4.2 Discrete Cosine Transform based EEG Compression

Discrete cosine transform (DCT) is signal independent based transform and it has two advantages. First one there is no imaginary part of the signal compared to FFT, so it can help easy quantization, second one is the entire power of the signal contained first few coefficients only, so we can concentrate on these first few coefficients means high resolution to this part can get good quality of synthesized signal. Huffman coding is also applicable to this technique. Its working procedure is taken from the reference [13].

4.2.1 Discrete cosine transform of the EEG signal

The DCT [9] is closely related to the discrete Fourier transform. It can reconstruct a sequence very accurately from only a few DCT coefficients, a useful property for applications requiring data reduction.

$$y(k) = w(k) \sum_{n=0}^{N} x(n) \cos \frac{\pi(2n-1)(k-1)}{2N}, k = 0,\ldots\ldots,N-1 \qquad \ldots\ldots\ldots\ldots 4.1$$

x is the input signal, y is DCT of the input signal

Where; $w(k) = \frac{1}{\sqrt{N}}, k = 0$,

$$\frac{2}{\sqrt{N}}, 1 <= k <= N$$

N is the length of x, and x and y are the same size.

4.2.2 Steps of DCT based EEG compression
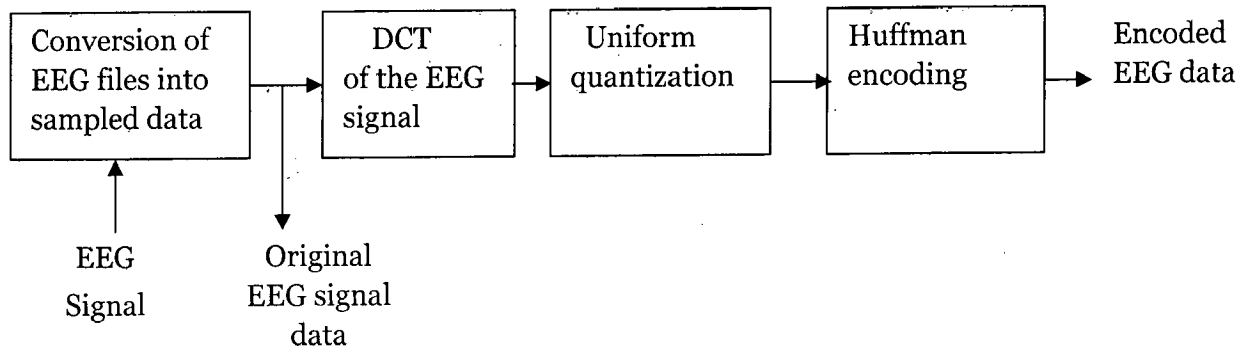
Fig4.1 Steps of DCT based EEG encoding [13]
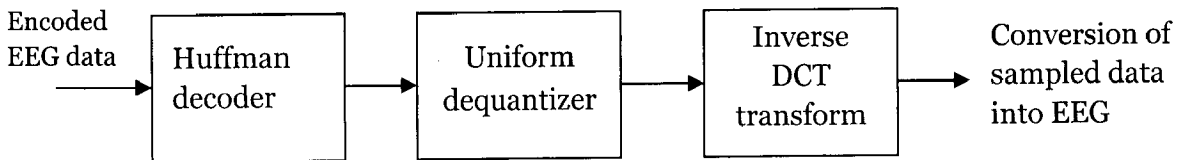
Fig4.2 Steps of DCT based EEG decoding [13]

4.2.3 Uniform quantization

Quantization is a process of mapping a set of continuously valued input data, to a set of discrete valued output data. In other words, the aim of quantization is to decrease the information found in the coefficients in such a way that this process brings perceptually no error [14]. The process of quantization is shown in figure 4.3.
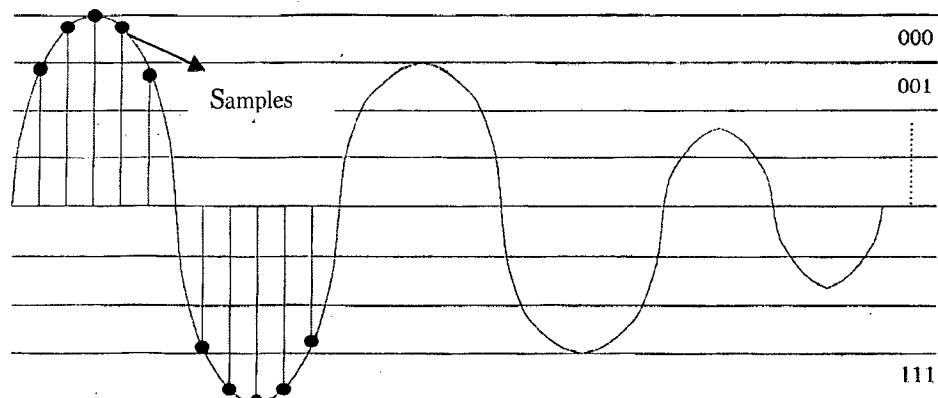
Figure 4.3 Sampling and quantization of the signal [14]

23

The floating point DCT coefficients are quantized to integer values in this process. These quantized coefficients are the indices to the quantization table; for example the use of DCT serves to process the original signal but to this point no actual compression of data has yet occurred. It means that at quantization step, the compression actually starts; it explains that the DCT analysis does not actually compress a signal, which allows the data to be compressed by standard entropy coding techniques which is further part of the quantization. Once the quantization process is done, the quantized value will be fed into the next stage of compression. Quantization is applied for two coding techniques DCT and Wavelet in this dissertation work.

4.2.4 Huffman encoding

The quantized data contains redundant information. It is waste of storage space if we were to save the redundancies of the quantized data. One way of overcoming this problem is to use Huffman encoding [15]. In this the probabilities of occurrence of the symbols in the signal are computed. These symbols are the indices to the quantization table. We will sort these symbols according to their probabilities of occurrence in descending order and build the binary tree and codeword table. Due to limitation in the implementation of a binary tree with recursive ability, this encoder uses an array-based binary tree that encodes and decodes the data in a sequence manner. Such an approach incurs expensive computation time. This is the draw back in this coding.

In the real time applications if we want to code any element we need to have minimum of 4 bits for any element in the binary coded decimal (BCD) numbering system. Even though our data is repeating for so many times then also we need to have 4 bits. So if we want to decrease the memory size or the bandwidth of the transmission line we have to represent the data with less number of bits. This could have been done by using Huffman coding. There are many different reasons for and ways of encoding data and one of these ways is Huffman coding. This is used as a compression method in digital imaging and video as well as in other areas. The idea behind Huffman coding is simply to use shorter bit patterns for more common characters, and longer bit patterns for less common characters. So it is necessary to know the probability of each data element in the data set. Once we know the data and corresponding probabilities it is possible to encode the data by using Huffman coding. The steps of Huffman coding [16]:

1. Consider each of the elements as a symbol with its probability.

2. Find the two symbols with the smallest probability and combine them into a new symbol with both letters by adding the probabilities.

3. Repeat step 2 until there is only one symbol left with a probability of 1

4. To see the code, redraw all the symbols in the form of a tree where each symbol contain either a single letter or splits up into two smaller symbols. Label all the left branches of the tree with a '0' and all the right branches with a '1'. The code for each of the letters is the sequence of 0's and 1's that lead to it on the tree, starting form the symbol with a probability of 1.

(a) Example: If want to encode the letters A (0.12), E (0.42), I (0.09), O (0.30), U (0.07) listed with their respective probabilities. By applying the above steps we can get the following tree.
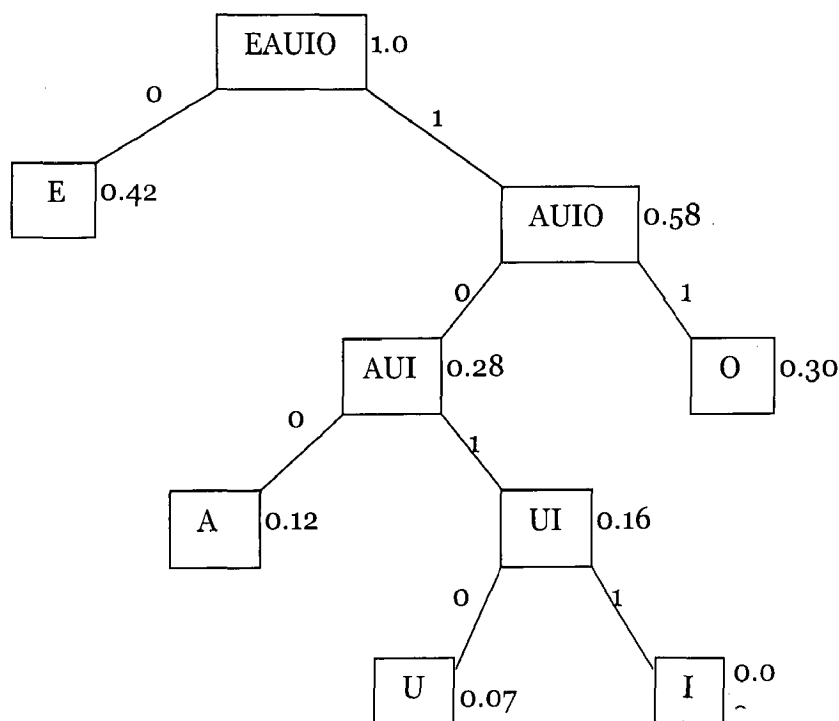
Figure 4.4 Huffman Coding Tree: An example [16]

From the above Huffman coding tree we can encode and decode the data. Example 'UEA' can be represented as 10100100. Similarly 10110 can be decoded as 'IE' and also any string of vowels can be written uniquely as well as each string of 0's and 1's can be uniquely decoded. To reconstruct the EEG signal, we have to reverse the process for three stages. Those are Huffman decoding, dequantization and inverse DCT then we can get the reconstructed EEG.

4.3 Wavelet based EEG Compression

4.3.1 Basics of wavelet transform

The fundamental idea behind wavelets is to analyze according to scale. The wavelet analysis procedure is to adopt a wavelet prototype function called an analyzing wavelet or mother wavelet. Any signal can then be represented by translated and scaled versions of the mother wavelet. Wavelet analysis is capable of revealing aspects of data that other signal analysis techniques such as Fourier analysis miss aspects like trends, breakdown points, discontinuities in higher derivatives, and self-similarity. Furthermore, because it affords a different view of data then those presented by traditional techniques, it can compress or de-noise a signal without appreciable degradation. Wavelets are functions that satisfy certain mathematical requirements and are used in representing data and other functions. However, in wavelet analysis, the scale that we use to look at data plays a special role. Wavelet algorithms process data at different scales or resolutions. If we look at a signal (or a function) through a large 'window', we would notice gross features. Similarly, if we look at a signal through a small 'window', we would notice small features.

Transform based techniques such as the discrete Fourier transform (DFT) or discrete cosine transform (DCT), and subband techniques such as the conjugate quadrature-mirror filter bank (QMF) are suitable for stationary signal analysis. However, they are not suitable for analysis of non stationary signals such as speech and audio (time frequency) or images (space-frequency), or video (time-space frequency), and for nonlinear perceptual distortion criteria. Consequently, these techniques have recently been extended to QMF trees with unequal-bandwidth branches and subband-DFT hybrids. A much more promising approach to time-frequency analysis is offered by wavelets [17].

a) **Fourier analysis:**

(a) Fourier transform [17]

26
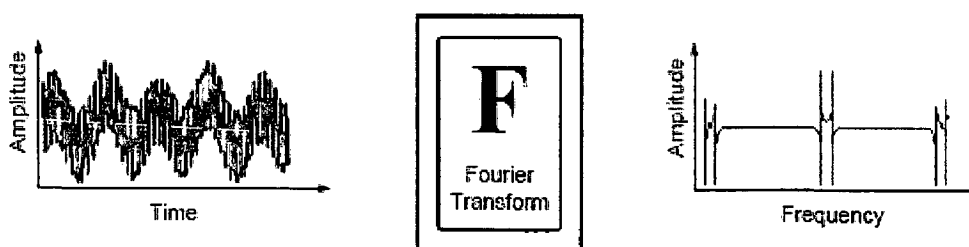
Figure 4.5 (c) shows a WFT, where the window is simply a square wave. The square wave window truncates the sine or cosine function to fit a window of a particular width. Because a single window is used for all frequencies in the WFT, the resolution of the analysis is the same at all locations in the time frequency plane. The drawback is that once choose a particular size for the time window, that window is the same for all frequencies. Many signals require a more flexible approach — one where we can vary the window size to determine more accurately either time or frequency.

c) Wavelet analysis:

Like Fourier analysis the wavelet transform can be viewed as transforming the signal form the time domain to the wavelet domain [18]. This new domain contains more complicated basis functions called wavelets, mother wavelets or analyzing wavelets.

Wavelet analysis represents the next logical step: a windowing technique with variable-sized regions. Wavelet analysis allows the use of long time intervals where we want more precise low-frequency information, shorter regions where we want high-frequency information. It is shown in figure below.

(d) wavelet transform [17]
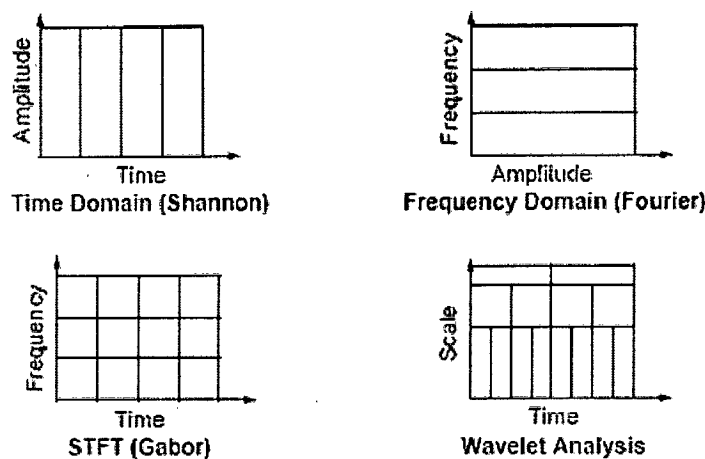
Figure 4.5 FT, STFT, Wavelet characteristics [17]

28

Fourier analysis breaks down the signal into constituent sinusoids of different frequencies. So these sines and cosines are the basis functions and the elements of Fourier synthesis. It is nothing but, it transforms the time based signal into frequency based signal [18]. Fourier analysis has a serious drawback. In transforming to the frequency domain, time information is lost. When looking at a Fourier transform of a signal, it is impossible to tell when a particular event took place.

b) Short-time Fourier analysis:

In an effort to correct this deficiency Fourier analysis, Dennis Gabor (1946) adapted the fourier transform to analyze only a small section of the signal at a time — a technique called windowing the signal. Gabor's adaptation, called the Short-Time Fourier Transform (STFT), maps a signal into a two-dimensional function of time and frequency.
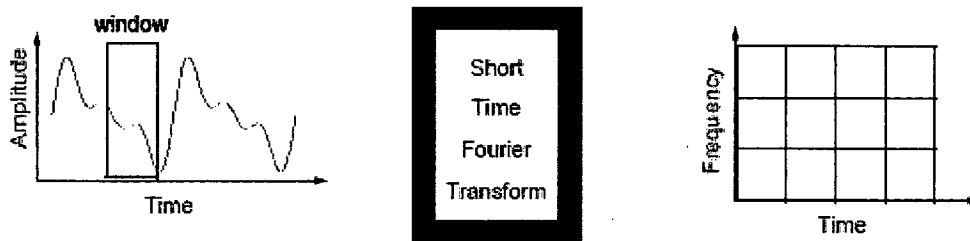
(b) short term Fourier transform [17]

The STFT represents a sort of compromise between the time and frequency based views of a signal. It provides some information about both when and at what frequencies a signal event occurs. However, you can only obtain this information with limited precision, and that precision is determined by the size of the window. This is called the Windowed Fourier Transform (WFT). WFT gives information about signals simultaneously in the time domain and in the frequency domain. To illustrate the time-frequency resolution consider the following figure 4.5(c) [17].
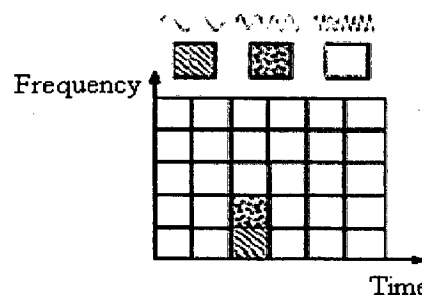
(c) Fourier basis functions and WFT resolution [17]

27

The above figure shows the difference between all the four methods discussed above those are time domain, Fourier analysis, short time Fourier analysis, and wavelet analysis [17, 18].

4.3.2 Continuous wavelet transform
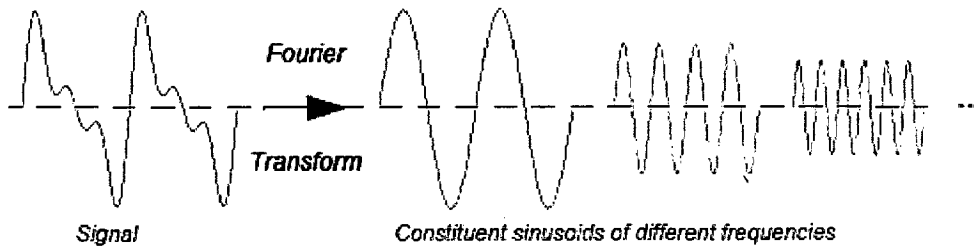
(a) Fourier Transform [18]

Mathematically, the process of Fourier analysis is represented by the Fourier transform [17]:

$$F(\omega) = \int_{-\infty}^{\infty} f(t)e^{-j\omega t}dt \qquad\qquad \dots \dots \dots \dots \dots \dots \dots \dots 4.2$$

Which is the sum over all time of the signal f (t) multiplied by a complex exponential. The results of the transformation are the Fourier coefficients F (ω), which when multiplied by a sinusoid of frequency of ω yields the constituent sinusoidal components of the original signal. Graphically, the process looks like similarly, the continuous wavelet transform (CWT) is defined as the sum over all time of the signal multiplied by scaled, shifted versions of the wavelet function Ψ [18]:

$$C(scale, position) = \int_{-\infty}^{\infty} f(t)\psi(scale, position, t)dt \qquad \dots \dots \dots \dots \dots \dots 4.3$$

The results of the CWT are many wavelet coefficients C, which are the function of scale and position. Multiplying each coefficient by the appropriately scaled and shifted wavelet yields the constituent wavelets of the original signal. Refer figure below:
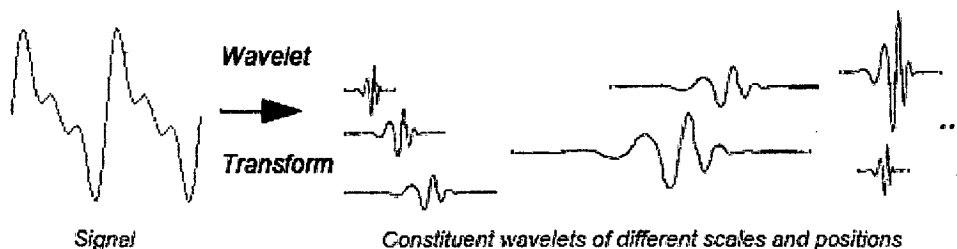
(b) Wavelet Transform [18]

29

The basis functions in both Fourier and wavelet analysis are localized in frequency making mathematical tools such as power spectra useful at picking out frequencies and calculating power distributions. The most important difference between these two kinds of transforms (FT&WT) is that individual wavelet functions are localized in space. In contrast Fourier sine and cosine functions are non-local and are active for all time t. This localization feature, along with wavelets localization of frequency, makes many functions and operators using wavelets sparse when transformed it to the wavelet domain. This sparseness, in turn results in a number of useful applications such as data compression, detecting features in images and de-noising signals. To illustrate the time-frequency resolution differences between the Fourier transform and the wavelet transform I considering the following figure 4.6 [17].
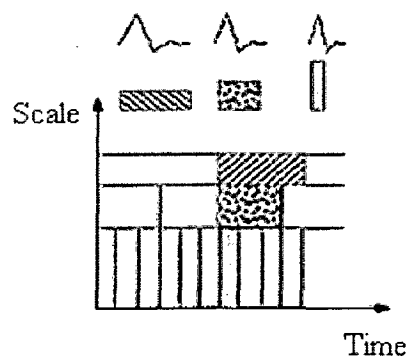
Figure 4.6 Daubechies wavelet basis functions and wavelets resolution [17].

Figure 4.6 shows a time-scale view for wavelet analysis rather than a time frequency region. Scale is inversely related to frequency. A low-scale compressed wavelet with rapidly changing details corresponds to a high frequency. A high scale stretched wavelet that is slowly changing has a low frequency. The figure 4.7 below illustrates four different types of wavelet basis functions.
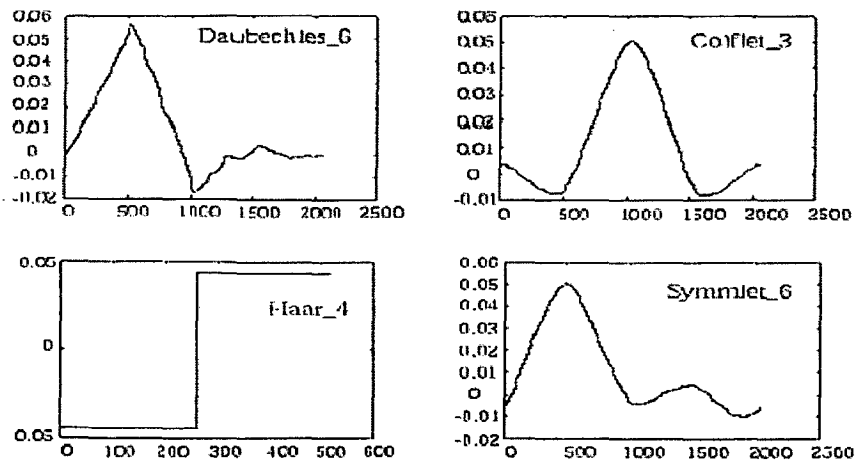
Figure 4.7 Different Wavelet Families [17]

An advantage of wavelet transform is that the windows vary. Wavelet analysis allows the use of long time intervals where we want more precise low-frequency information, and shorter regions where we want high frequency information. A way to achieve this is to have short high-frequency basis functions and long low-frequency ones. The different families make trade-offs between how compactly the basis functions are localized in space and how smooth they are. Within each family of wavelets are wavelet subclasses distinguished by the number of filter coefficients and level of iteration. Wavelets are most often classified with in a family by the number of vanishing moments. This is an extra set of mathematical relationships for the coefficients that must be satisfied. The extent of compactness of signals depends on the number of vanishing moments of the wavelet function used. A more detailed discussion is provided in the next section.

4.3.3 Discrete wavelet transform (DWT)

Calculating wavelet coefficients at every possible scale is a fair amount of work, and it generates lot of data. If we choose scales and positions based on powers of two, then our analysis will be much more efficient and accurate. We obtain such an analysis from the DWT. The mother wavelet is rescaled or dilated by powers of two and translated by integers. Specifically, a function $f(t) = L^2(R)$ (defines space of square integral functions) can be represented as:

$$f(t) = \sum_{j=1}^{L} \sum_{k=-\infty}^{\infty} d(j,k)\psi(2^{-j}t - k) + \sum_{k=-\infty}^{\infty} a(L,k)\phi(2^{-L}t - k) \quad \ldots \ldots \ldots \ldots 4.4$$

The function ψ (t) is known as the mother wavelet, while ϕ (t) is the scaling function. The set of functions $\{ \sqrt{2^{-l}}\phi(2^{-L}t - k), \sqrt{2^{-j}}\psi(2^{-j}t - k) \mid j \leq L, j,k,L \in Z \}$, where Z is the set of integers, is an orthonormal basis for $L^2(R)$. The numbers a(L, k) are known as the approximation coefficients at scale L, while d(j, k) are known as the detail coefficients at scale j. The approximation and detail coefficients can be expressed as:

$$a(L,k) = \frac{1}{\sqrt{2^L}} \int_{-\infty}^{\infty} f(t)\phi(2^{-L}t - k)dt \quad \ldots \ldots \ldots \ldots \ldots \ldots .4.5$$

$$d(j,k) = \frac{1}{\sqrt{2^j}} \int_{-\infty}^{\infty} f(t)\psi(2^{-j}t - k)dt \quad \ldots \ldots \ldots \ldots \ldots .4.6$$

To provide some understanding of the above coefficients consider a projection f_l (t) of the function f (t) that provides the best approximation (in the sense of minimum error energy) to f (t) at a scale l. This projection can be constructed form the coefficients a (L, k), using the equation

$$f_l(t) = \sum_{k=-\infty}^{\infty} a(l,k)\phi(2^{-l}t - k) \qquad \dots\dots\dots\dots\dots .4.7$$

As the scale l decreases, the approximation becomes finer, converging to f (t) as $l \rightarrow 0$. The difference between the approximation at scale $l + 1$ and that at l, $f_{l+1}(t) - f_l$ (t), is completely described by the coefficients d (j, k) using the equation-

$$f_{l+1}(t) - f_l(t) = \sum_{k=-\infty}^{\infty} d(l,k)\psi(2^{-l}t - k) \qquad \dots\dots\dots\dots\dots .4.8$$

Using these relations, given by a (L, k) and {d (j, k) | j ≤ L}, it is clear that we can build the approximation at any scale. Hence the wavelet transform breaks up the signal into a coarse approximation f_L (t). As each layer of detail is added, the approximation at the next finer scale is achieved.

a) Vanishing Moments

The number of vanishing moments of a wavelet indicates the smoothness of the wavelet function as well as the flatness of the frequency response of the wavelet filters. Typically a wavelet with p vanishing moments satisfies the following equation.

$$\int_{-\infty}^{\infty} t^m \psi(t)dt = 0 \qquad \text{for m=0... p-1,} \qquad \dots\dots\dots\dots\dots .4.9$$

Or equivalently,

$$\sum_{k} (-1)^k k^m c(k) = 0 \qquad \text{for m=0... p-1} \qquad \dots\dots\dots\dots .4.10$$

For the representation of smooth signals, a higher number of vanishing moments leads to a fast decay rate of wavelet coefficients. Thus, wavelets with a higher number of vanishing moments lead to a more compact signal representation and hence are useful in coding applications. However, in general, the length of the filters increase with the number of vanishing moments and the complexity of computing the DWT coefficients increase with the size of the wavelet filters.

4.3.4 The Fast Wavelet Transform Algorithm

The Discrete Wavelet Transform (DWT) coefficients can be computed by using Mallat's Fast Wavelet Transform algorithm [17]. This algorithm is sometimes referred to as the two-channel sub-band coder and involves filtering the input signal based on the wavelet function used. Consider the following equations:

$$\phi(t) = \sum_k c(k)\phi(2t-k) \qquad \dots \dots \dots \dots 4.11$$

$$\psi(t) = \sum_k (-1)^k c(1-k)\phi(2t-k) \qquad \dots \dots \dots \dots 4.12$$

$$\sum_k c_k c_{k-2m} = 2\delta_{0,m} \qquad \dots \dots \dots \dots 4.13$$

The first equation is known as the twin-scale relation (or the dilation equation) and defines the scaling function ϕ. The next equation expresses the wavelet ψ in terms of the scaling function ϕ. The third equation is the condition required for the wavelet to be orthogonal to the scaling function and its translates the coefficients c (k) or $\{c_0, \dots\dots c_{2N-1}\}$ in the above equations represent the impulse response coefficients for a low pass filter of length 2N, with a sum of 1 and a norm of $\frac{1}{\sqrt{2}}$. The high pass filter is obtained from the low pass filter using the relationship $g_k = (-1)^k c(1-k)$, where k varies over the range (1-(2N-1)) to 1. The equation (4.11) shows that the scaling function is essentially a low pass filter and is used to define the approximations. The wavelet function defined by the equation (4.13) is a high pass filter and defines the details. Starting with a discrete input signal vector s, the first stage of the FWT algorithm decomposes the signal into two sets of coefficients. These are the approximation coefficients cA_1 (low frequency information) and the detail coefficients cD_1 (high frequency information), as shown in the figure below.

The coefficient vectors are obtained by convolving s with the low-pass filter Lo_D for approximation and with the high-pass filter Hi_D for details. This filtering operation is then followed by dyadic decimation or down sampling by a factor of 2.Mathematically the two-channel filtering of the discrete signal s is represented by the expressions:

$$cA_1 = \sum_k c_k s_{2i-k}, \qquad cD_1 = \sum_k g_k s_{2i-k}. \qquad \dots \dots \dots \dots 4.14$$
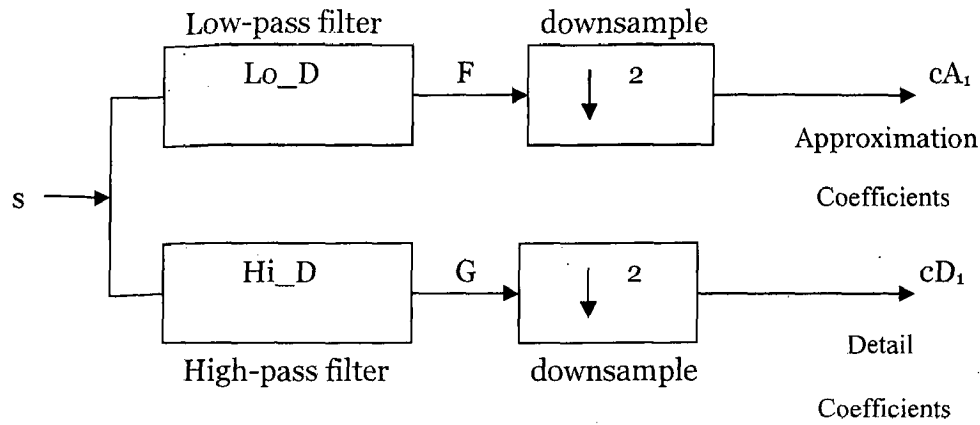
Figure 4.8 Filtering operation of DWT

These equations implement a convolution plus down sampling by a factor 2 and give the forward fast wavelet transform. If the length of the each filter is equal to 2N and the length of the original signal s is equal to n, then the corresponding lengths of the coefficients of cA_1 and cD_1 are given by the formula:

$$floor(\frac{n-1}{2}) + N \qquad \ldots \ldots \ldots \ldots \ldots \ldots 4.15$$

This shows that the total length of the wavelet coefficients is always slightly greater than the length of the original signal due to the filtering process used.

a) Multilevel decomposition

The decomposition process can be iterated, with successive approximations being decomposed in turn, so that one signal is broken down into many lower resolution components. This is called the wavelet decomposition tree [18].

The wavelet decomposition of the signal s analyzed at level j has the following structure [cA_j, cD_j, cD_1].
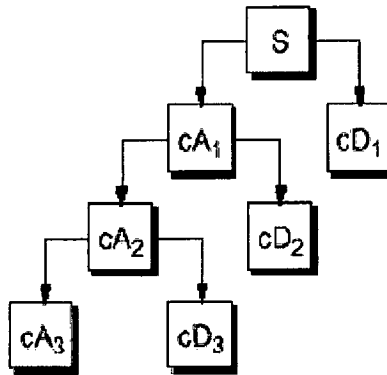
Figure 4.9 (a) Decomposition of DWT coefficients [17]
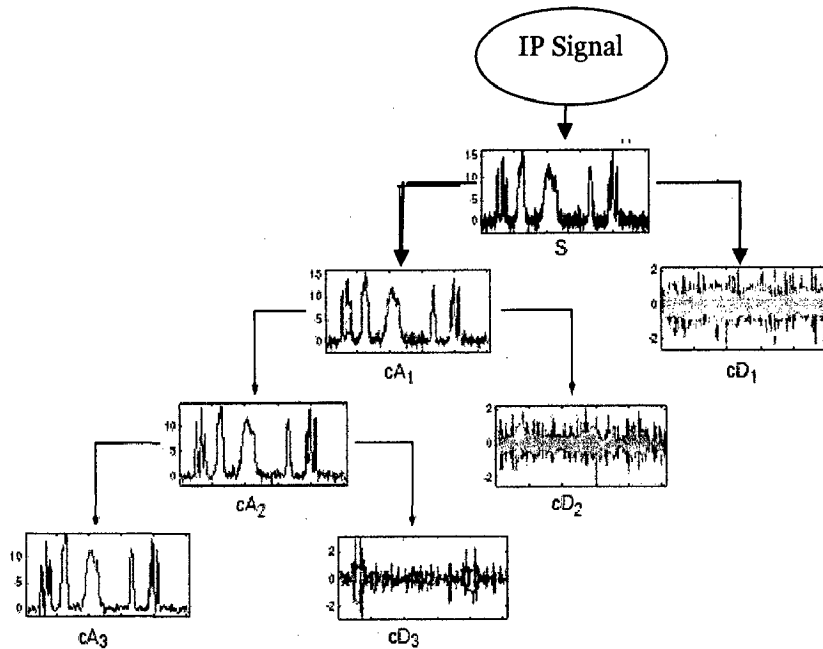
Figure 4.9 (b) Level 3 decomposition of sample signal [18]

Since the analysis process is iterative, in theory, it can be continued indefinitely. In reality, the decomposition can only proceed until the vector consists of a single sample. Normally, however, there is little or no advantage gained in decomposing a signal beyond a certain level. The selection of the optimal decomposition level in the hierarchy depends on the nature of the signal being analyzed or some other suitable criterion, such as low pass filter cut off.

4.3.5 Signal Reconstruction

The original signal can be reconstructed or synthesized using the inverse discrete wavelet transform (IDWT). The synthesis starts with the approximation and detail coefficients cA_j and cD_j, and then reconstructs cA_{j-1} by up sampling and filtering with the reconstruction filters.

The reconstruction filters are designed in such a way to cancel out the effects of aliasing introduced in the wavelet decomposition phase. The reconstruction filter (Lo_R and Hi_R) together with the low and high pass decomposition filters forms a system known as quadrature mirror filters (QMF). For a multilevel analysis, the reconstruction process can itself be iterated producing successive approximations at finer resolutions and finally synthesizing the original signal.

Upsample   Low-pass filter

cAj ──────▶ [↑ 2] ──────▶ [Lo_R]
                                          ────▶ cA_{j-1}

cDj ──────▶ [↑ 2] ──────▶ [Hi_R]

level j   Upsample   High-pass filter   level j-1

Where: [↑ 2]   Insert zeros at odd-indexed elements.

           [X]   Convolve with filter X (Lo_R, Hi_R).
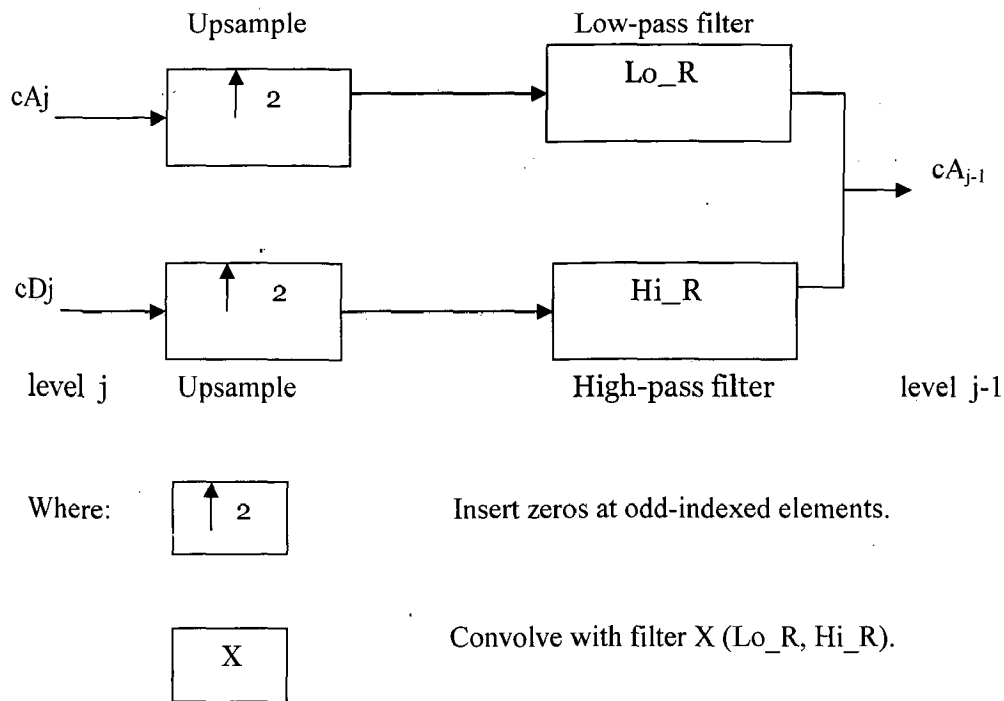
Figure 4.10 Wavelets Reconstruction

For many signals, the low-frequency content is the most important part. The high frequency component on the other hand imparts noise. Consider the human voice. If we remove the high frequency components, the voice sounds different, but we can still tell what's being said. However, if we remove the low frequency components, you hear gibberish. In wavelet analysis often speak of approximations and details. The approximations are the high-scale, low frequency components of the signal. The details are the low scale, high frequency components. The original signal passes through two complementary filters and emerges as two signals.

The original and reconstructed approximations are shown in figure 4.11
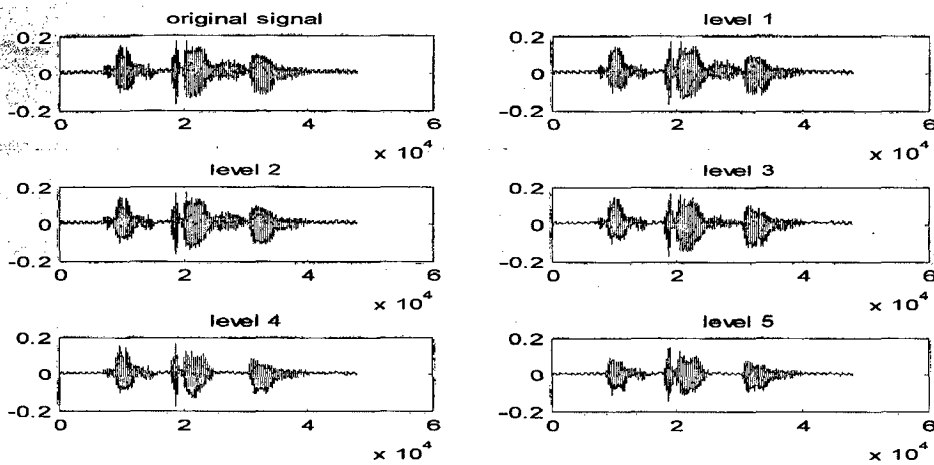
Figure 4.11 Original signal and reconstructed approximations

a) Optimal decomposition level in wavelet transforms

The figure above shows a simple EEG signal and approximations of the signal, at five different scales. These approximations are reconstructed form the coarse low frequency coefficients in the wavelet transform vector [19]. Figure 4.11 is showing that by keep on increasing the level of decomposition the energy in the approximation part of the signal is decreasing.

b) Retained Energy in First N/2 Coefficients

A suitable criterion for selecting optimum mother wavelets is related to the amount of energy a wavelet basis function can concentrate into the level 1-approximation coefficients. An EEG signal is divided into frames of size 600 samples and then analyzed using different wavelets. The wavelet transform is computed to scale 5. The signal energy retained in the first N/2 transform coefficients are given in the table given below. This energy is equivalent to the energy stored in the level 1-approximation coefficients [19].

Table 4.1 Average energy concentrated by different wavelets in N/2 coefficients

Wavelet	Avg signal energy retained
Haar	92.57
Db4	83.16
Db6	96.74
Db8	96.81
Db10	96.76

37

4.3.6 Steps of Wavelet Speech Compression

The following Figures 4.12 and 4.13 represents the encoding and decoding blocks of wavelet EEG compression.
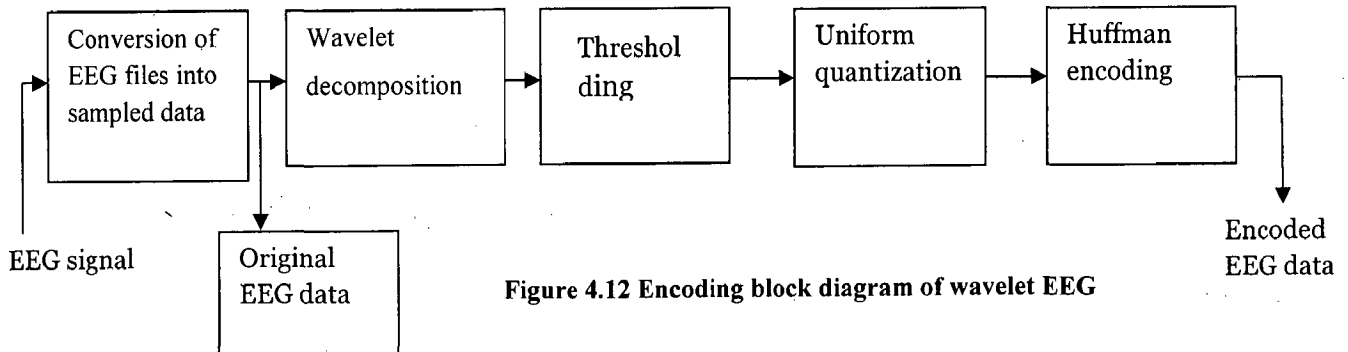
Figure 4.12 Encoding block diagram of wavelet EEG
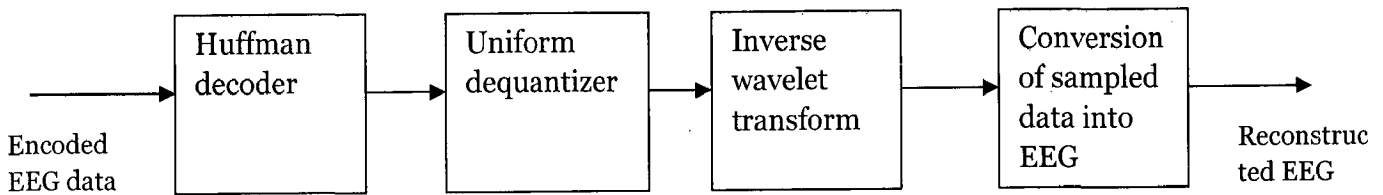
Figure 4.13 Decoding block diagram of wavelet EEG compression

The process of compressing an EEG signal using wavelets involves the following steps [9], [14]:

a) Wavelet Decomposition

The choice of the mother-wavelet function used in designing high quality EEG coders is of prime importance. Choosing a wavelet that has compact support in both time and frequency in addition to a significant number of vanishing moments is essential for an optimum wavelet EEG compressor [20]. Several different criteria's can be used in selecting an optimal wavelet function. The objective is to minimize reconstructed variance and maximize quality. In general optimum wavelets can be selected based on the energy conservation properties in the approximation part of the wavelet coefficients.

In [20], it was shown that the Battle-Lemarie wavelet concentrates more than 97.5% of the signal energy in the approximation part of the coefficients. This is followed very closely by the Daubedhies D20, D12, D10, D8 wavelets, all concentrating more than 96% of the signal energy in the level one approximation coefficients. By comparing all wavelets "Db10" is used in this dissertation work.
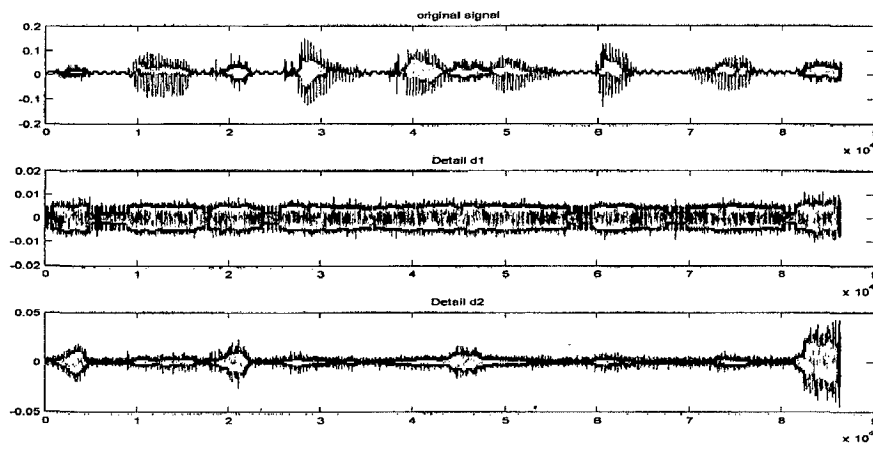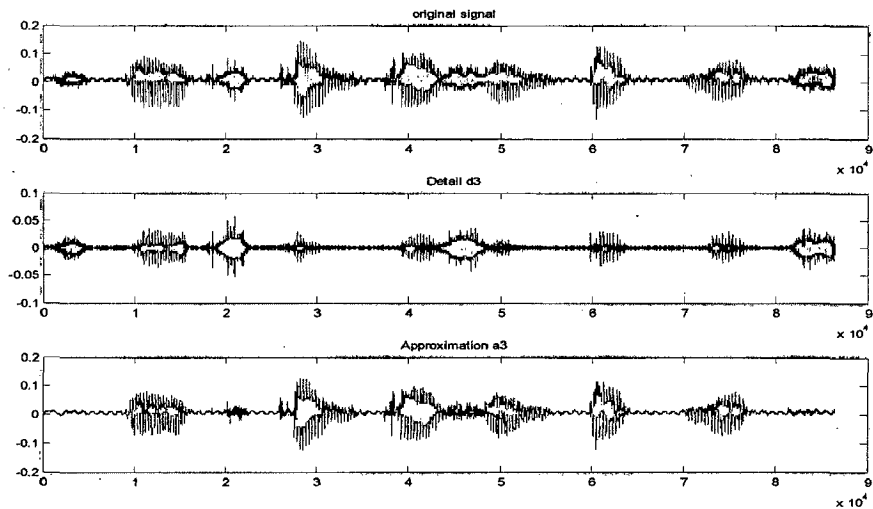
Figure 4.14 Approximation and detail parts of the EEG signal

Wavelets with more vanishing moments provide better reconstruction quality, as they introduce less distortion into the processed EEG and concentrate more signal energy in a few neighboring coefficients. However the computational complexity of the DWT increases with the number of vanishing moments and hence for real time applications it is not practical to use wavelets with an arbitrarily high number of vanishing moments [20]. Wavelets work by decomposing a signal into different resolutions or frequency bands, and this task is carried out by choosing the wavelet function and computing the Discrete Wavelet Transform (DWT). Signal compression is based on the concept that selecting a small number of approximation coefficients (at a suitably chosen level) and some of the detail coefficients can accurately represent regular signal components. Choosing a decomposition level for the DWT usually depends on the type of signal being analyzed or some other suitable criterion

39

such as entropy. For the processing of EEG signals decomposition up to scale five is adequate [20], with no further advantage gained in processing beyond scale 5.

b) Thresholding

After calculating the wavelet transform of the EEG signal, many of the wavelet coefficients are close to or equal to zero. Thresholding can modify the coefficients to produce more zeros. We have two types of thresholding one is level dependent thresholding and another is global thresholding. Level dependent thresholds are calculated using the Brige-Massart strategy [18]. This thresholding scheme is based on an approximation result from Brige and Massart and is well suited for signal compression. This strategy keeps all of the approximation coefficients at the level of decomposition J. The numbers of detail coefficients to be kept at level I starting form 1 to J are given by the formula:

$$n_i = M / (J+2-i)^a \qquad \qquad \dots \dots \dots \dots \dots .4.16$$

Where a_i is compression parameter and its value is typically 1.5. The value of M denotes the how scarcely distributed the wavelet coefficients are in the transform vector. If L denotes the length of the coarsest approximation coefficients then M takes on the values in table, depending on the signal being analyzed. For high scarceness M value is L, for medium scarceness M value is 1.5*L and for low M value is 2*L thus this approach to thresholding selects the highest absolute valued coefficients at each level. In the case of global thresholding we select the threshold value in between '0' to Cmax, where Cmax is the maximum coefficient in the decomposition. However, this value comes from the final approximation sub signal, and increases the level of decomposition [15].

The use of wavelets and thresholding serves to process the original signal but to this point no actual compression of data has yet occurred. This explains that the wavelet analysis does not actually compress a signal, which allows the data to be compressed by standard entropy coding technique. The floating point Wavelet coefficients are quantized to integer values in this process. These quantized coefficients are the indices to the quantization table. Once the quantization process is done, the quantized value will be fed into the next stage of compression. The next step is the Huffman coding which has been explained in DCT technique. To reconstruct the EEG signal, we have to reverse the process for three stages. Those are Huffman decoding, dequantization and inverse WT then we can get the reconstructed EEG.

4.4 LPC based EEG Compression

4.4.1 LPC Analysis

A second form of source coding for EEG [7, 8].compression is provided by vocoders. These devices extract the characteristic parameters of EEG, by analyzing the mechanisms of EEG formation, to derive an algorithm for providing additional compression of the data to be transmitted to the receiver.

Accordingly, instead of attempting to produce a close replica of the input signal at the output of the decoder, the appropriate set of source parameters is found in order to characterize the input signal sufficiently closely for a given duration of time. First, a decision must be made as to whether the current EEG segment to be encoded is stable or unstable. Then the corresponding source parameters must be specified. In the case of unstable EEG, the source parameter is the time between periodic excitation pulses, which is often referred to as the pitch P. In the case of stable EEG, the variance or power of the noise-like excitation must be determined. The parameters are quantized and transmitted to the decoder in order to synthesize a replica of the original signal. Vocoder schematic is shown in the figure 4.16. The encoder is a simple EEG analyzer, determining the current source parameters. After initial EEG segmentation, it computes the linear predictive filter coefficients a_i i=1....p, which characterize the spectral shaping transfer function H (z). A stable/unstable decision is carried out, and the corresponding pitch frequency and noise energy parameters are determined [21]. These are then quantized, multiplexed, and transmitted to the EEG decoder, which is an EEG synthesizer.
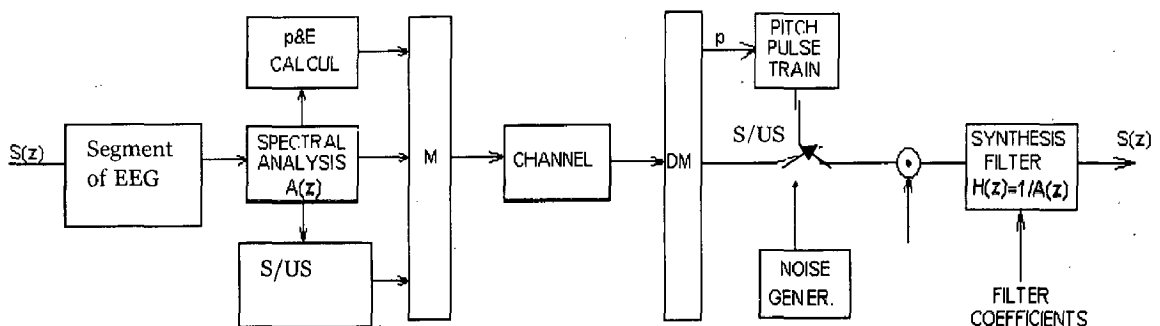
Figure 4.15 Vocoder schematic [21].

The associated EEG quality of this type of systems may be predetermined by the adequacy of the source model, rather than by the accuracy of the quantization of these parameters. In linear predictive coding (LPC), often more complex excitation models are used to describe the generating source. Once the tract apparatus has been described by the help of its spectral domain transfer function H (z), the central problem of coding is to decide how to find the simplest adequate excitation for high quality parametric EEG representation.

In the linear prediction signal is modeled as a linear combination of its past values and present and past values of a hypothetical input to a system whose output is the given signal [12]. Linear predictive coding is a standard model for speech coders. In this model all-pole model is used to describe the transfer function of the vocal tract. Here it is showing the procedure to get the synthetic EEG [22]. Assume that the present sample of the EEG is predicted by the past P samples of the EEG such that

$$S'(n) = \sum_{i=1}^{p} a_i S(n-i) \qquad \dots \dots \dots \dots \dots .4.17$$

Where $S'(n)$ is the prediction of $S(n)$, $S(n-k)$ is the kth step previous sample, and $\{a_i\}$ are the linear prediction coefficients. The residual error between the actual sample and the predicted one can be expressed as $/$

$$e(n) = S(n) - S'(n) = S(n) - \sum_{i=1}^{p} a_i S(n-i) \qquad \dots \dots$$

The sum of the squared error to be minimized is expressed as

$$E = \sum_{n} e^2(n) = \sum_{n} \left(S(n) - \sum_{i=1}^{p} a_i S(n-i) \right)^2 \qquad \dots \dots \dots$$

We would like to minimize the sum of the squared error. By setting to zerc E with respect to a_i, one obtains

$$2\sum_{n} S(n-k) \left(S(n) - \sum_{i=1}^{p} a_i S(n-i) \right) = 0 \qquad \dots \dots . \qquad .4.20$$

$$/$$

for k=1, 2, 3 $\cdots$ p

$$E\{S(n)S(n-k)\} = E\left\{\sum_{i=1}^{p} a_i S(n-i)S(n-k)\right\} \qquad \ldots\ldots\ldots\ldots\ldots .4.21$$

Upon exchange the order of the summation and expected value computation at the right hand side of equation 4.21 we get following equation.

$$E\{S(n)S(n-k)\} = \sum_{i=1}^{p} a_i E\{S(n-i)S(n-k)\} \quad k=1, p \qquad \ldots\ldots\ldots\ldots .4.22$$

By observing the above equation

$$C(k,i) = E\{S(n-k)S(n-i)\} \qquad \ldots\ldots\ldots\ldots\ldots .4.23$$

Equation 4.20 represents the input signal's covariance coefficients. The covariance coefficients C (k, i) are now computed form the following short-term expected value expression:

$$C(k,i) = \sum_{n=0}^{L_a+p-1} S(n-k)S(n-i), \quad \begin{array}{l} k=1,\ldots p, \\ i=1,\ldots p. \end{array} \qquad \ldots\ldots\ldots\ldots .4.24$$

Upon setting m=n-k, equation 3.8 can be expressed as

$$C(k,i) = \sum_{m=0}^{L_a-1-(k-i)} S(m)S(m+k-i) \qquad \ldots\ldots\ldots\ldots .4.25$$

$$\sum_{i=1}^{p} a_i C(k,i) = C(i,0) \quad i=1\ldots p \qquad \ldots\ldots\ldots\ldots .4.26$$

Which suggests that C (k, i) is the short-time autocorrelation of the input signal s (m) evaluated at a displacement of (k-i), giving:

$$C (k, i) = r (k-i) \qquad \ldots\ldots\ldots\ldots\ldots .4.27$$

Where

$$r(j) = \sum_{n=0}^{L_a-1-j} S(n)S(n+j) = \sum_{n=j}^{L_a-1} S(n)S(n-j) \qquad \ldots\ldots\ldots\ldots .4.28$$

Where r (j) represents the EEG autocorrelation coefficients. Then the set of p equations can now be reformulated as

$$\sum_{i=1}^{p} a_i r(|k-i|) = r(i) \quad k=1\ldots p \qquad \ldots\ldots\ldots\ldots .4.29$$

Equation (4) results in P unknowns in P equations.

The EEG signal is divided into segments each with N samples. If the length of each segment is short enough, the EEG signal in the segment may be stationary. In other words, the vocal tract model is fixed over the time period of one segment. If there are N samples in the sequence indexed from 0 to N-1 such that $\{S(n)\} = \{S(0),S(1),S(2),\cdots\cdot S(N-2),S(N-1)\}$, Equation can be expressed in terms of matrix equation.

$$\begin{bmatrix} r(0) & r(1) & \cdots & r(p-1) \\ r(1) & r(0) & \cdots & r(p-2) \\ \cdot & \cdot & & \cdot \\ \cdot & \cdot & & \cdot \\ r(p-1) & r(p-2) & \cdots & r(0) \end{bmatrix} \begin{bmatrix} a_1 \\ a_2 \\ \cdot \\ \cdot \\ a_p \end{bmatrix} = \begin{bmatrix} r(1) \\ r(2) \\ \cdot \\ \cdot \\ r(p) \end{bmatrix}$$

$$[R] \, [a] = \text{ r} \qquad \ldots\ldots\ldots\ldots .4.30$$

Where; $\qquad r(k) = \sum_{n=0}^{N-1-k} S(n)S(n-k) \qquad \ldots\ldots\ldots\ldots .4.31$

To solve the matrix equation 4.30 any of the following methods are used [25].

- o The Gaussian elimination method.
- o Any matrix inversion method (MATLAB).
- o The Levinson-Durbin recursion.

Out of those three algorithms Levinson-Durbin algorithm gives better results. Here the Levinson-Durbin algorithm has been given.

$E(0) = r(0)$

For k=1 to p do

$$i_k = \left[r(k) - \sum_{j=1}^{k-1} a_j^{(k-1)} r(k-j) \right] / E(k-1) \qquad \ldots\ldots\ldots\ldots .4.32$$

$$a_k^{(k)} = i_k$$

For j=1 to k-1 do

$$a_j^{(k)} = a_j^{(k-1)} - i_k a_{k-j}^{(k-1)} \qquad\qquad \dots \dots \dots \dots \dots .4.33$$

$$E(i) = (1 - i_k^2)E(k-1). \qquad\qquad \dots \dots \dots \dots \dots 4.34$$

The final solution after p iterations is given by:

$$a_j = a_j^{(p)} \qquad J=1,\dots\dots, P. \qquad\qquad \dots \dots \dots \dots \dots 4.35$$

FLOW CHART OF LEVINSON ALGORITHM
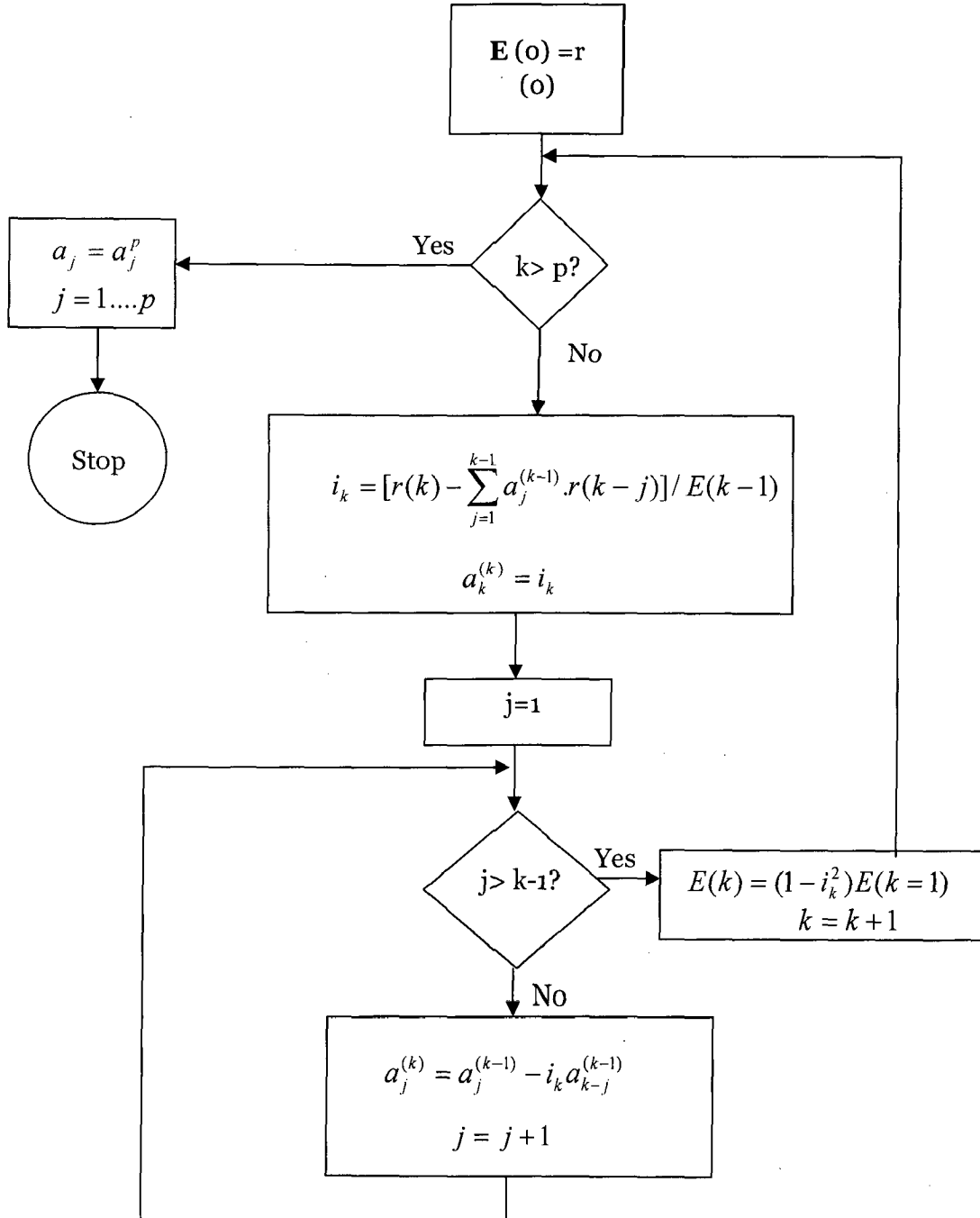
Figure 4.16 Flow chart of levinson algorithm [21].

Once the linear prediction coefficients $\{a_i\}$ are computed, equation 4.15 can be used to compute the residual error sequence e (n). The implementation of equation 4.15, where s (n) is the input and e (n) is the output, is called the analysis filter and is shown in figure 4.18
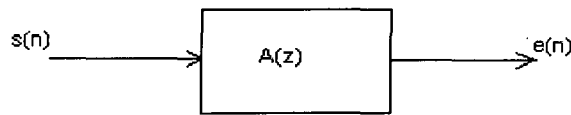
Fig. 4.17 EEG analysis filter

The transfer function is given by

$$A(z) = 1 - \sum_{i=1}^{p} a_i z^{-i} \qquad \dots\dots\dots\dots\dots\dots \quad 4.36$$

Because e (n) has less standard deviation than EEG itself, smaller number of bits is needed to quantize the error sequence.

Equation 4.15 can be rewritten as the difference equation of a digital filter whose input is e (n) and output is S (n) such that

$$S(n) = \sum_{i=1}^{p} a_i S(n-i) + e(n) \qquad \dots\dots\dots\dots\dots \quad 4.37$$

the implementation of Equation 4.35 is called the synthesis filter and is shown in Figure 4.19.
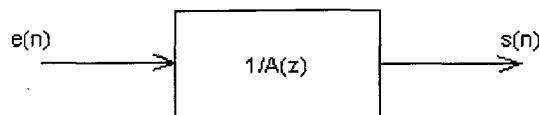
Fig. 4.18 EEG synthesis filter

If both the linear prediction coefficients and the error sequence are available, the EEG can be reconstructed using the synthesis filter [23].

4.4.2 Correlation

The correlation is one of the most common and most useful statistics. A correlation is a single number that describes the degree of relationship between two variables. Correlation between groups of data implies that they move or change with respect to each other in a structured way. In the case of signals, signals have to be digitized and that therefore form groups of data. For N pairs of data {x (n), y (n)}, the coefficient is defined as;

46

$$r_{xy} = \frac{\sum_{n=1}^{N}\{x(n) - \overline{x}\}\{y(n) - \overline{y}\}}{\sqrt{\sum_{n=1}^{N}\{x(n) - \overline{x}\}^2 \sum_{n=1}^{N}\{y(n) - \overline{y}\}^2}} \quad \ldots \ldots \ldots \ldots \ldots 4.38$$

If the finite length signals are to be analyzed, then the definition of the cross correlation function of the two signals is given.

$$r_{xy}(k) = \frac{\sum_{n=1}^{N}\{x(n) - \overline{x}\}\{y(n+k) - \overline{y}\}}{\sqrt{\sum_{n=1}^{N}\{x(n) - \overline{x}\}^2 \sum_{n=1}^{N}\{y(n) - \overline{y}\}^2}} \quad \ldots \ldots \ldots \ldots \ldots .4.39$$

In the case when the two input signals are the same, the cross correlation function becomes the autocorrelation function of that signal. Thus, the autocorrelation function is defined as

$$r_{xx}(k) = \frac{\sum_{n=1}^{N}\{x(n) - \overline{x}\}\{x(n+k) - \overline{x}\}}{\sum_{n=1}^{N}\{x(n) - \overline{x}\}^2} \quad \ldots \ldots \ldots \ldots \ldots .4.40$$

Autocorrelation is useful to determine the pitch period of the EEG signals and also this is useful in the determination of unstable and stable frames in the EEG signals.

4.4.3 Pitch Detection

Pitch period is important factor in the case of unstable EEG coding methods. Accurate estimation of the pitch period or the lag in the pitch filter is very important. It is difficult to measure exact pitch period due to the following reasons [24]:

- The reliable measurement of pitch is limited by the inherent difficulty in defining the exact beginning and end of each pitch period during voiced speech segments.

- Another difficulty in pitch detection is distinguishing between stable EEG and low level unstable EEG. In many cases, transitions between stable EEG segments and low level unstable EEG segments are very subtle, and thus are extremely hard to pinpoint.

- In practical application, the background ambient noise can also seriously affect the performance of the pitch detector. This is especially serious in mobile communication environments where a high level of noise is present.

Pitch diction methods can be classified in the following categories [24]:

I. Pitch detectors which utilize the frequency domain properties of EEG signals.

II. Pitch detectors which utilize the time domain properties of EEG signals.

III. Pitch detectors which utilize both the frequency and time domain properties of EEG signals.

In this dissertation work I am mainly interested in pitch detectors which utilize the time domain properties of EEG signals. One major property of periodic signals is that the distant similarity of the waveform in time domain. The main principle of pitch detection algorithms (PDAs) which rely on waveform similarities is to find the pitch by comparing the similarity between the original signal and its shifted version. If the shifted distance is equal to the pitch, the two signal waveforms should have the greatest similarity. The majority of existing PDAs are based on this concept. Among them, the auto-correlation (AC) method and the average magnitude difference function (AMDF) are the two most widely used. Out of these two we are concentrating on only auto-correlation method.

The key problem of PDAs which are based on the waveform similarity methods is the quantitative definition of similarity [24]. There are a number of different similarity measures which result in different PDAs and performance. They are mainly based on the minimization of a quadratic cost function. The direct distance measurement is the most popular criterion, examining the similarity between two waveforms which can be expressed as;

$$E(\tau) = \frac{1}{N}\sum_{n=0}^{N-1}[s(n) - s(n+\tau)]^2 \qquad \ldots\ldots\ldots\ldots 4.41$$

Where N is the analysis frame length and τ is the shifted distance. The above equation assumes that the average signal level is fixed. The assumption in the case of auto-correlation method is that the signal is stationary. The error criterion of equation (4.25) can be rewritten as

$$E(\tau) = [R(0) - R(\tau)] \qquad \ldots\ldots\ldots\ldots\ldots 4.42$$

Where; $$R(\tau) = \sum_{n=0}^{N-1} s(n)s(n+\tau) \qquad \ldots\ldots\ldots\ldots\ldots 4.43$$

The minimization of the estimation error, E (τ), in equation 4.25 is equivalent to maximizing the auto-correlation R (τ). The variable τ is called lag or delay, and the pitch is equal to the value of τ, which results in the maximum R (τ).
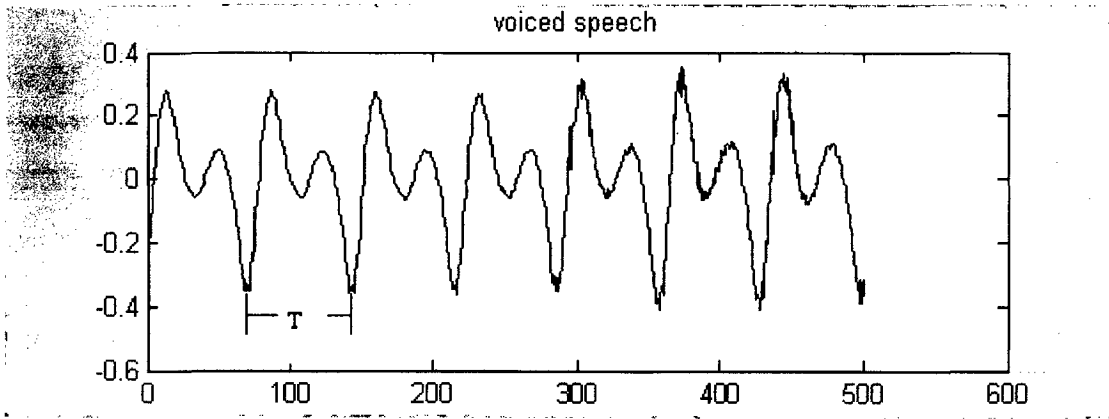
Figure 4.19 Illustration of pitch period [25]

In the above figure 4.19 has been shown that the pitch period (T) of the EEG signal. Pitch period is a variable parameter. Its value changes from person to person's EEG signal.

4.4.4 Stable/ Unstable Decision

By calculating the auto correlation coefficient we can say that the particular frame is stable or unstable. Auto correlation coefficient can be calculated by using the equation (4.26). If the auto correlation coefficient is maximum, only once in a frame then we can say that, that frame is unvoiced. If the auto correlation coefficient is giving maximum value repeatedly with particular interval then we can say that the frame is unstable with pitch period of T. Detection of stable, unstable and pitch period is showing in the figure (4.20).
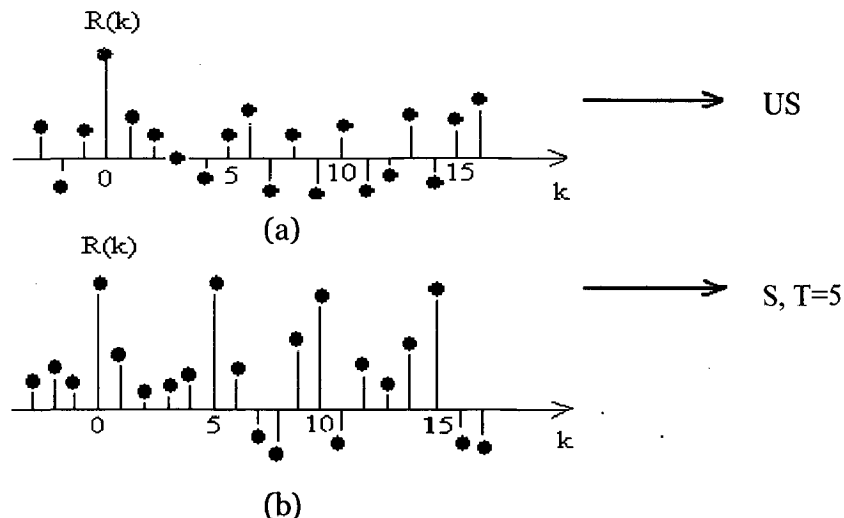
Figure 4.20 Stable/Unstable Decisions [25]

Chapter - 5

SIGNAL ACQUISATION, INSTRUMENTS AND DATABASE

5.1 Introduction

The database has taken from three varieties of signals from different sources. The first two were taken from standard website [26] archive of physiological signals. The third database has been taken from EEG machine, laboratory of Electrical Engineering department, IIT Roorkee.

5.2 Effect of Deep Brain Stimulation on Parkinsonian Tremor

The recordings of this database are of rest tremor velocity in the index finger of 16 subjects with Parkinson's disease (PD) who receive chronic high frequency electrical deep brain stimulation (DBS) either uni- or bi-laterally within one of three targets:

- Vim = the ventro-intermediate nucleus of the thalamus (n=3),
- GPi = the internal Globus pallidus (n=7), or
- STN = the subthalamic nucleus (n=6).
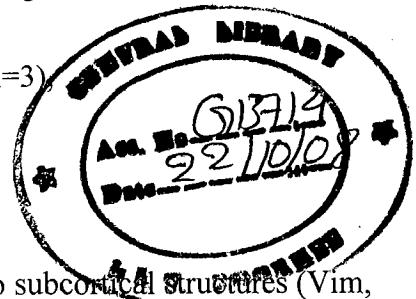
This surgical procedure involves implanting an electrode into subcortical structures (Vim, GPi or STN) for long-term stimulation at frequencies greater than 100 Hz. The mechanism by which high frequency DBS suppresses tremor and reduces other symptoms in PD is unknown.

Parkinson's disease is characterized by the progressive loss of dopamine neurons in the substantia nigra of the midbrain, and is associated with motor symptoms including tremor (usually rest tremor, though sometimes postural tremor), bradykinesia and rigidity. In Parkinson's disease, tremor becomes more regular or harmonic, its frequency is shifted to a lower range (typically 4-6 Hz), its amplitude increases, the shape of its oscillations changes, and it fluctuates over time. These changes are subtle and intermittent at first, becoming more permanent and obvious as the disease progresses. Chronic high frequency deep brain stimulation of the Vim can decrease tremor amplitude in a spectacular way. Deep brain stimulation of the GPi and STN has been shown to relieve not only tremor but also other

symptoms of PD such as rigidity and dyskinesia. See figure 5.1 for an example of the effect of deep brain stimulation of the GPi on tremor.
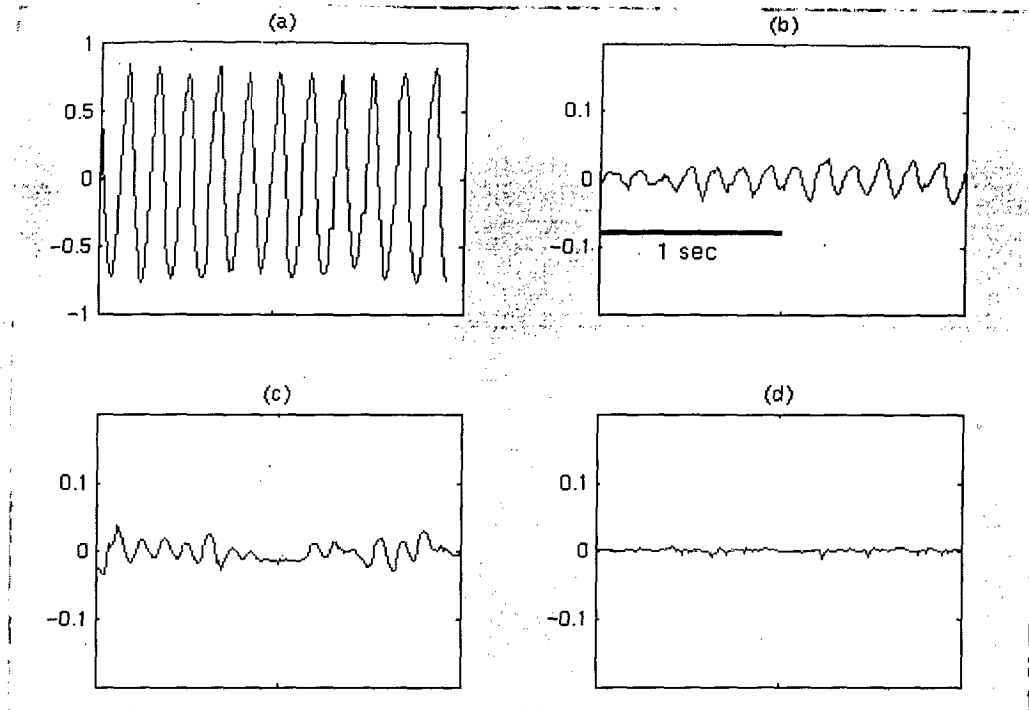
Figure 5.1 Two seconds of Parkinsonian rest tremor velocity (metres/second) recordings from subject g2 (stimulator implanted in the GPi) under four conditions: (a) no stimulation and no medication, (b) deep brain stimulation and no medication, (c) no stimulation and 150% medication, (d) deep brain stimulation and 150% medication. Note the zoomed vertical scale in (b), (c) and (d) [26].
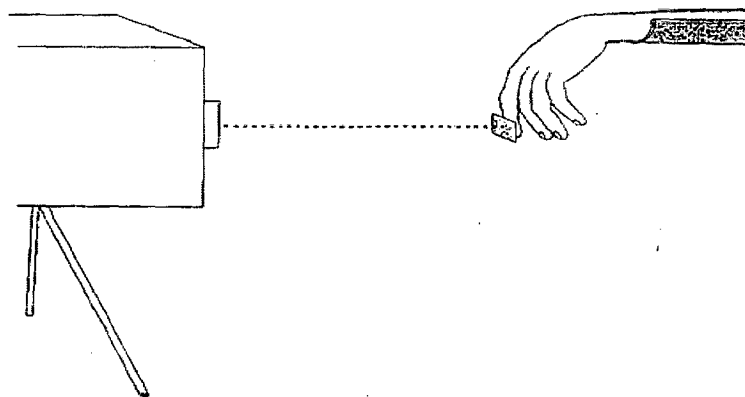
Figure5. 2 Velocity laser recording of rest tremor [26].

The raw data were obtained using a low intensity velocity-transducing laser that was directed at a piece of reflective paper on the subject's index finger tip (figure 5.2), with the output voltage proportional to the velocity of the finger.

(a) DBS/Medication conditions:

Tremor was recorded for approximately 60 seconds under various conditions:

1. Two conditions of DBS (on-off) and two conditions of medication (L-dopa on-off) [total: 55 recordings of approx 60 seconds each]
2. every 15 minutes when DBS was stopped for 60 minutes (medication off) [total: 46 recordings of approx 60 seconds each]

Subjects were tested under all conditions.

For the 'medication off' condition, the subject did not take any medication for at least 12 hours. For the 'medication on' condition, the subject took 150% morning dose of dispersible Modopar and testing began after the neurologist determined the medication had taken effect (approximately 40 minutes) [26].

(b) Subjects:

The 16 subjects can be divided into two groups:

1. Subjects 1-8 with high amplitude tremor (HAT) those are receiving DBS to relieve tremor (Group 1), and
2. Subjects 9-16 with low amplitude tremor (LAT) those are receiving DBS to relieve other symptoms such as rigidity or dyskinesias (Group 2).

The file description.txt [26] contains information on the 16 subjects. They have been explained in the next chapter.

(c) The file name structure of the records is:

- 2 character subject identification: stimulation target (v=Vim, s=STN, g=GPi) and subject number (1-16)
- 1 character tremor type: r = resting tremor
- 1 character DBS condition: e = effective (> 100 Hz), o = no stimulation
- (optional) 2 character time since stimulator arrest: if a 2 digit number follows the DBS condition, it indicates the number of minutes since the stimulation was stopped
- 1 character medication condition: n= medication on, f=medication off

- 3 character extension indicates the side tested: let = left index finger tremor, rit = right index finger tremor

Table 5 .1 Subject description table of parkinsonian Tremor

Information	Description
SUBJECT	Character subject identification: Stimulation target (v=Vim, s=STN, g=GPi), and Subject number (1-16)
AGE	Age at the time of testing (years)
GENDER	Male (n=11) or female (n=5)
STIM TARGET	Vim = ventro-intermediate nucleus of the thalamus GPi = internal Globus Pallidus STN=subthalamic nucleus
BI/UNI-LATERAL	Bilateral stimulation (n=12) or unilateral stimulation (n=4)
EFF FREQ	Frequency (Hz) of effective stimulation (> 100 Hz)
INEFF FREQ	Frequency (Hz) of so-called ineffective stimulation (< 100 Hz)
INTENSITY	Stimulation intensity (V)
PULSE WIDTH	Stimulation pulse width (μsec)
MODE	Cont = continuous stimulation, Cycl=cyclic stimulation (e.g. 1 minute on, 1 second off)
STIM CONTACTS	Listed in order of proximal distal direction on Quadripolar stimulating electrode: - negative polarity + positive polarity . not stimulated
YEAR DIAGNOSED	Year diagnosed with Parkinson's disease
YEAR DBS RIGHT	Year of right brain DBS surgery
YEAR DBS LEFT	Year of left brain DBS surgery
TOT DAILY MED	Total medication of morning, noon and evening doses (mg)
150% SINGLE DOSE	Dose taken before testing "medication on" condition (mg)

(d) Filename examples:

- s6ren.let contains a recording (approx. 60 sec) of rest tremor in the left index finger of subject 6 in the "dbs on and medication on" condition: the subject had taken 150 % morning dose of L-dopa and was receiving "effective" stimulation of the STN.

- v4rof.rit contains a recording (approx. 60 sec) of rest tremor in the right index finger of subject 4 in the "dbs off and medication off" condition: the subject was off medication for at least 12 hours and the subject's stimulator (implanted in the Vim) was switched off.

- g1r30of.rit contains a recording (approx. 60 sec) of rest tremor in the right index finger of subject 1 at 30-minutes after the stimulator (implanted in the GPi) was switched off. Also, this subject was off medication for at least 12 hours.

(e) Tremor recordings:

The rest tremor recordings can be classified as one of 8 categories, for subjects with high amplitude tremor (HAT) and for subjects with low amplitude tremor (LAT):

Case 1: **ren:** Deep brain stimulation on, Medication on
  HAT subjects: n=5 recordings
  LAT subjects: n=8 recordings

Case 2: **ref:** Deep brain stimulation on, Medication off
  HAT subjects: n=5 recordings
  LAT subjects: n=8 recordings

Case 3: **ron:** Deep brain stimulation off, Medication on
  HAT subjects: n=7 recordings
  LAT subjects: n=8 recordings

Case 4: **rof:** Deep brain stimulation off, Medication off
  HAT subjects: n=6 recordings
  LAT subjects: n=8 recordings

Case 5: **r15of:** Deep brain stimulation off for 15 minutes, Medication off

HAT subjects: n=3 recordings

LAT subjects: n=8 recordings

Case 6: **r30of:** Deep brain stimulation off for 30 minutes, Medication off

HAT subjects: n=4 recordings

LAT subjects: n=8 recordings

Case 7: **r45of:** Deep brain stimulation off for 45 minutes, Medication off

HAT subjects: n=3 recordings

LAT subjects: n=8 recordings

Case 8: **r60of:** Deep brain stimulation off for 60 minutes, Medication off

HAT subjects: n=4 recordings

LAT subjects: n=8 recordings

HAT subjects: n=37 recordings, LAT subjects: n=64 recordings all are shown in [26].

5.3 Noise Enhancement of Sensorimotor Function

This database contains postural sway [26] measurements for 15 healthy young (mean age 23, standard deviation 2), and 12 healthy elderly (mean age 73, standard deviation 3) volunteers. Each subject's postural sway is recorded during a test of 10 minutes for the young subjects, or 5 minutes for the elderly subjects, in all cases with a 2-minute seated break midway through the test. Each test was divided into 30-second trials, and each file of the database contains data for one of these 30-second trials.

In each shoe, subjects wore a gel-based insole, which included vibrating elements (tactors) beneath the forefoot and heel. The vibrations were generated using a digitized uniform white noise signal, low-pass filtered with 100 Hz cutoff. Before beginning the test, each subject adjusted the amplitude of the vibrations produced by the tactors to a level that could be felt only slightly. The stimulation level was then reduced by 10% so that the vibrations were subsensory.

The data from the young and elderly subjects are contained within the yng (young) and eh (elderly healthy) directories respectively. Within these, separate directories for each subject contain the data for that subject. For each subject, sub sensory vibration applied

during half of the 30-second trials (those recorded in the database files within the STIM subdirectories of the subject directories), and no stimulus was applied during the remaining (control) trials (those in the NULL subdirectories). The sequence of noise and control trials was randomized in a pair wise fashion, so that subjects were not aware of the presence or absence of the stimulus in any given trial.

An example should make this arrangement clear. Within the eh directory are subdirectories for each of the 12 healthy elderly volunteers, designated as MT1502, MT1503, etc. Within the directory for the first of these, MT1502, are subdirectories NULL and STIM, containing control and noise trial data for subject MT1502. Within each of these are the data files, with names that indicate their positions within the sequence of trials for that subject. For example, the data for the first trial, fMT150201.txt, are found in the NULL subdirectory, so this indicates that subject MT1502's first trial was a control trial.

The data files are two-column text files, and the data are measurements of the displacement of a reflective marker placed on the subject's shoulder to characterize whole body postural sway. A Vicon motion analysis system has been used to record the mediolateral (side-to-side) and anteroposterior (front-to-back) displacement (normalized by the height of the marker) in columns 1 and 2 respectively, at a rate of 60 samples per second, throughout each 30 second trial.

5.4 EEG machine data

This data base has been taken from EEG laboratory in Electrical Engineering department, IIT Roorkee. It is computer based machine named "RMS EEG-24" supplied by "Recorders Medicare Systems" belongs to Punjab, India.

Machine has two software supporting EEG signal processers are existing, one "EEG Acquire" and "Analysis", by using EEG acquire we can record the data up to 24 channels by using gel based non invasive type of electrodes. This software provides number of varieties to take data means reference changing, patient details changing and so on. The "Analysis" software can support processing the recorded data means Average, RMS, splitting into different frequency bands and so on. The sampling frequency exists between 40—60Hz.

RESULTS AND DISCUSSIONS

6.1 Evaluation details

The work is carried out on a Pentium IV PC operating at 2.00 GHz clock with a 512RAM. In this work MATLAB 7.5.0.324(R2007b) is used for the implementation of EEG compression techniques. The EEG signals are downloaded from internet and also recorded from EEG machine using software called 'superspec'. Three types of signals have been taken and tested with the three algorithms, and forty-five patient data have been taken for comparative evaluation.

In this work EEG signals are compressed using DCT, Wavelets and LPC techniques. In Wavelets best among all Wavelets 'Db10' is used by using level dependent thresholding. Compression is achieved in two ways one by thresholsing (or) bit assigning and another by Huffman coding. These three results of the each sampled EEG signal are tabulated and all the three coding technique performance are compared.

6.2 Parameters for Comparative Evaluation

The following parameters for the comparative evaluation of the EEG compression techniques have been implemented in this dissertation work.

1. Compression Ratio (CR)

2. Compression Factor (%) (CF)

3. Signal to Noise Ratio (dB) (SNR)

4. Percent Residual difference (%) (PRD)

The above quantities are calculated using the following formulae:

1. **Compression Ratio**

$$C = \frac{\text{Memory required for sampled original data}}{\text{Memory required for encoded data}}$$

2. **Compression Factor (%)**

The reduction in storage requirement is usually expressed as a percentage using a figure of merit called the compression factor (CF).

$$CF(\%) = \frac{U_S - C_S}{U_S} \times 100$$

U_S Is the original data size and C_s is the compressed data size.

3. **Signal to Noise Ratio**

$$SNR = 10 \log_{10}(\frac{\sigma_x^2}{\sigma_e^2})$$

σ_x^2 Is the mean square of the speech signal and σ_e^2 is the mean square difference between the original and reconstructed signals.

4. **Percent Residual Difference**

The reconstruction error is often expressed using a distortion metric called the percent residual difference (PRD), defined as

$$PRD(\%) = \sqrt{\frac{\sum_{i=1}^{N}(x_i - y_i)^2}{\sum_{i=1}^{N} x_i^2}} \times 100$$

x is the original signal, y is the reconstructed signal, and N is the segment length.

6.3 Subjects with High Amplitude Tremor

This database contains "Effect of deep brain stimulation on parkinonian tremor" signals. These are further divided into HAT and LAT. First of all HAT signals have been used. For these

signals two coding techniques were applied one DCT and another Wavelet. For both techniques, Huffman coding was applied to further compress the data. Compression ratio (C.R), compression factor (C.F %), signal to noise ratio (SNR) and percent residual difference (PRD %) are calculated for each coding technique. Original EEG signal data and encoded EEG signal data are stored in the '.mat' file. The size of the original and reconstructed EEG signal data that has been represented in the result tables are in "KB (kilobytes)" and "Bytes".

In HAT [26], there are eight varieties of condition are available, those are as follows:

```
# FILES FOR SUBJECTS WITH HIGH AMPLITUDE TREMOR:
#
#-------------------------------------------------------------
# SUBJECTS WITH HIGH AMPLITUDE TREMOR:
# REST TREMOR, CONDITION: DBS ON, MEDICATION ON (n=5 files)
#-------------------------------------------------------------
SUBJ    FILE        RANGE VELOCITY LASER   RATE SAMPLES
#
g1      g1ren.let 0.5   mm/s      0-0.2   100  6234
g2      g2ren.rit 0.2   mm/s      0-0.2   100  7680
v3
v4
v5
s6      s6ren.let 0.2   mm/s      0-0.2   100  6288
s7      s7ren.rit 0.5   mm/s      0-0.2   100  6468
s8      s8ren.let 0.2   mm/s      0-0.2   100  6252
#
#-------------------------------------------------------------
# SUBJECTS WITH HIGH AMPLITUDE TREMOR:
# REST TREMOR, CONDITION: DBS ON, MEDICATION OFF (n=5 files)
#-------------------------------------------------------------
SUBJ    FILE        RANGE VELOCITY LASER   RATE SAMPLES
#
g1      g1ref.let 0.5   mm/s      0-0.2   100  6690
g2      g2ref.rit 0.2   mm/s      0-0.2   100  6336
v3
v4
v5
s6      s6ref.let 0.2   mm/s      0-0.2   100  7260
s7      s7ref.rit 0.5   mm/s      0-0.2   100  6402
s8      s8ref.let 0.2   mm/s      0-0.2   100  7896
#
#-------------------------------------------------------------
# SUBJECTS WITH HIGH AMPLITUDE TREMOR:
# REST TREMOR, CONDITION: DBS OFF, MEDICATION ON (n=7 files)
#-------------------------------------------------------------
SUBJ    FILE        RANGE VELOCITY LASER   RATE SAMPLES
#
g1      g1ron.let 0.5   mm/s      0-0.2   100  6264
g2      g2ron.rit 0.5   mm/s      0-0.2   100  7134
v3
v4      v4ron.rit 2.0   m/s       0-1     100  6432
```

```
v5        v5ron.let 1.0    m/s        0-0.2   100   7344
s6        s6ron.let 0.5    mm/s       0-0.2   100   7356
s7        s7ron.rit 0.5    mm/s       0-0.2   100   6234
s8        s8ron.let 0.2    mm/s       0-0.2   100   6720
#
#-------------------------------------------------------------
# SUBJECTS WITH HIGH AMPLITUDE TREMOR:
# REST TREMOR, CONDITION: DBS OFF, MEDICATION OFF (n=6 files)
#-------------------------------------------------------------
SUBJ      FILE        RANGE VELOCITY LASER   RATE  SAMPLES
#
g1
g2        g2rof.rit 2.0    m/s        0-1     100   7176
v3
v4        v4rof.rit 2.0    m/s        0-1     100   6282
v5        v5rof.let 2.0    m/s        0-1     100   3400
s6        s6rof.let 1.0    m/s        0-1     100   9114
s7        s7rof.rit 0.5    mm/s       0-0.2   100   6264
s8        s8rof.let 2.0    m/s        0-1     100   6216
#
#-------------------------------------------------------------------
# SUBJECTS WITH HIGH AMPLITUDE TREMOR:
# REST TREMOR, 15 MINUTES AFTER DBS STOPPED (MEDICATION OFF) (n=3
files)
#-------------------------------------------------------------------
SUBJ      FILE        RANGE VELOCITY LASER   RATE  SAMPLES
#
g1
g2        g2r15of.rit 2.0    m/s      0-1     100   6150
v3
v4
v5
s6        s6r15of.let 1.0    m/s      0-1     100   7104
s7
s8        s8r15of.let 2.0    m/s      0-1     100   8598
#
#-------------------------------------------------------------------
# SUBJECTS WITH HIGH AMPLITUDE TREMOR:
# REST TREMOR, 30 MINUTES AFTER DBS STOPPED (MEDICATION OFF) (n=4
files)
#-------------------------------------------------------------------
SUBJ      FILE        RANGE VELOCITY LASER   RATE  SAMPLES
#
g1
g2        g2r30of.rit 2.0    m/s      0-1     100   9144
v3
v4
v5
s6        s6r30of.let 1.0    m/s      0-1     100   7200
s7        s7r30of.rit 0.5    mm/s     0-0.2   100   6510
s8        s8r30of.let 2.0    m/s      0-1     100   8616
#
#-------------------------------------------------------------------
# SUBJECTS WITH HIGH AMPLITUDE TREMOR:
# REST TREMOR, 45 MINUTES AFTER DBS STOPPED (MEDICATION OFF) (n=3
files)
#-------------------------------------------------------------------
```

```
SUBJ   FILE           RANGE VELOCITY LASER   RATE SAMPLES
#
g1
g2     g2r45of.rit    2.0   m/s       0-1    100  6354
v3
v4
v5
s6     s6r45of.let    1.0   m/s       0-1    100  8232
s7
s8     s8r45of.let    2.0   m/s       0-1    100  8652
#----------------------------------------------------------------
# SUBJECTS WITH HIGH AMPLITUDE TREMOR:
# REST TREMOR, 60 MINUTES AFTER DBS STOPPED (MEDICATION OFF) (n=4
files)
#----------------------------------------------------------------
#
SUBJ   FILE           RANGE VELOCITY LASER   RATE SAMPLES
g1
g2     g2r60of.rit    2.0   m/s       0-1    100  6162
v3
v4
v5
s6     s6r60of.let    1.0   m/s       0-1    100  7218
s7     s7r60of.rit    0.5   mm/s      0-0.2  100  6300
s8     s8r60of.let    2.0   m/s       0-1    100  6726
#
#===============================================================
#
# SUBJ:  g = GPi = Globus Pallidus interna
#        v = Vim = Ventro-intermediate nucleus of the thalamus
#        s = STN = subthalamic nucleus
# RANGE:    Range (V)   Precision (+/- mm/s)
#              2.0          1.0
#              1.0          0.5
#              0.5          0.25
#              0.2          0.1
#              0.1          0.05
# VELOCITY: units of velocity in recordings
#           (mm/s or m/s)
# LASER: laser speed setting
#        (0-0.2 m/s or 0-1 m/s)
# RATE: sampling rate in Hz
# SAMPLES: number of samples in recording
#
#---------------------------------------------------------------
```

The above database is the 51 files of 8 HAT patients. The different patients are considering s->subthalmic nucleas, g-> globus pallidus interna, v-> ventro-intermediate nucleas of the thalamus. From above files it is considered only one patient data for compression, because one file can give good comparative study of compression algorithms. The considered data file is 's6' because it is appearing in 8 varieties of conditions. The remaining details are available in the above description text it self.

a) Original and reconstructed waveforms

Original and reconstructed waveforms for different conditions of patient '6' are shown figure 6.1 and 6.2 respectively.
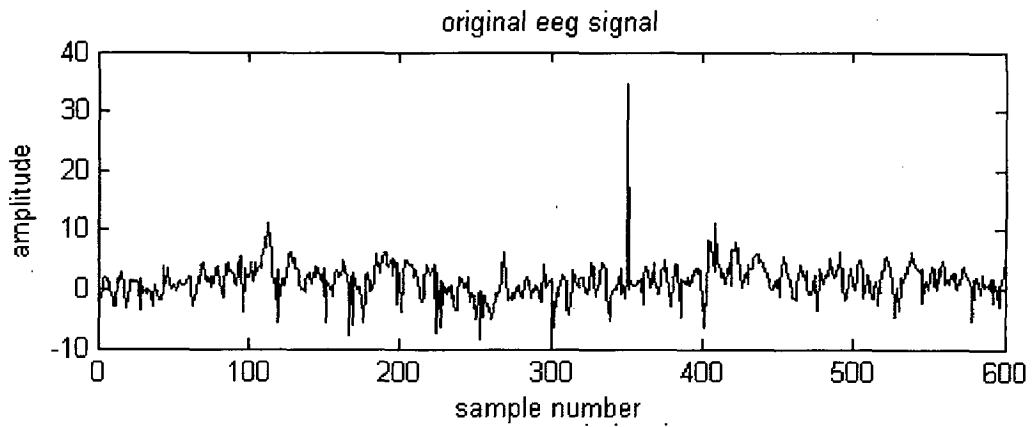
(a) "S6ren.let"
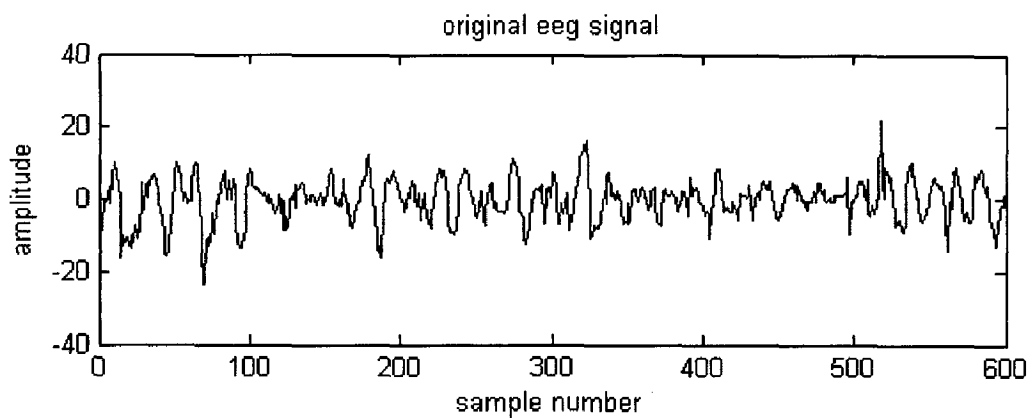
(b) "S6ref.let"
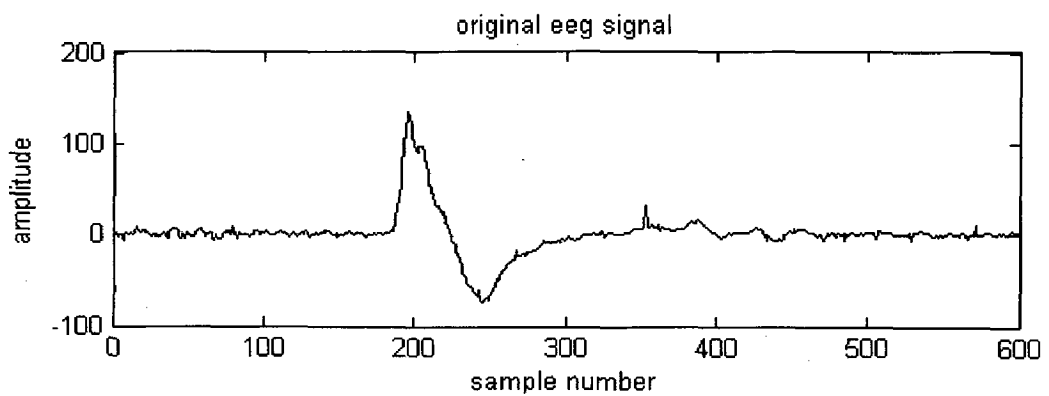
(c) "S6ron.let"
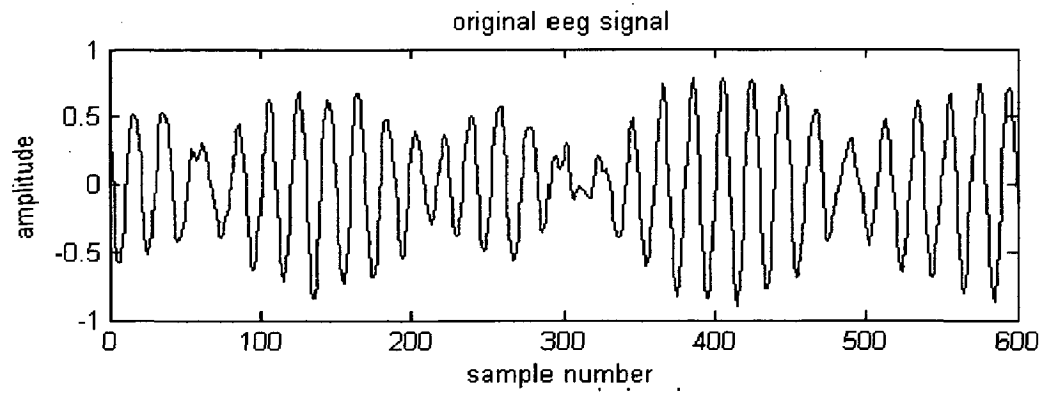
(d) "S6rof.let"
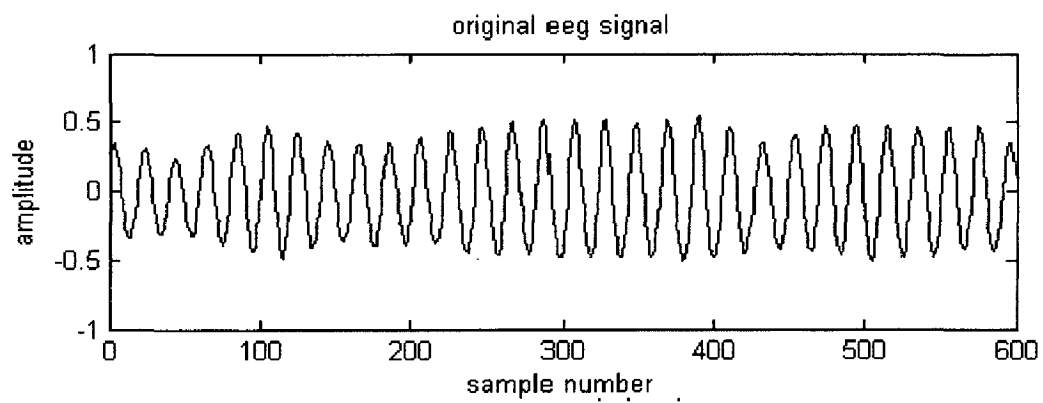
(e) "S6r15of.let"
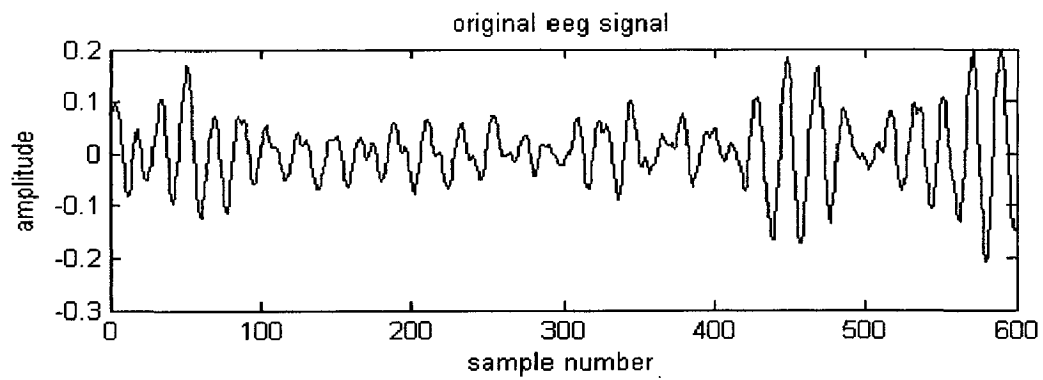
(f) "S6r45of.let"

Fig 6.1 Original EEG signals of patient s6
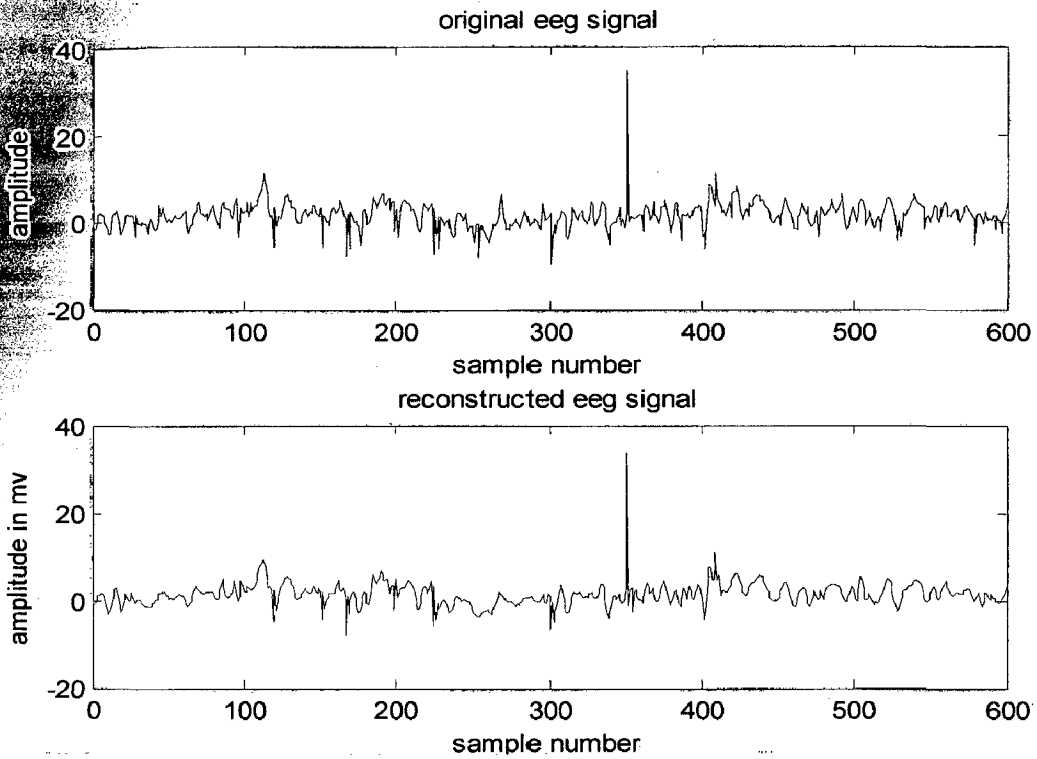
(a) original and reconstructed EEG signal "s6ren.let" at 6 bits for sample in DCT coding
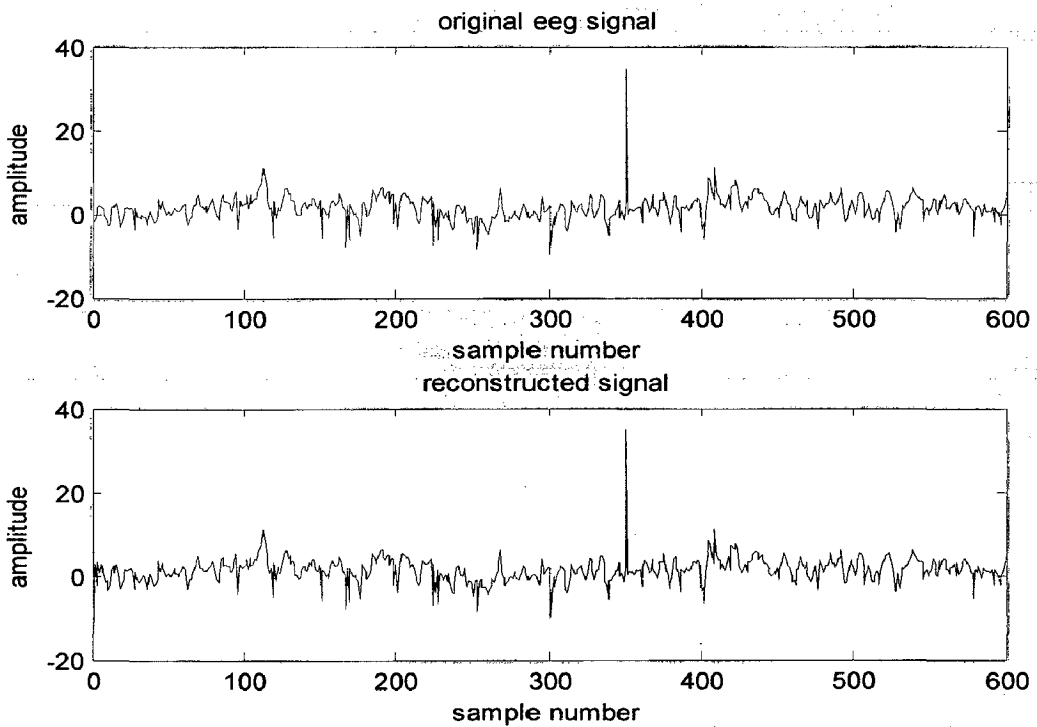
(b) original and reconstructed EEG signal "s6ren.let" at level 3 decomposition in Wavelet

Fig. 6.2 Original and reconstructed EEG signal "s6ren.let"

b) Representation of results in tabular form

The performance index for two EEG signals (s6ren.let and s6ref.let) are presented in tables 6.1 to 6.4 using DCT and Wavelet coding.

Table 6.1 Performance index for EEG signal 1 ("s6ren.let") using DCT coding

No of bits per sample	Original signal size in KB	Size of encoded data in bytes	C.R	Compression Factor (%)	SNR in dB	PRD (%)
3	1.28	324	4.0454	75.2808	- 3.9272	157.1674
4	1.28	381	3.7342	70.9320	2.2660	77.0369
5	1.28	470	2.7888	64.1418	8.2182	38.8231
6	1.28	567	2.3117	56.7413	14.2762	19.3280
7	1.28	662	1.9799	49.4934	20.3891	9.5619
8	1.28	768	1.7067	41.4063	26.4641	4.7511
9	1.28	854	1.5348	34.8450	32.4037	2.3978

Table 6.2 Performance index for EEG signal 1 ("s6ren.let") using Wavelet coding

Level of decomposition	Original signal size in KB	Size of encoded data (bytes)	C.R	Compression Factor (%)	SNR in dB	PRD (%)
1	1.28	723	1.8129	44.8395	19.7365	10.3080
2	1.28	580	2.2599	55.7495	12.3566	24.1086
3	1.28	438	2.9925	66.5833	7.8116	40.6837
4	1.28	364	3.6009	72.2290	5.1406	55.3312
5	1.28	319	4.1088	75.6622	3.9803	63.2393
6	1.28	300	4.3691	77.1118	3.3999	67.6087

Table 6.3 Performance index for EEG signal 1 ("s6ref.let") using DCT coding

No of bits per sample	Original signal size in KB	Size of encoded data (bytes)	C.R	Compression Factor (%)	SNR in dB	PRD (%)
3	1.39	342	4.1620	75.9723	-3.3563	147.1692
4	1.39	362	3.9320	74.5672	3.1145	69.8677
5	1.39	441	3.2277	69.0170	9.4333	33.7547
6	1.39	541	2.6311	61.9913	15.2857	17.2073
7	1.39	631	2.2558	55.6683	21.3626	8.5481
8	1.39	728	1.9552	48.8534	27.2075	4.3614
9	1.39	821	1.7337	42.3196	33.2903	2.1651

Table 6.4 Performance index for EEG signal 1 ("s6ref.let") using Wavelet coding

Level of decomposition	Original signal size in KB	Size of encoded data (bytes)	C.R	Compression Factor (%)	SNR in dB	PRD (%)
1	1.39	761	1.8704	46.5350	22.3779	7.6051
2	1.39	589	2.4166	58.6190	14.4228	19.0047
3	1.39	461	3.0876	67.6118	7.9612	39.9891
4	1.39	366	3.8891	74.2862	3.9201	63.6788
5	1.39	323	4.4068	77.3072	2.0749	78.7507
6	1.39	295	4.8251	79.2744	1.4995	84.1444

It is observed from above tables that, by increasing the number of bits per sample C.R and PRD are decreasing while SNR increases. For Wavelet, by increasing the level of decomposition C.R and PRD are increasing while SNR is decreasing. By comparing DCT and WT it is observed that WT is giving good results at 8 bits per sample.

The performance index (s6ron.let and s6rof.let) are presented in tables 6.5 to 6.8.

Table 6.5 Performance index for EEG signal 1 ("s6ron.let") using DCT coding

No of bits per sample	Original signal size in KB	Size of encoded data (bytes)	C.R	Compression Factor (%)	SNR in dB	PRD (%)
3	1.14	344	3.3935	70.5318	-2.9982	141.2253
4	1.14	358	3.2608	69.3325	3.3060	68.3439
5	1.14	381	3.0639	67.3623	9.6903	32.7708
6	1.14	416	2.8062	64.3640	16.0869	15.6912
7	1.14	475	2.4576	59.3099	22.2813	7.6901
8	1.14	554	2.1071	52.5425	28.5460	3.7385

Table 6.6 Performance index for EEG signal 1 ("s6ron.let") using Wavelet coding

Level of decomposition	Original signal size in KB	Size of encoded data (bytes)	C.R	Compression Factor (%)	SNR in dB	PRD (%)
1	1.14	564	2.0699	51.6859	29.8294	3.2250
2	1.14	453	2.5770	61.1945	27.7073	4.1175
3	1.14	367	3.1809	68.5615	25.1218	5.5451
4	1.14	314	3.7178	73.1017	22.5133	7.4875
5	1.14	293	3.9843	74.9006	19.6695	10.3878
6	1.14	279	4.1842	76.0999	16.7720	14.5010

Table 6.7 Performance index for EEG signal 1 ("s6rof.let") using DCT coding

No of bits per sample	Original signal size in KB	Size of encoded data (bytes)	C.R	Compression Factor (%)	SNR in dB	PRD (%)
3	2.22	318	7.1487	86.0114	-5.4920	188.1913
4	2.22	326	6.9733	85.6595	0.6689	92.5885
5	2.22	360	6.3147	84.1639	6.7922	45.7499
6	2.22	398	5.7118	82.4923	13.0137	22.3519
7	2.22	434	5.2380	80.9086	19.2607	10.8884
8	2.22	495	4.5925	78.2253	25.4499	5.3396
9	2.22	545	4.1712	76.0258	31.5349	2.6501

Table 6.8 Performance index for EEG signal 1 ("s6rof.let") using Wavelet coding

Level of decomposition	Original signal size in KB	Size of encoded data (bytes)	C.R	Compression Factor (%)	SNR in dB	PRD (%)
1	2.22	741	3.0679	67.4039	38.4467	1.1958
2	2.22	568	4.0023	75.0141	28.6983	3.6736
3	2.22	461	4.9312	79.7209	15.7542	16.3038
4	2.22	354	6.4217	84.4278	5.5642	52.6972
5	2.22	310	7.3332	86.3633	2.5328	74.7068
6	2.22	293	7.7586	87.1111	1.2497	86.5994

Similar are the results observed in tables 6.5 to 6.8.

The performance index (s6r15of.let and s6r45of.let) are presented in tables 6.5 to 6.8 by same DCT and Wavelet techniques.

Table 6.9 Performance index for EEG signal 1 ("s6r15of.let") using DCT coding

No of bits per sample	Original signal size in KB	Size of encoded data (bytes)	C.R	Compression Factor (%)	SNR in dB	PRD (%)
3	2.17	315	7.0542	85.8241	-10.1294	320.9750
4	2.17	318	6.9877	85.6891	-4.0504	159.4108
5	2.17	330	6.7336	85.1490	2.1068	78.4625
6	2.17	343	6.4784	84.5640	8.2999	38.4598
7	2.17	367	6.0547	83.4839	14.6052	18.6096
8	2.17	401	5.5413	81.9538	21.0865	8.8242
9	2.17	461	4.8201	79.2537	27.6119	4.1630

Table 6.10 Performance index for EEG signal 1 ("s6r15of.let") using Wavelet coding

Level of decomposition	Original signal size in KB	Size of encoded data (bytes)	C.R	Compression Factor (%)	SNR in dB	PRD (%)
1	2.17	733	3.0315	67.0129	40.7376	0.9186
2	2.17	552	4.0255	75.1584	34.9604	1.7864
3	2.17	441	5.0387	80.1537	17.9454	12.6687
4	2.17	350	6.3488	84.2490	6.0067	50.0803
5	2.17	305	7.2855	86.2741	1.7148	82.0843
6	2.17	294	7.5581	86.7692	0.9900	89.2273

Table 6.11 Performance index for EEG signal 1 ("s6r45of.let") using DCT coding

No of bits per sample	Original signal size in KB	Size of encoded data (bytes)	C.R	Compression Factor (%)	SNR in dB	PRD (%)
3	1.96	335	5.9912	83.3088	-5.7986	194.9535
4	1.96	354	5.6696	82.3621	0.3810	95.7079
5	1.96	376	5.3379	81.2659	6.6337	46.5922
6	1.96	416	4.8246	79.2730	12.9710	22.4620
7	1.96	460	4.3631	77.0807	19.1416	11.0387
8	1.96	519	3.8671	74.1410	25.3441	5.4050
9	1.96	590	3.4018	70.6035	31.7439	2.5871

Table 6.12 Performance index for EEG signal 1 ("s6r45of.let") using Wavelet coding

Level of decomposition	Original signal size in KB	Size of encoded data (bytes)	C.R	Compression Factor (%)	SNR in dB	PRD (%)
1	1.96	723	2.7760	63.9768	34.9114	1.7965
2	1.96	559	3.5904	72.1480	28.2224	3.8804
3	1.96	433	4.6352	78.4259	13.9475	20.0737
4	1.96	347	5.7840	82.7109	6.0434	49.8687
5	1.96	315	6.3716	84.3052	2.7817	72.5967
6	1.96	303	6.6239	84.9031	1.1097	88.0061

The results from tables 6.9 to 6.12 show the higher C.R and SNR. It is because of low frequency variation in the signal. In the tables 6.11 and 6.12, the average C.R in DCT and WT are 4.2356

and 5.4236, respectively. By observing the HAT results parameters variation are not wide among tables, but overall it is observed that there is always some change in these parameters.

By observing high amplitude tremor signals the compression ratios are existing in between 3 to 7. In DCT and Wavelet there is trade of between these two in respective to bits per sample or level of decomposition, but overall Wavelets show better results. The 6 verities of data (ren, ref, ron, rof, r15of, r45of) of left indexed tremor (let) of patient 's6' are shown results similarly in each table by respective coding. It indicates the algorithms DCT and Wavelet are signal independent algorithms.

c) Representation of results in graphical form

Fig 6.3 shows one representation graph for file 's6ren.let'.
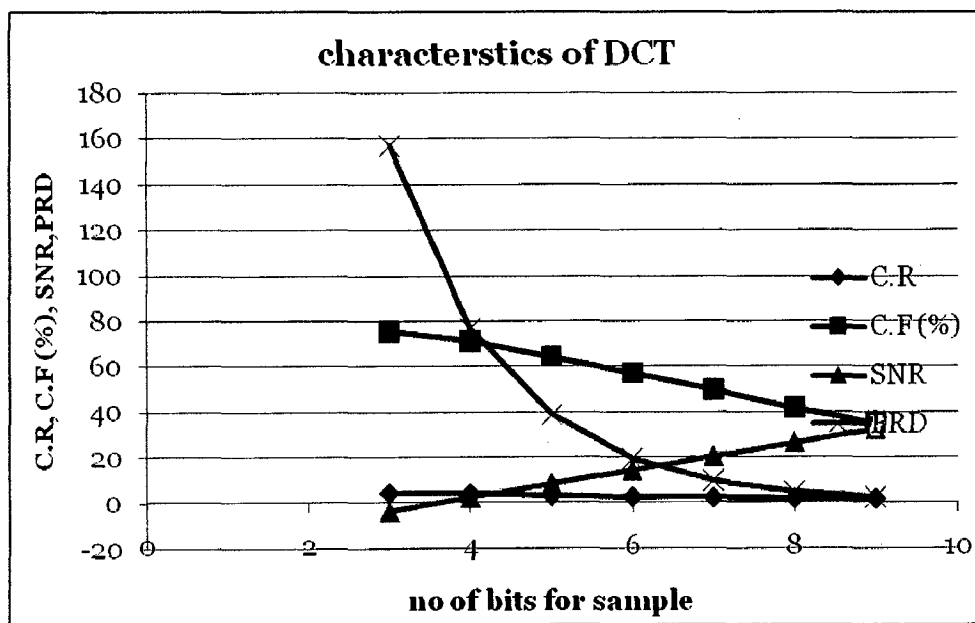
(a) comparative graph of "S6ren.lit" using DCT coding

The tabular results presented earlier are presented in graphical form here. Variations in different parameters obtained are clearly visible here.
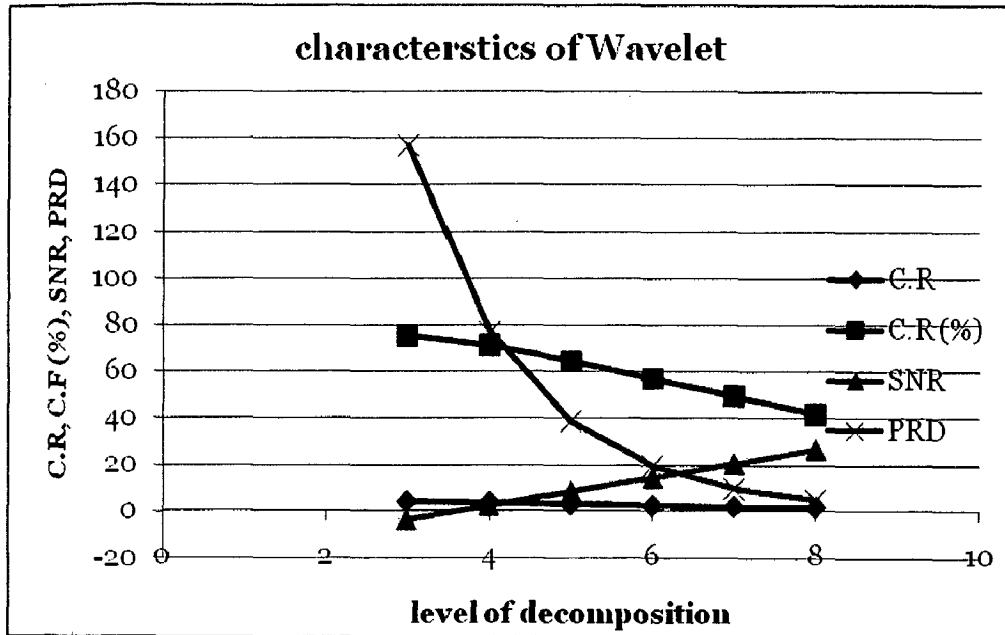
(b) comparative graph of "S6ren.lit" using Wavelet coding

Fig 6.3 Comparative graph for different coding

Similarly, variations in different parameters obtained clearly visible here by Wavelet.

6.4 Subjects with Low Amplitude Tremor

Similar to high amplitude tremor LAT [26] signals also 8 varieties are available, those are as follows

```
# FILES FOR SUBJECTS WITH LOW AMPLITUDE TREMOR:
#-----------------------------------------------------------
# SUBJECTS WITH LOW AMPLITUDE TREMOR:
# REST TREMOR, CONDITION: DBS ON, MEDICATION ON (n=8 files)
#-----------------------------------------------------------
#
SUBJ    FILE          RANGE  VELOCITY  LASER    RATE  SAMPLES
g9      g9ren.rit     0.5    mm/s      0-0.2    100   6276
g10     g10ren.let    0.5    mm/s      0-0.2    100   6180
g11     g11ren.let    0.1    mm/s      0-0.2    100   6276
g12     g12ren.rit    0.2    mm/s      0-0.2    100   6492
g13     g13ren.rit    0.1    mm/s      0-0.2    100   6282
s14     s14ren.rit    0.5    mm/s      0-0.2    100   6408
s15     s15ren.rit    0.5    mm/s      0-0.2    100   7284
s16     s16ren.let    0.2    mm/s      0-0.2    100   6300
#-----------------------------------------------------------
# SUBJECTS WITH LOW AMPLITUDE TREMOR:
# REST TREMOR, CONDITION: DBS ON, MEDICATION OFF (n=8 files)
#-----------------------------------------------------------
#
SUBJ    FILE          RANGE  VELOCITY  LASER    RATE  SAMPLES
g9      g9ref.rit     0.5    mm/s      0-0.2    100   6174
g10     g10ref.let    0.5    mm/s      0-0.2    100   6252
```

```
    g11    g11ref.let 0.1   mm/s    0-0.2  100  6396
    g12    g12ref.rit 0.2   mm/s    0-0.2  100  6714
    g13    g13ref.rit 0.2   mm/s    0-0.2  100  6564
    s14    s14ref.rit 0.5   mm/s    0-0.2  100  6282
    s15  . s15ref.rit 0.5   mm/s    0-0.2  100  6228
    s16    s16ref.let 0.2   mm/s    0-0.2  100  7128
    #------------------------------------------------------------
    # SUBJECTS WITH LOW AMPLITUDE TREMOR:
    # REST TREMOR, CONDITION: DBS OFF, MEDICATION ON (n=8 files)
    #------------------------------------------------------------
    #
    SUBJ   FILE       RANGE VELOCITY LASER  RATE SAMPLES
    g9     g9ron.rit  0.5   mm/s    0-0.2  100  9156
    g10    g10ron.let 0.5   mm/s    0-0.2  100  12108
    g11    g11ron.let 0.1   mm/s    0-0.2  100  6366
    g12    g12ron.rit 0.2   mm/s    0-0.2  100  7176
    g13    g13ron.rit 0.2   mm/s    0-0.2  100  6234
    s14    s14ron.rit 0.5   mm/s    0-0.2  100  6228
    s15    s15ron.rit 0.5   mm/s    0-0.2  100  6102
    s16    s16ron.let 0.5   mm/s    0-0.2  100  6696
    #------------------------------------------------------------
    # SUBJECTS WITH LOW AMPLITUDE TREMOR:
    # REST TREMOR, CONDITION: DBS OFF, MEDICATION OFF (n=8 files)
    #------------------------------------------------------------
    #
    SUBJ   FILE       RANGE VELOCITY LASER  RATE SAMPLES
    g9     g9rof.rit  0.5   mm/s    0-0.2  100  6354
    g10    g10rof.let 0.5   mm/s    0-0.2  100  6180
    g11    g11rof.let 0.1   mm/s    0-0.2  100  6306
    g12    g12rof.rit 0.2   mm/s    0-0.2  100  6360
    g13    g13rof.rit 0.2   mm/s    0-0.2  100  7230
    s14    s14rof.rit 0.5   mm/s    0-0.2  100  6492
    s15    s15rof.rit 0.5   mm/s    0-0.2  100  6300
    s16    s16rof.let 0.5   mm/s    0-0.2  100  6594
    #------------------------------------------------------------
    # SUBJECTS WITH LOW AMPLITUDE TREMOR:
    # REST TREMOR, 15 MINUTES AFTER DBS STOPPED (MEDICATION OFF) (n=8
    files)
    #------------------------------------------------------------
    #
    SUBJ   FILE        RANGE VELOCITY LASER  RATE SAMPLES
    g9     g9r15of.rit  0.5   mm/s    0-0.2  100  6306
    g10    g10r15of.let 0.5   mm/s    0-0.2  100  6132
    g11    g11r15of.let 0.1   mm/s    0-0.2  100  6258
    g12    g12r15of.rit 0.2   mm/s    0-0.2  100  6348
    g13    g13r15of.rit 0.2   mm/s    0-0.2  100  6558
    s14    s14r15of.rit 0.5   mm/s    0-0.2  100  6726
    s15    s15r15of.rit 0.5   mm/s    0-0.2  100  6252
    s16    s16r15of.let 0.5   mm/s    0-0.2  100  6486
    #------------------------------------------------------------
    # SUBJECTS WITH LOW AMPLITUDE TREMOR:
    # REST TREMOR, 30 MINUTES AFTER DBS STOPPED (MEDICATION OFF) (n=8
    files)
    #------------------------------------------------------------
    #
    SUBJ   FILE        RANGE VELOCITY LASER  RATE SAMPLES
    g9     g9r30of.rit  0.5   mm/s    0-0.2  100  6318
```

```
g10    g10r30of.let 0.5    mm/s    0-0.2  100  6198
g11    g11r30of.let 0.1    mm/s    0-0.2  100  6594
g12    g12r30of.rit 0.2    mm/s    0-0.2  100  6354
g13    g13r30of.rit 0.2    mm/s    0-0.2  100  7140
s14    s14r30of.rit 0.5    mm/s    0-0.2  100  6276
s15    s15r30of.rit 0.5    mm/s    0-0.2  100  6438
s16    s16r30of.let 0.5    mm/s    0-0.2  100  6588
#-------------------------------------------------------------------
# SUBJECTS WITH LOW AMPLITUDE TREMOR:
# REST TREMOR, 45 MINUTES AFTER DBS STOPPED (MEDICATION OFF) (n=8
files)
#-------------------------------------------------------------------
#
SUBJ   FILE         RANGE VELOCITY LASER  RATE SAMPLES
g9     g9r45of.rit  0.5    mm/s    0-0.2  100  6240
g10    g10r45of.let 0.5    mm/s    0-0.2  100  6210
g11    g11r45of.let 0.1    mm/s    0-0.2  100  6318
g12    g12r45of.rit 0.2    mm/s    0-0.2  100  6300
g13    g13r45of.rit 0.2    mm/s    0-0.2  100  6264
s14    s14r45of.rit 0.5    mm/s    0-0.2  100  6282
s15    s15r45of.rit 0.5    mm/s    0-0.2  100  7104
s16    s16r45of.let 0.5    mm/s    0-0.2  100  6744
#-------------------------------------------------------------------
# SUBJECTS WITH LOW AMPLITUDE TREMOR:
# REST TREMOR, 60 MINUTES AFTER DBS STOPPED (MEDICATION OFF) (n=8
files)
#-------------------------------------------------------------------
#
SUBJ   FILE         RANGE VELOCITY LASER  RATE SAMPLES
g9     g9r60of.rit  0.5    mm/s    0-0.2  100  6312
g10    g10r60of.let 0.5    mm/s    0-0.2  100  6180
g11    g11r60of.let 0.1    mm/s    0-0.2  100  6282
g12    g12r60of.rit 0.2    mm/s    0-0.2  100  6342
g13    g13r60of.rit 0.2    mm/s    0-0.2  100  6342
s14    s14r60of.rit 0.5    mm/s    0-0.2  100  6342
s15    s15r60of.rit 0.5    mm/s    0-0.2  100  6516
s16    s16r60of.let 0.5    mm/s    0-0.2  100  7302
#-------------------------------------------------------------------
#
# SUBJ:  g = GPi = Globus Pallidus interna
#        v = Vim = Ventro-intermediate nucleus of the thalamus
#        s = STN = subthalamic nucleus
# RANGE:    Range (V)  Precision (+/- mm/s)
#              2.0         1.0
#              1.0         0.5
#              0.1         0.05
# VELOCITY: units of velocity in recordings
#           (mm/s or m/s)
# LASER: laser speed setting
#        (0-0.2 m/s or 0-1 m/s)
# RATE: sampling rate in Hz
#-------------------------------------------------------------
```

Similarly the above description has 8 patient of database of LAT containing 51 files. Remaining details are same as explained above.

a) Original and reconstructed waveforms

Original and reconstructed waveforms for different conditions of patient '12' are shown
figure 6.4 and 6.5 respectively.
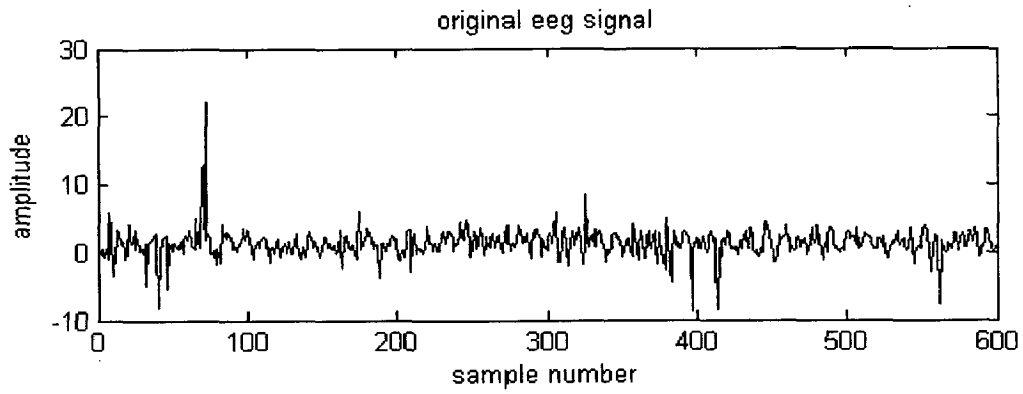
(a) "g12ren.rit"
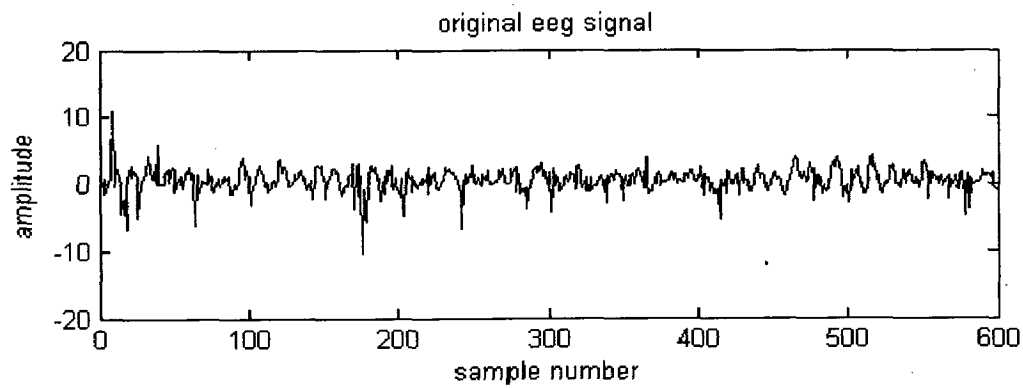
(b) "g12ref.rit"
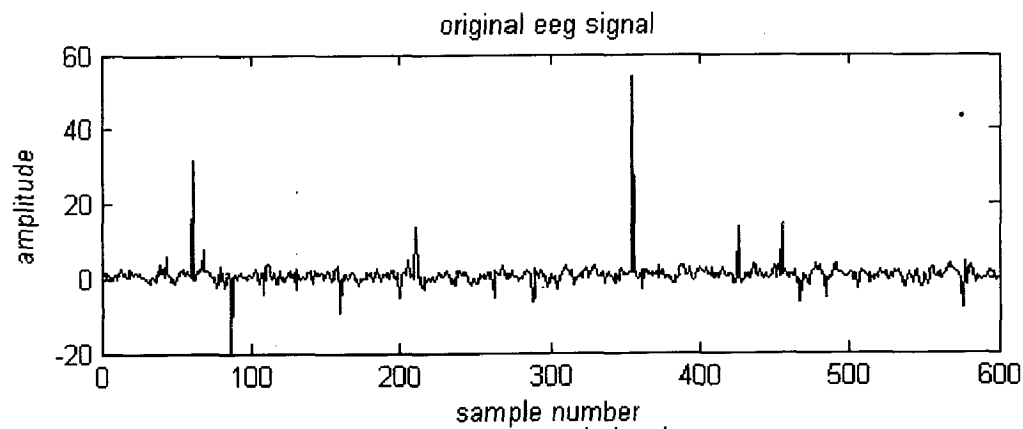
(c) "g12ron.rit"
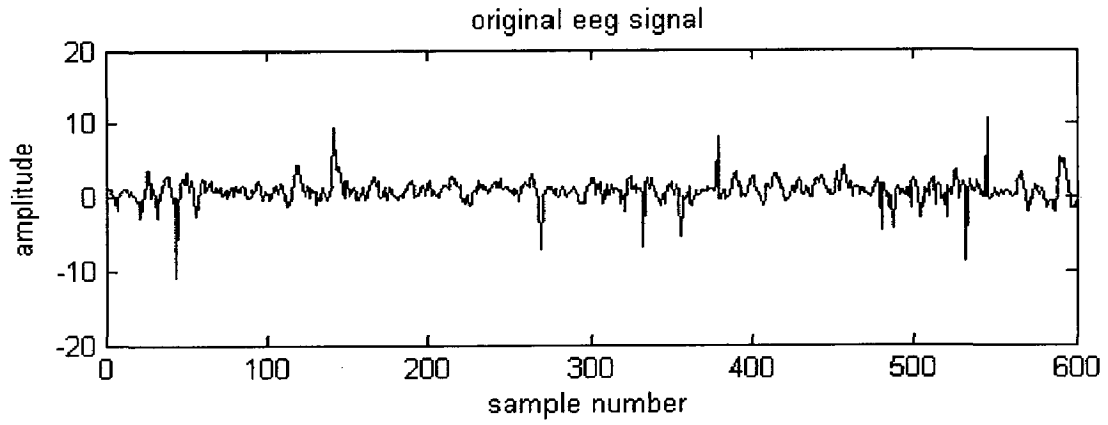
(d) "g12rof.rit"
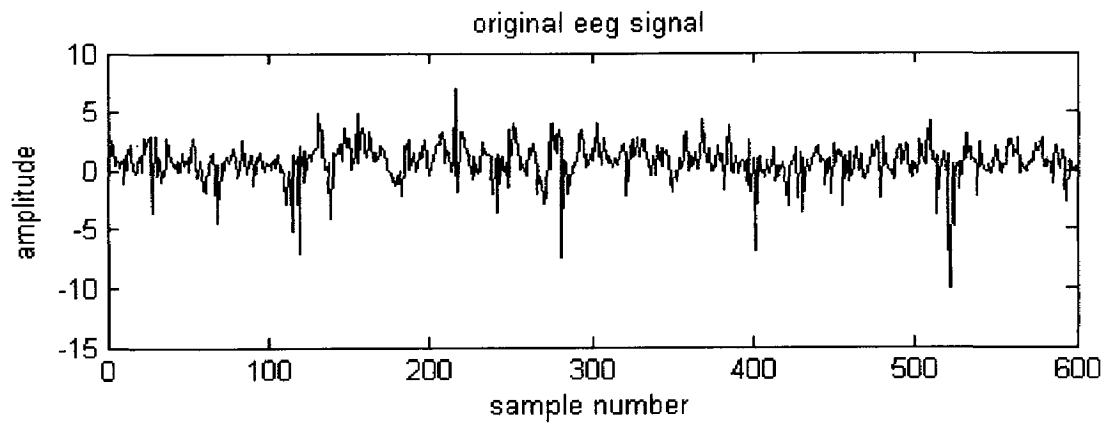
(e) "g12r15of.rit"
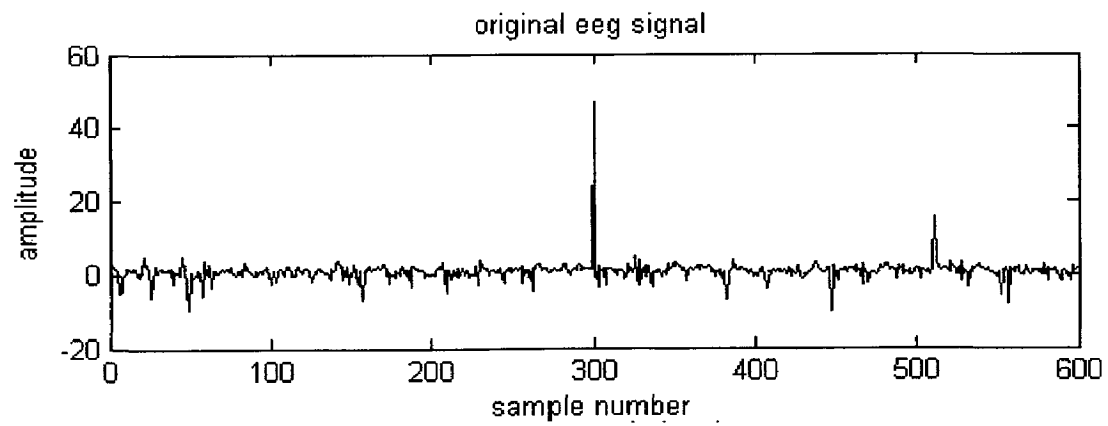
(f) "g12r45of.rit"

Fig. 6.4 Original EEG signals of patient g12
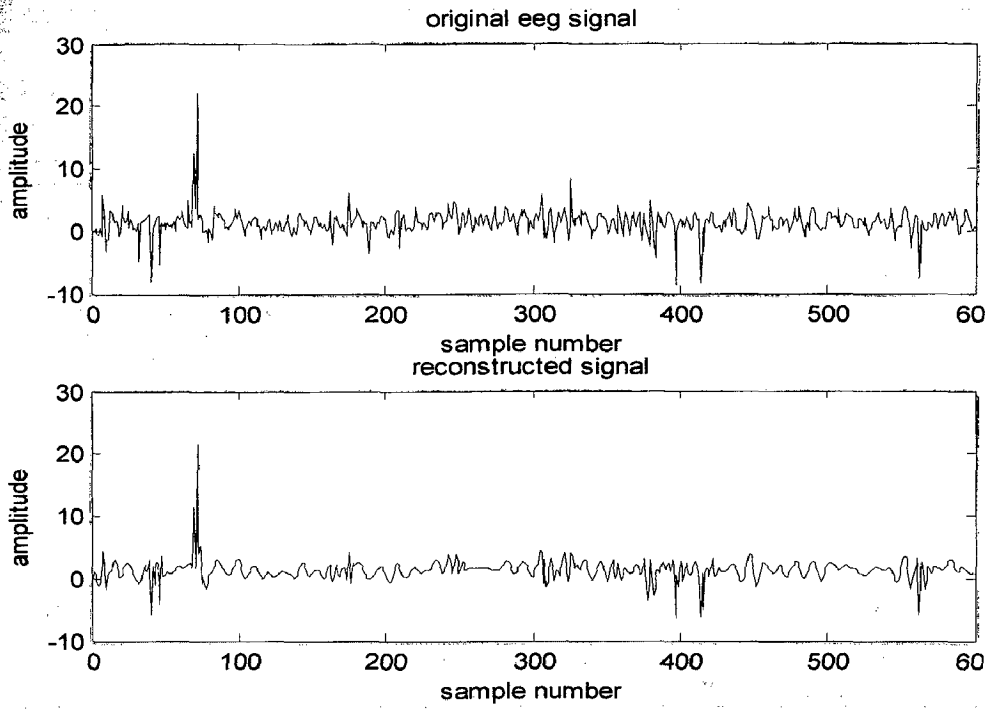
(a) original and reconstructed EEG ("g12ren.rit") signals at 6 bits for sample in DC
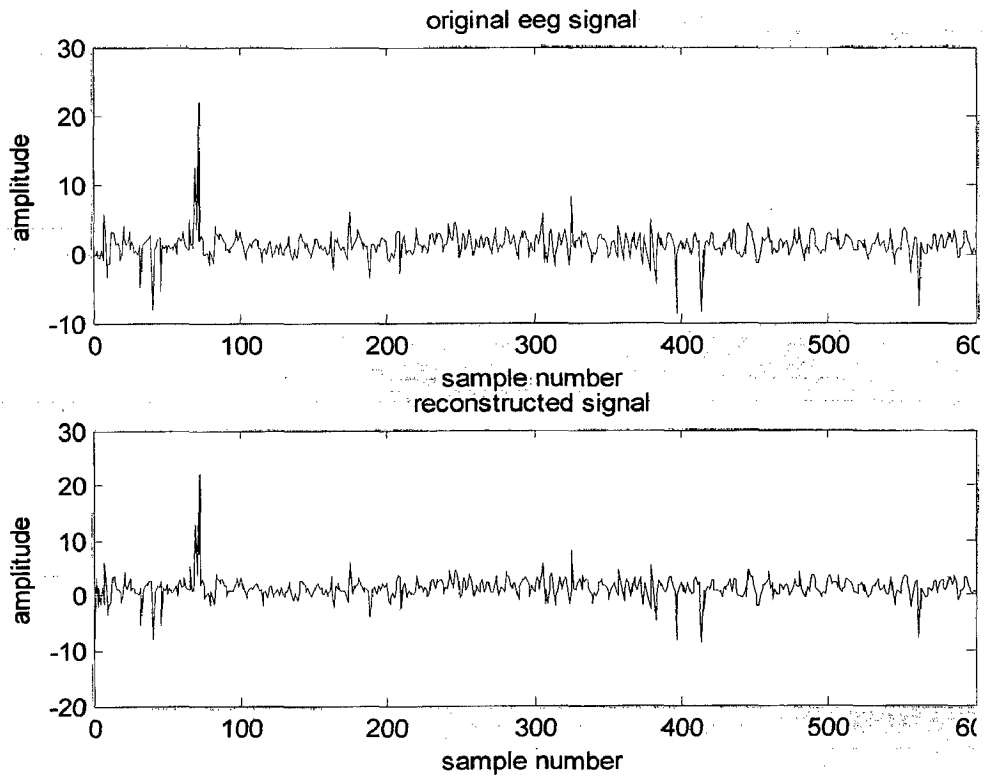
(b) original and reconstructed EEG signals ("g12ren.rit") at level 3 decompositio

6.5 Original and reconstructed EEG signal "g12ren.rit"

b) Representation of results in tabular form

The performance index for two EEG signals (g12ren.rit and g12ref.rit) are presented in tables 6.13 to 6.16 using DCT and Wavelet coding.

Table 6.13 Performance index for EEG signal 1 ("g12ren.rit") using DCT coding

No of bits per sample	Original signal size in KB	Size of encoded data (bytes)	C.R	Compression Factor (%)	SNR in dB	PRD (%)
3	1.19	314	3.8809	74.2319	-6.1395	202.7557
4	1.19	350	3.4817	71.2776	0.3622	95.9155
5	1.19	432	2.8208	64.5483	6.0825	49.6449
6	1.19	526	2.3167	56.8343	12.1117	24.7979
7	1.19	624	1.9529	48.7920	18.3849	12.0435
8	1.19	718	1.6972	41.0780	24.4417	5.9967

Table 6.14 Performance index for EEG signal 1 ("g12ren.rit") using Wavelet coding

Level of decomposition	Original signal size in KB	Size of encoded data (bytes)	C.R	Compression Factor (%)	SNR in dB	PRD (%)
1	1.19	698	1.7458	42.7193	18.7673	11.5249
2	1.19	563	2.1645	53.7979	11.0525	28.0141
3	1.19	441	2.7633	63.8097	6.7229	46.1164
4	1.19	375	3.2496	69.2260	4.6608	58.4735
5	1.19	316	3.8563	74.0678	3.5956	66.1031
6	1.19	300	4.0620	75.3808	3.3439	68.0467

Table 6.15 Performance index for EEG signal 1 ("g12ref.rit") using DCT coding

No of bits per sample	Original signal size in KB	Size of encoded data (bytes)	C.R	Compression Factor (%)	SNR in dB	PRD (%)
3	1.18	348	3.4722	71.1997	-0.9830	111.9821
4	1.18	422	2.8633	65.0755	4.9134	56.7979
5	1.18	521	2.3192	56.8823	10.7613	28.9692
6	1.18	619	1.9521	48.7718	16.9223	14.2522
7	1.18	712	1.6971	41.0752	23.0243	7.0597
8	1.18	806	1.4992	33.2958	28.9263	3.5784
9	1.18	883	1.3684	26.9233	35.0850	1.7610

Table 6.16 Performance index for EEG signal 1 ("g12ref.rit") using Wavelet coding

Level of decomposition	Original signal size in KB	Size of encoded data (bytes)	C.R	Compression Factor (%)	SNR in dB	PRD (%)
1	1.18	760	1.5899	37.1028	16.6174	14.7615
2	1.18	589	2.0515	51.2546	9.7280	32.6287
3	1.18	445	2.7153	63.1720	5.6948	51.9108
4	1.18	361	3.3471	70.1238	2.9181	71.4656
5	1.18	317	3.8117	73.7652	1.8308	80.9952
6	1.18	300	4.0277	75.1721	1.1732	87.3658

It is observed from above tables that, by increasing the number of bits per sample C.R and PRD are decreasing while SNR increases. For Wavelet by increasing the level of decomposition C.R and PRD are increasing while SNR is decreasing. By comparing DCT and WT it is observed that WT is giving good results at 8 bits per sample.

Table 6.17 Performance index for EEG signal 1 ("g12ron.rit") using DCT coding

No of bits per sample	Original signal size in KB	Size of encoded data (bytes)	C.R	Compression Factor (%)	SNR in dB	PRD (%)
3	1.19	360	3.3849	70.4569	0.5492	93.8727
4	1.19	454	2.6841	62.7429	6.5414	47.0900
5	1.19	562	2.1683	53.8800	12.8104	22.8812
6	1.19	647	1.8834	46.9045	18.6354	11.7012
7	1.19	753	1.6183	38.2058	24.8894	5.6955
8	1.19	839	1.4524	31.1482	31.0791	2.7928
9	1.19	933	1.3061	23.4342	36.8807	1.4321

Table 6.18 Performance index for EEG signal 1 ("g12ron.rit") using Wavelet coding

Level of decomposition	Original signal size in KB	Size of encoded data (bytes)	C.R	Compression Factor (%)	SNR in dB	PRD (%)
1	1.19	636	1.9160	47.8072	21.1527	8.7572
2	1.19	534	2.2819	56.1778	13.2946	21.6406
3	1.19	418	2.9152	65.6972	8.5819	37.2310
4	1.19	352	3.4618	71.1134	5.7338	51.6784
5	1.19	308	3.9564	74.7243	4.2987	60.9627
6	1.19	291	4.1875	76.1194	3.6441	65.7351

Table 6.19 Performance index for EEG signal 1 ("g12rof.rit") using DCT coding

Table 6.19 Performance index for EEG signal 1 ("g12rof.rit") using DCT coding

No of bits per sample	Original signal size in KB	Size of encoded data (bytes)	C.R	Compression Factor (%)	SNR in dB	PRD (%)
3	1.13	327	3.5386	71.7402	-4.8325	174.4322
4	1.13	366	3.1615	68.3697	1.4110	85.0059
5	1.13	446	2.5944	61.4560	7.4844	42.2452
6	1.13	544	2.1271	52.9867	13.2462	21.7615
7	1.13	642	1.8024	44.5174	19.3170	10.8181
8	1.13	741	1.5616	35.9617	25.4285	5.3527
9	1.13	842	1.3743	27.2331	31.3585	2.7044

Table 6.20 Performance index for EEG signal 1 ("g12rof.rit") using Wavelet coding

Level of decomposition	Original signal size in KB	Size of encoded data (bytes)	C.R	Compression Factor (%)	SNR in dB	PRD (%)
1	1.13	749	1.5449	35.2703	19.6326	10.4321
2	1.13	572	2.0229	50.5669	12.1437	24.7069
3	1.13	452	2.5600	60.9375	7.4457	42.4341
4	1.13	364	3.1789	68.5426	4.9992	56.2395
5	1.13	326	3.5494	71.8266	3.4292	67.3813
6	1.13	289	4.0039	75.0242	2.7491	72.8694

In the tables 6.17 to 6.20 comparing to high amplitude tremor signals low amplitude tremor signals are showing lesser compression ratios. For WT, by increasing the level of decomposition C.R, PRD are increasing slowly. In DCT at bit level 6 and in Wavelets at level 3 decomposition all the parameters are with in the acceptable range.

Table 6.21 Performance index for EEG signal 1 ("g12r15of.rit") using DCT coding

No of bits per sample	Original signal size in KB	Size of encoded data (bytes)	C.R	Compression Factor (%)	SNR in dB	PRD (%)
3	1.16	329	3.6103	72.3027	-3.9532	157.6381
4	1.16	382	3.1094	67.8408	2.3570	76.2342
5	1.16	465	2.5544	60.8533	8.2519	38.6727
6	1.16	566	2.0986	52.3505	14.4321	18.9842
7	1.16	667	1.7808	43.8477	20.3371	9.6194
8	1.16	768	1.5466	35.3448	26.3175	4.8320

Table 6.22 Performance index for EEG signal 1 ("g12r15of.rit") using Wavelet coding

Level of decomposition	Original signal size in KB	Size of encoded data (bytes)	C.R	Compression Factor (%)	SNR in dB	PRD (%)
1	1.16	759	1.5650	36.1025	16.6962	14.6282
2	1.16	599	1.9830	49.5723	9.6454	32.9405
3	1.16	466	2.5489	60.7691	5.8420	51.0387
4	1.16	369	3.2190	68.9352	4.0389	62.8134
5	1.16	323	3.6774	72.8078	2.9967	70.8211
6	1.16	305	3.8944	74.3231	2.3626	76.1851

Table 6.23 Performance index for EEG signal 1 ("g12r45of.rit") using DCT coding

No of bits per sample	Original signal size in KB	Size of encoded data (bytes)	C.R	Compression Factor (%)	SNR in dB	PRD (%)
3	1.15	342	3.4433	70.9579	-0.0362	100.4178
4	1.15	441	2.6703	62.5510	6.0976	49.5588
5	1.15	543	2.1687	53.8893	12.0553	24.9596
6	1.15	643	1.8314	45.3974	17.9942	12.5977
7	1.15	743	1.5849	36.9056	23.9332	6.3583
8	1.15	830	1.4188	29.5177	30.0001	3.1623
9	1.15	909	1.2955	22.8091	36.0804	1.5703

Table 6.24 performance index for EEG signal 1 ("g12r45of.rit") using Wavelet coding

Level of decomposition	Original signal size in KB	Size of encoded data(bytes)	C.R	Compression Factor (%)	SNR in dB	PRD (%)
1	1.15	630	1.8692	46.5014	19.4343	10.6729
2	1.15	548	2.1489	53.4647	11.7469	25.8616
3	1.15	433	2.7196	63.2303	7.9556	40.0145
4	1.15	353	3.3360	70.0238	5.6606	52.1157
5	1.15	312	3.7744	73.5054	4.3231	60.7920
6	1.15	292	4.0329	75.2038	3.6507	65.6846

Similar are the results observed in tables 6.21 to 6.24.

Coming to end of the parkinsonian tremor disease results, we can observe the variations in the C.R, SNR, PRD and C.F all most similar in each table for respective algorithm. At bit

level 4-6 DCT giving better results and Wavelet giving better results at 3-5 decomposition level. At last the conclusion about these results is Wavelet is some what better than the DCT.

c) Representation of results in graphical form

Fig 6.6 shows one representation graph for file 'g12ren.rit'.
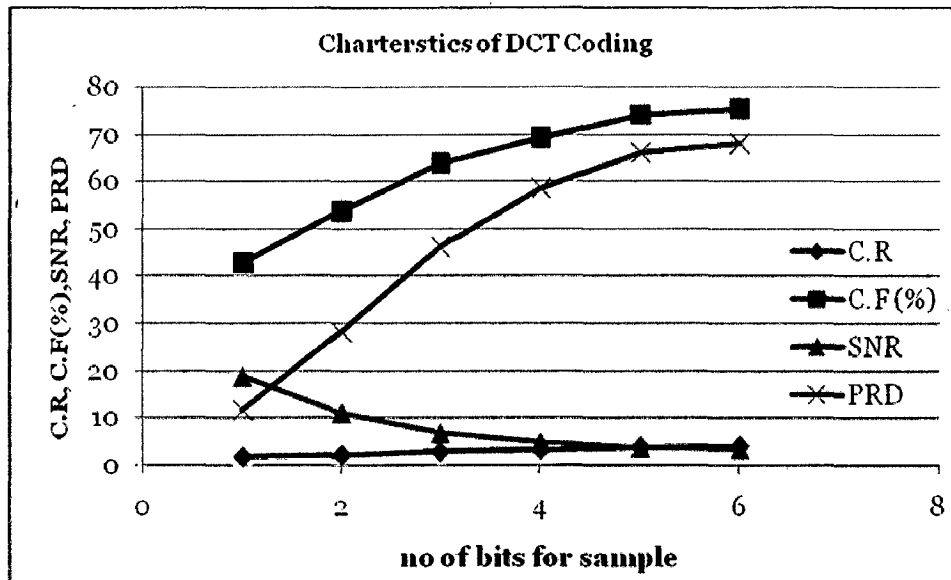
(a) comparative graph of "g12ren.rit" using DCT coding
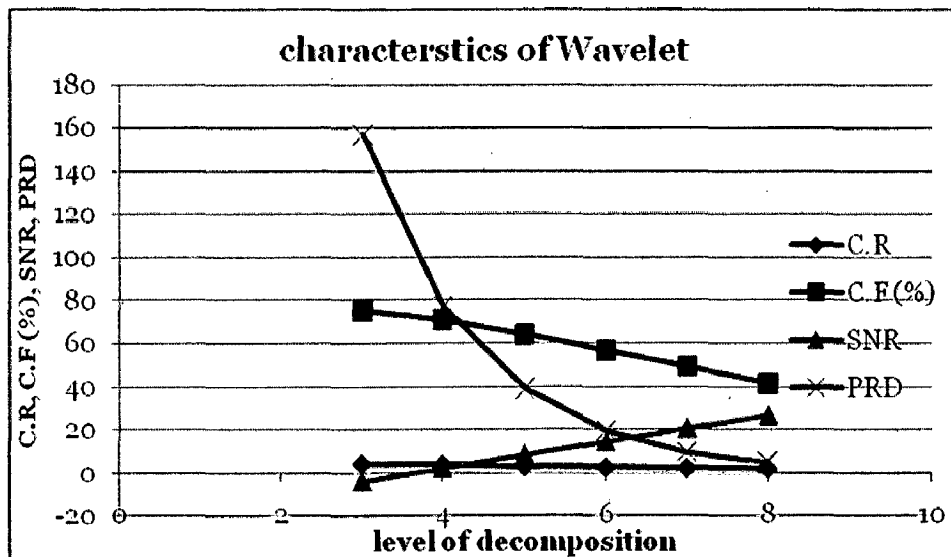
(b) comparative graph of "g12ren.rit" using Wavelet coding

Fig 6.6 Comparative graph for different coding

The tabular results presented earlier are presented in graphical form here. Variations in different parameters obtained are clearly visible here.

6.5 Subjects with Sensorimotor Function

This database contains "Noise enhancement of sensorimotor function [26]" signals. In this database there are 15 young and 12 elder subjects are existed, from this I have chosen 3 young and 3 elder subject's data. Coming to compression techniques DCT and Wavelet transform are implemented, for this fixed bit rate (12) and fixed decomposition level (3) were chosen.

There are two channels data existing in these files, hence, I have compressed the two channels data and results are tabulated separately for each channel.

Details of the files are, sampling frequency 60Hz and no of samples for each file 1800 (mean 30 seconds data).

a) Original and reconstructed waveforms

Original and reconstructed waveforms for subject MT1415 are shown in figure 6.7.

STIM 'MT1415' using DCT and Wavelet
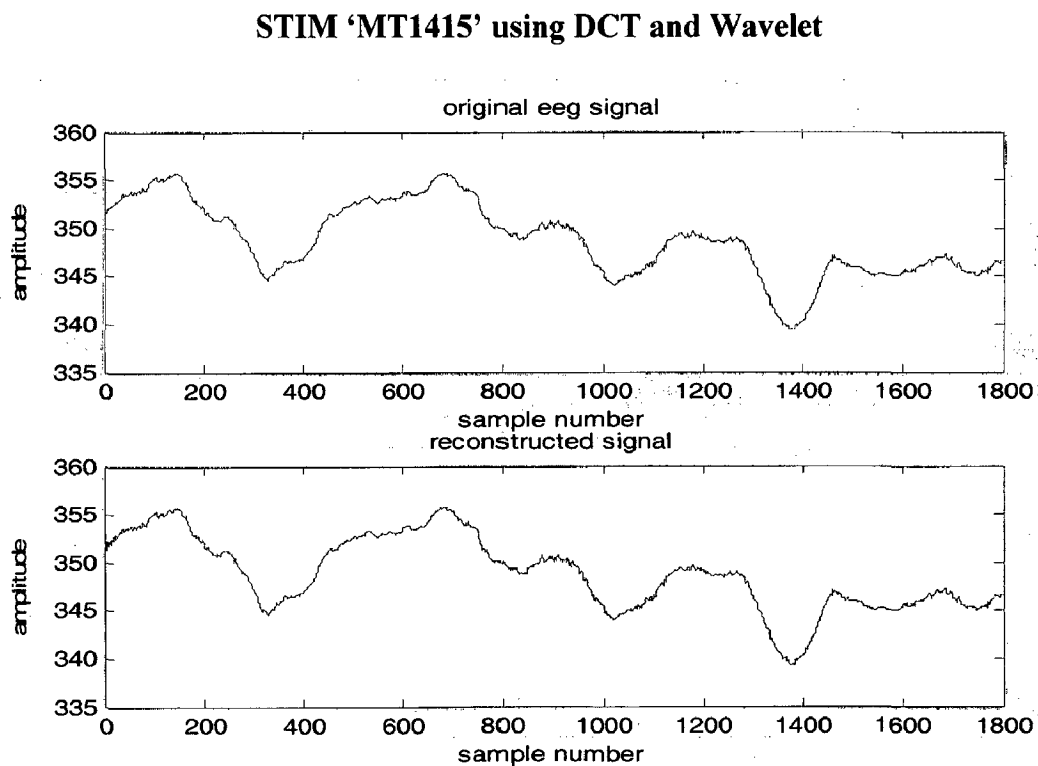
(a) original and reconstructed EEG signals at 12 bits for sample in DCT

81
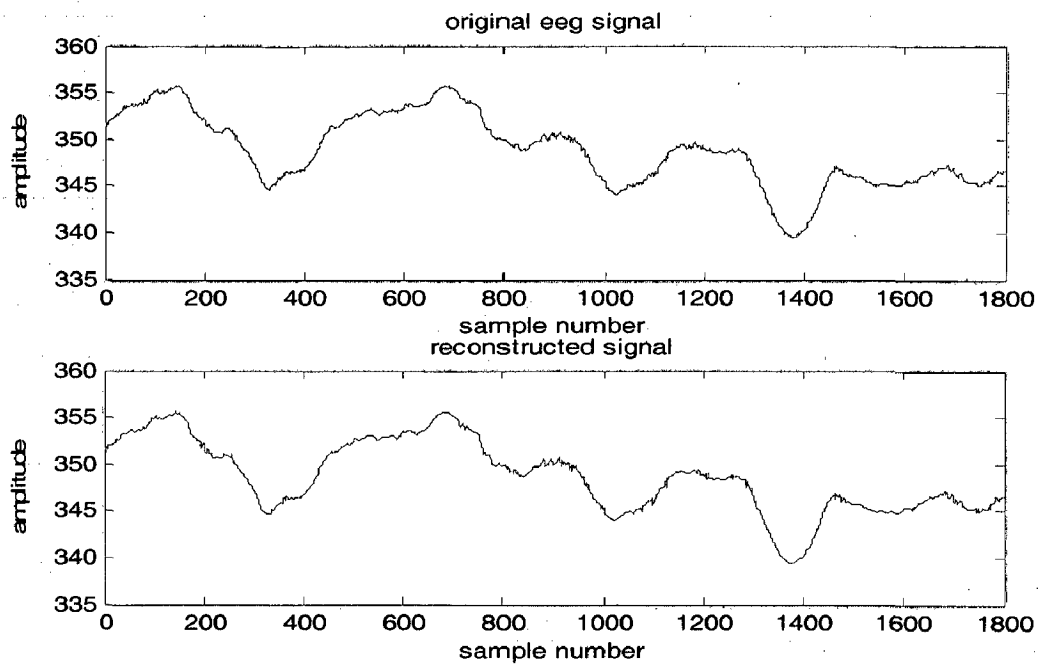
(b) original and reconstructed EEG signals at level 3 decomposition in Wavelet

Fig 6.7 Original and reconstructed EEG signals of patient MT1415

b) Representation of results in tabular form

The performance index for EEG signals ('NULL' channel 1 and channel 2) are presented in tables 6.25 to 6.28 using DCT (at 12 bits per sample) and Wavelet coding (level 3 decomposition).

Table 6.25 Performance index for EEG signal 2 channel 1 ("NULL") using DCT coding

Subject No	Original signal size in KB	Size of encoded data (bytes)	C.R	Compression Factor (%)	SNR in dB	PRD (%)
MT1415	11.2	1003	11.4345	91.2545	73.7444	0.0205
MT1424	11.1	949	11.9772	91.6508	74.0485	0.0198
MT1433	11.1	928	12.2483	91.8356	74.3176	0.0192
MT1504	11.2	1.05KB	10.6667	90.6250	75.0177	0.0177
MT1512	11.1	1.00KB	11.1000	90.9910	75.0955	0.0176
MT1523	11.5	1.07KB	10.7477	90.6957	75.0091	0.0178

Table 6.26 Performance index for EEG signal 2 channel 2("NULL") using DCT coding

Subject No	Original signal size in KB	Size of encoded data (bytes)	C.R	Compression Factor (%)	SNR in dB	PRD (%)
MT1415	11.3	1015	11.4002	91.0942	75.4208	0.0169
MT1424	11.5	1.15KB	10.00	90.0000	73.3791	0.0214
MT1433	12.5	1.24 KB	10.0806	90.0800	74.1933	0.0195
MT1504	12.6	1.37 KB	9.1971	89.1270	74.3529	0.0192
MT1512	11.2	1.07 KB	10.4673	90.4464	73.2341	0.0218
MT1523	11.5	996	11.8233	91.5400	73.2391	0.0218

Table 6.27 Performance index for EEG signal 2 channel 1("NULL") using Wavelet coding

Subject No	Original signal size in KB	Size of encoded data (bytes)	C.R	Compression Factor (%)	SNR in dB	PRD (%)
MT1415	11.2	606	18.9254	94.7161	67.8141	0.0407
MT1424	11.1	629	18.0706	94.4611	67.7036	0.0412
MT1433	11.1	611	18.6029	94.6245	67.7629	0.0409
MT1504	11.2	636	18.0327	94.4545	66.3154	0.0483
MT1512	11.1	612	18.5725	94.6157	66.8260	0.0456
MT1523	11.5	715	16.4699	93.9283	66.6334	0.0466

Table 6.28 Performance index for EEG signal 2 channel 2 ("NULL") using Wavelet coding

Subject No	Original signal size in KB	Size of encoded data (bytes)	C.R	Compression Factor (%)	SNR in dB	PRD (%)
MT1415	11.3	655	17.6660	94.3394	67.9818	0.0399
MT1424	11.5	751	15.6804	93.6226	65.6556	0.0521
MT1433	12.5	778	16.4524	93.9218	64.2520	0.0613
MT1504	12.6	796	16.2090	93.8306	55.3376	0.1710
MT1512	11.2	686	16.7184	94.0816	66.2158	0.0489
MT1523	11.5	667	17.6552	94.3359	67.4639	0.0423

It is observed from above tables that, at fixed bit rate and decomposition level better results are obtained compare to parkinsonian tremor signals. It is because of the low frequency variation in the signal. By comparing DCT and WT it is observed that WT is giving good results at 8 bits per sample.

83

The performance index for EEG signals ('STIM' channel 1 and channel 2) are presented in tables 6.29 to 6.32 using DCT (at 12 bits per sample) and Wavelet coding (level 3 decomposition).

Table 6.29 Performance index for EEG signal 2 channel 1 ("STIM") using DCT coding

Subject No	Original signal size in KB	Size of encoded data (bytes)	C.R	Compression Factor (%)	SNR in dB	PRD (%)
MT1415	11.1	925B	12.2880	91.8650	73.2672	0.0217
MT1424	11.2	943B	12.1620	91.7777	74.3043	0.0193
MT1433	11.1	964B	11.7909	91.5189	73.1689	0.0220
MT1504	11.3	1.16 KB	9.7414	89.7345	73.3890	0.0214
MT1512	11.1	1008B	11.2762	91.1318	73.1087	0.0221
MT1523	11.4	1.02 KB	11.1765	91.0526	75.3988	0.0170

Table 6.30 Performance index for EEG signal 2 channel 2("STIM") using DCT coding

Subject No	Original signal size in KB	Size of encoded data (bytes)	C.R	Compression Factor (%)	SNR in dB	PRD (%)
MT1415	11.4	967B	12.0720	91.7164	74.0983	0.0197
MT1424	11.6	1.14 KB	10.1754	90.1724	73.3669	0.0215
MT1433	11.6	1.20 KB	9.6667	89.6552	73.2956	0.0216
MT1504	11.9	1.45 KB	8.2069	87.8151	75.3267	0.0171
MT1512	11.1	1.00 KB	11.1000	90.9910	75.5737	0.0166
MT1523	11.6	995B	11.9381	91.6235	73.3946	0.0214

Table 6.31 Performance index for EEG signal 2 channel 1("STIM") using Wavelet coding

Subject No	Original signal size in KB	Size of encoded data (bytes)	C.R	Compression Factor (%)	SNR in dB	PRD (%)
MT1415	11.1	605	18.7874	94.6773	67.4605	0.0424
MT1424	11.2	616	18.6122	94.6289	57.6117	0.1316
MT1433	11.1	586	19.3966	94.8445	67.6262	0.0416
MT1504	11.3	700	16.5303	93.9505	64.6576	0.0585
MT1512	11.1	639	17.7878	94.3782	66.8342	0.0455
MT1523	11.4	695	16.7965	94.0464	66.6973	0.0463

Table 6.32 Performance index for EEG signal 2 channel 2 ("STIM") using Wavelet coding

Subject No	Original signal size in KB	Size of encoded data (bytes)	C.R	Compression Factor (%)	SNR in dB	PRD (%)
MT1415	11.4	682	17.1167	94.1578	57.1967	0.1381
MT1424	11.6	722	16.4521	93.9217	65.3430	0.0541
MT1433	11.6	752	15.7957	93.6692	64.4574	0.0599
MT1504	11.9	829	14.6992	93.1969	59.3511	0.1078
MT1512	11.1	655	17.3533	94.2374	67.1833	0.0437
MT1523	11.6	687	17.2902	94.2164	57.3024	0.1364

It is observed from above tables that, once again the WT showing better results compared to DCT in terms of C.R. PRD is very less in the sensorimotor signals.

At the end of sensorimotor function results, the average C.R and SNR in DCT are 11 and 73.567 and in Wavelets 17 and 62. It is observed higher compression ratios obtained with good signal quality. It is because of the low frequency the signals, means these signals are low frequency signals similar to 'thita' and 'alpha' waves of EEG. The results are concluded among DCT and WT, Wavelets are better in Sensorimotor function than DCT.

c) Comparative table for different coding

The performance index for EEG signals (MT415,MT1504) are presented in tables 6.33 and 6.34 using DCT (at 12 bits per sample) and Wavelet coding (level 3 decomposition).

Table 6.33 Comparative table of noise enhancement of sensorimotor signals (NULL condition)

Channel & technique	Original signal size in KB	Size of encoded data (bytes)	C.R	Compression Factor (%)	SNR in dB	PRD (%)
MT1415						
1(DCT)	11.2	1003	11.4345	91.2545	73.7444	0.0205
1(Wavelet)	11.2	0606	18.9254	94.7161	67.8141	0.0407
2(DCT)	11.3	1015	11.4002	91.0942	75.4208	0.0169
2(Wavelet)	11.3	0655	17.6660	94.3394	67.9818	0.0399
MT1504						
1(DCT)	11.2	1.05 KB	10.6667	90.6250	75.0177	0.0177
1(Wavelet)	11.2	636 Bytes	18.0327	94.4545	66.3154	0.0483
2(DCT)	12.6	1.37 KB	9.1971	89.1270	74.3529	0.0192
2(Wavelet)	12.6	796 Bytes	16.2090	93.8306	55.3376	0.1710

In the above table comparison between one young and one elder patient is done. It is observed that WT giving very better results compare to DCT in both the cases.

Table 6.34 Comparative table of noise enhancement of sensorimotor signals (STIM condition)

| Channel & technique	Original signal size in KB	Size of encoded data (bytes)	C.R	Compression Factor (%)	SNR in dB	PRD (%)
MT1415						
1(DCT)	11.1	925	12.2880	91.8650	73.2672	0.0217
1(Wavelet)	11.1	605	18.7874	94.6773	67.4605	0.0424
2(DCT)	11.4	967	12.0720	91.7164	74.0983	0.0197
2(Wavelet)	11.4	682	17.1167	94.1578	57.1967	0.1381
MT1504						
1(DCT)	11.3	1.16 KB	9.7414	89.7345	73.3890	0.0214
1(Wavelet)	11.3	700Bytes	16.5303	93.9505	64.6576	0.0585
2(DCT)	11.9	1.45 KB	8.2069	87.8151	75.3267	0.0171
2(Wavelet)	11.9	829Bytes	14.6992	93.1969	59.3511	0.1078

Similar results are observed in the above comparative table. Finally it is concluded that Wavelet transform technique is suitable for sensorimotor signals with good SNR and least PRD.

6.6 Subjects with EEG Machine data from Biomedical lab.

This database I have taken from biomedical and instrumentation lab of Electrical department, of IIT Roorkee. In this single eye blink, double eye blink, relaxation data's are compressed using DCT, Wavelet and LPC. But LPC technique results are not tabulated, because of the signal reconstruction was not good and quantization was not implemented. The samples in each file are 2560 and the gel based electrodes are used for recording the EEG. It has 4 subjects database. For recording the EEG, the interface supported machine is attached to the computer and there are two software's existing for supporting data acquisition and analysis. 24 electrodes system is available for data acquisition.

The results are as follows,

a) Original and reconstructed waveforms
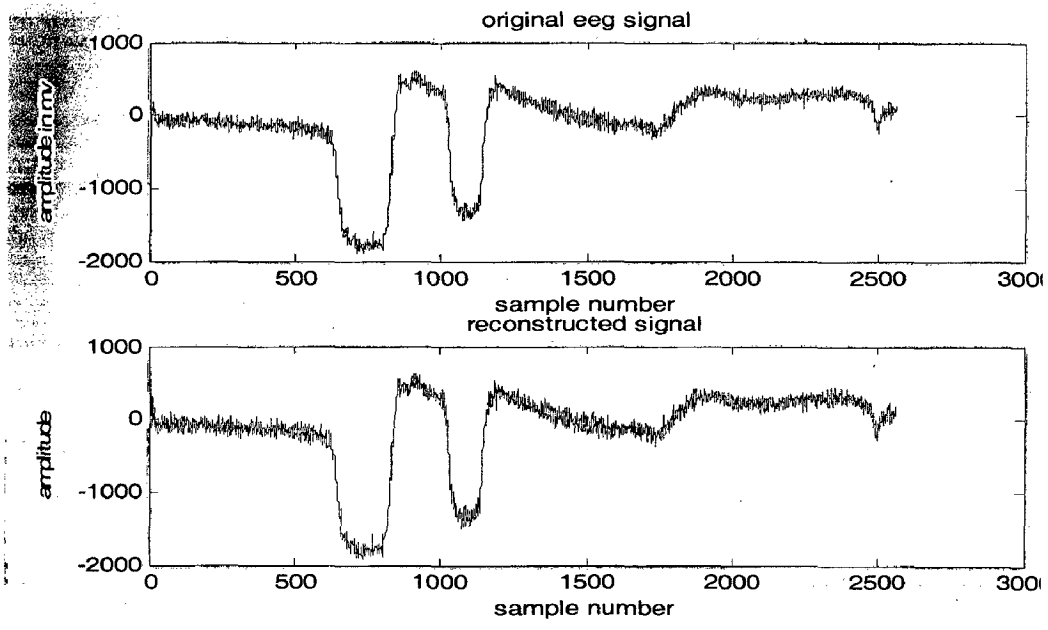
(a) original and reconstructed "double eye blink" EEG signals at in DCT coding
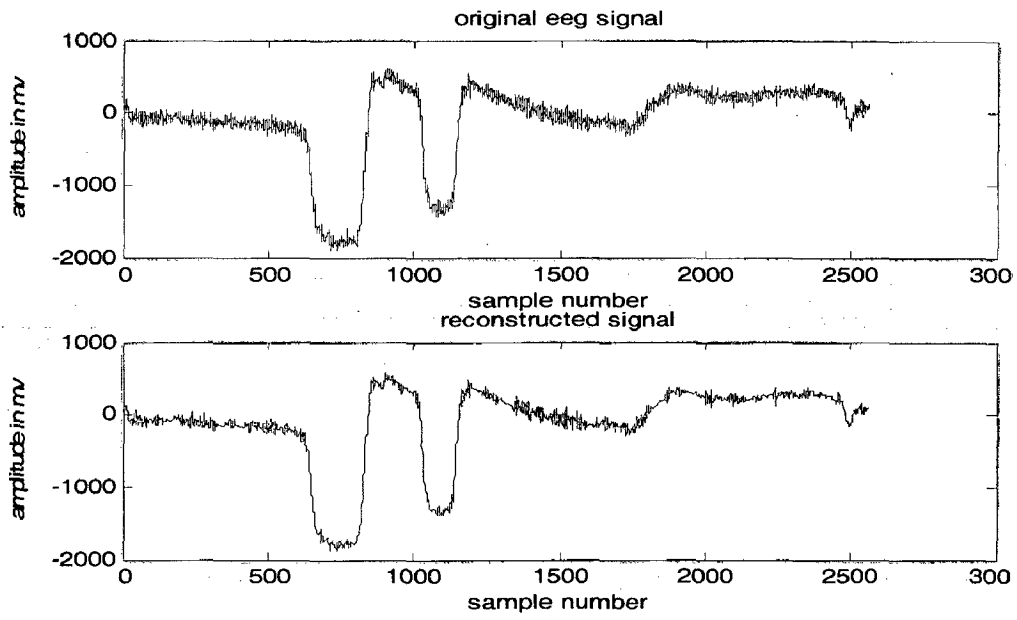
(b) original and reconstructed EEG signals at level 3 decomposition in Wavelet

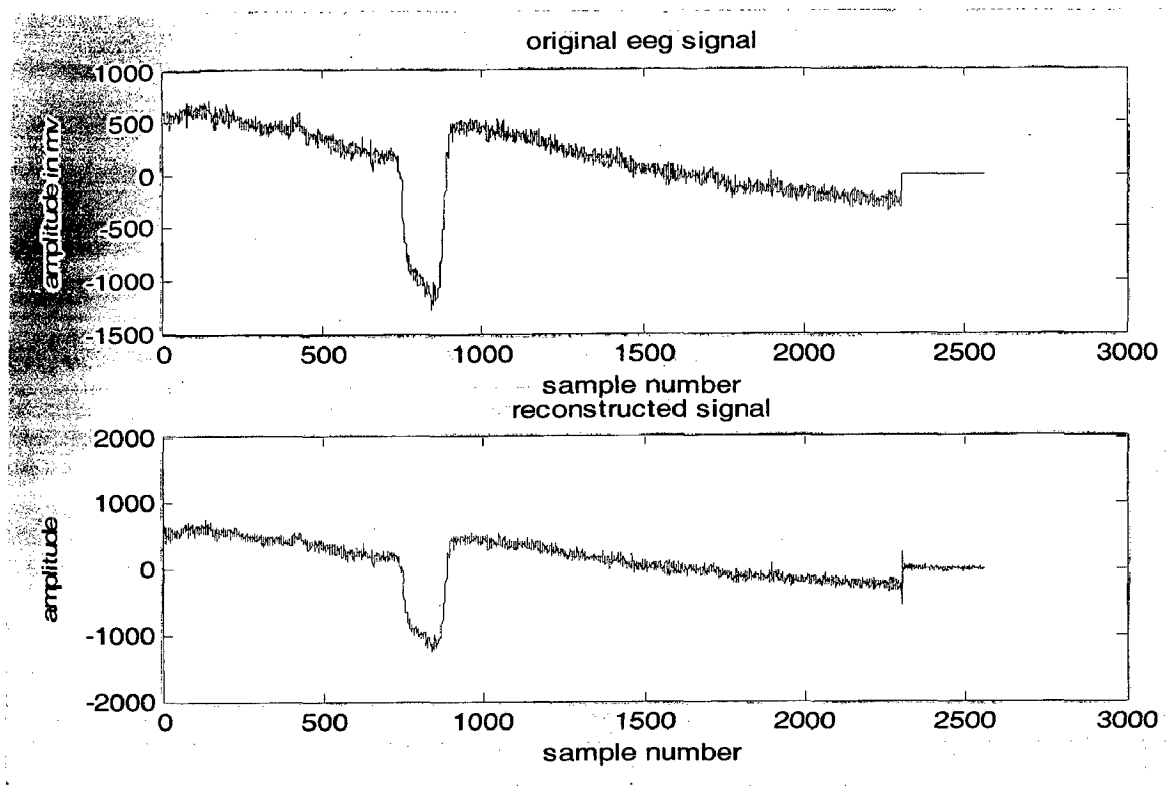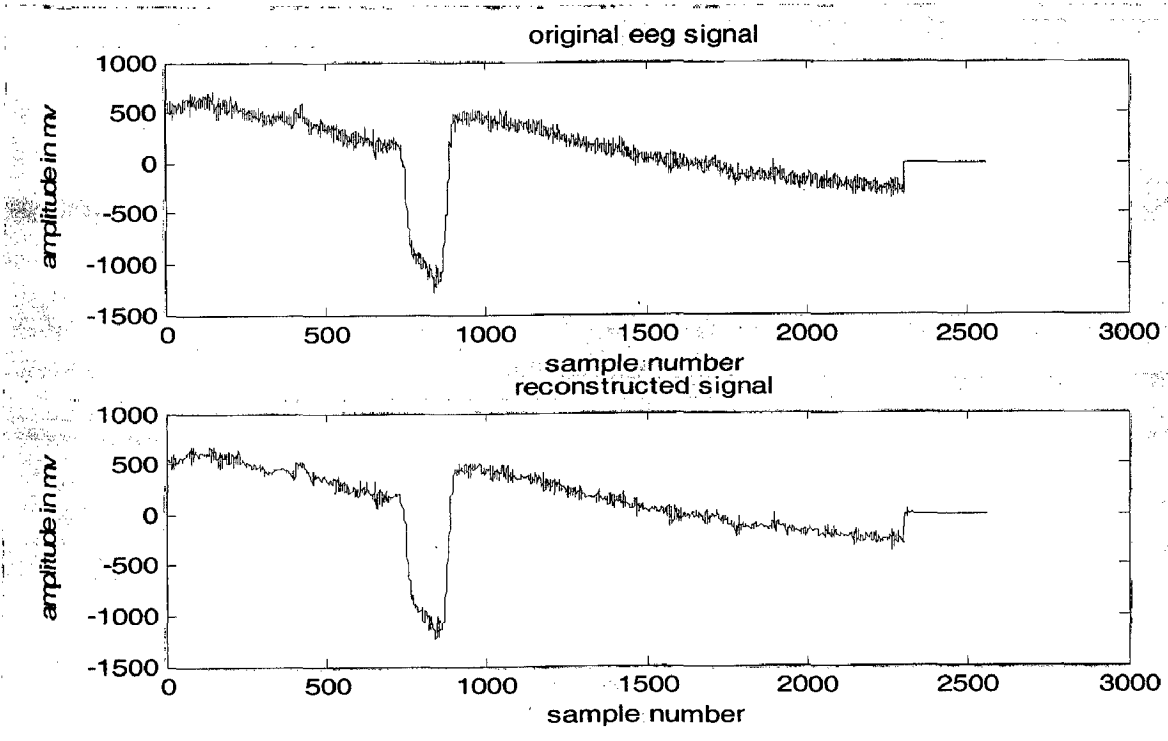Fig 6.8 Original and reconstructed EEG signals of subject db8

(a) original and reconstructed EEG signals at 6 bits for sample in DCT coding

(b) original and reconstructed EEG signals at level 3 decomposition

Fig 6.9 Original and reconstructed EEG signals of subject sb8

b) Representation of results in tabular form

The performance index for EEG signals (Single eye blink, double eye blink, relaxation) are presented in tables 6.35 and 6.36 using DCT (at 6 bits per sample) and Wavelet coding (level 3 decomposition).

Table 6.35 Performance index for EEG signal 3 ("Eye blink") using DCT coding at fixed bits (6) for sample

File name	Original signal size in KB	Size of encoded data (bytes)	C.R	Compression Factor (%)	SNR in dB	PRD (%)
sb8	3.06	626	5.0055	80.0220	12.5647	23.5379
sb4	3.13	913	3.5105	71.5143	18.4615	11.9378
sb6	3.39	776	4.4734	77.6456	14.4735	18.8941
db4	3.34	862	3.9677	74.7965	19.6099	10.4593
db8	3.2	1.05 KB	3.0476	67.1875	20.8763	9.0404
db9	3.58	1006	3.6441	72.5580	20.1919	9.7814
rel1 12	3.42	1.94 KB	1.7629	43.2794	38.0591	1.2504

Table 6.36 Performance index for EEG signal 3 ("Eye blink") using Wavelet coding at level 3 decomposition.

File name	Original signal size in KB	Size of encoded data (bytes)	C.R	Compression Factor (%)	SNR in dB	PRD
sb8	3.06	753	4.1613	75.9689	26.9507	4.4923
sb4	3.13	921	3.4800	71.2647	22.2426	7.7245
sb6	3.39	844	4.1130	75.6868	21.3020	8.6079
db4	3.34	814	4.2017	76.1999	29.9236	3.1902
db8	3.20	860	3.8102	73.7549	22.2234	7.7416
db9	3.58	956	3.8346	73.9220	23.2135	6.9076
rel1	3.42	1.02 KB	3.3529	70.1754	9.4942	33.5190

It is observed above tables that both in DCT and Wavelet fixed compression ratios exist. In the case of SNR and PRD Wavelets are showing better results than DCT.

Finally coming to end of the results, Wavelets are good in three signals. DCT is good in parkinsonian tremor and eye blink. But overall Wavelets have shown better results in all aspects of data compression.

Chapter - 7

CONCLUSIONS AND SCOPE FOR FUTURE WORK

7.1 Conclusions

In this dissertation work, three types of compression techniques namely, DCT Wavelet Transform and LPC coding have been implemented. This work mainly concentrated on compression of recorded EEG signals without significant loss of quality. Comparative evaluation was performed with respect to compression ratio, compression factor, SNR, and PRD. These three algorithms are tested on different EEG signals taken by variety of sources.

Implementation of DCT coding technique gives the average compression ratio of 3.2412, 11.3456, 3.5674 with respective to parkinsonian tremor, sensorimotor and eye blink signals with very less variation in compression ratio with respective to number of bits per sample. The average SNR, PRD at bit level 6 are 16.0869, 15.6912 in parkinsonian tremor and 20.1919, 13.2456 in eye blink signals. In The case of Sensoirmotor function signals SNR and PRD are 74.3176 and 0.0195 respectively. This indicates better quality output EEG from this technique.

In wavelet transform based EEG compression, different wavelets like 'Db10', 'Haar', 'coiflet', 'symlet', and 'discrete mayor' are used for the analysis purpose. In the analysis it shows that 'Db10' gives more compression ratio than that of all other wavelets. 'Discrete mayor' wavelet produces least compression ratio 1.5643. In all other cases, compression ratio are nearly equal to 4 at level of decomposition 3. Quality is more in the case of 'Db10' wavelet and less in the case of 'Haar' wavelet. The compression ratio can be changed in the case of wavelet transform based EEG compression by changing the level of decomposition. At decomposition level 3, this technique is giving compression ratio of about 60 and at level 5 it is giving 75 in ratios. But there is drastic change in the quality after level 3. Thus, for the comparative evaluation purpose 'db10' wavelet has been used at decomposition level 3 considering quality as an important factor.

A significant advantage of using wavelets for neurological signals compression is that the trade off between compression ratio and quality can be achieved while for LPC technique compression ratio is nearly fixed with fixed quality. In the case of wavelet transform based

EEG compression average compression ratio is 4.9312, 17.7878 and 3.9102 with respective to parkinsonian tremor, sensorimotor and eye blink signals respectively. The average SNR and PRD at level of decomposition three are 15.7542 and 16.3038 in high amplitude tremor and 7.4457 and 42.4341 in low amplitude tremor signals. In The case of sensorimotor signals average SNR and PRD are 64.4574 and 0.0599 and in eye blink these are 20.8763 and 9.0404. One disadvantage in the wavelet transform based neurological signals compression is that, with respect to other two techniques this involves much more computation.

It is clear that compression ratio is increasing with respect to level of decomposition in the case of WT while decreasing with number of bits per sample in DCT. In this work, it is also concluded that one more task achieved variable compression ratio of the neurological signals is obtained by the Wavelet transform. Finally coming to end of the conclusion WT is high in all aspects of the EEG compression techniques in three signals. At fixed bit rate DCT was showing better results, it was observed in parkinsonian tremor. LPC results are not tabulated because it is working only for eye blink signals and giving poor results in the case of SNR and PRD. For Telemedicine point of view we need higher compression ratio while maintaining the signal qualities which is achieved by DCT in parkinsonian tremor, eye blinking and WT by sensorimotor, eye blinking and parkinsonian tremor.

7.2 Scope for Future Work

In this dissertation work, EEG compression techniques like DCT technique, Wavelet transform and LPC coding has been implemented and compared with respect to compression ratio. The work can be further extended to any one of the directions:

1. For better compression ratios, further data compression ratio is possible by exploiting the redundancy in the encoded transform coefficients.

2. Implementation of the algorithms can be done by using the higher level languages like C, C++ for faster processing.

3. DCT, Wavelet transform implementation can be done on DSP kit for real time application for transmission of neurological signals.

4. In this work objective quality measuring methods like SNR are used for the comparative evaluation, a subjective quality measuring methods like mean opinion score, diagnostic acceptability measure can also be tried for comparison purpose.

REFERENCES

[1] Aviyente, Selin, "Compressed Sensing Framework for EEG Compression," *14th Workshop on Statistical Signal Processing, SSP '07. IEEE*, Aug 26-29, 2007.

[2] Y Wongsawat, S Oraintara, T Tanaka and K.R Rao, "Lossless Multi-channel EEG Compression," *Proceedings 2006 IEEE International Symposium on circuits and systems, ISCAS 2006*, May21-24, 2006.

[3] N.sriraam and C.Eswaran, "Performance of Perceptron Predictors for Lossless EEG Signal Compression," http://ieeexplore.ieee.org/search/, 2003.

[4] Tarun madav, Rajeev Agarwal and M.N.S swamy, "Compression of Long term EEG using Power Spectral Density," *Proceedings of the 26th Annual International Conference of the IEEE EMBS*, San Francisco, CA, USA, September 1-5, 2004.

[5] Z. Sijercic, G.C Agarwal and C.W Anderson, "EEG Signal Compression with ADPCM Subband Coding," *Proceedings of the 39th Midwest symposium on Circuits and Systems of IEEE*, Volume 2, Aug 18-21, 1996.

[6] F.bartloni, V.cappilini and S.Nerozzi, "Recurrent Neural Network Predictors for EEG signal Compression," *International Conference on Acoustics, Speech, and Signal Processing, ICASSP-95 IEEE*, Volume 5, May 9-12, 1995.

[7] Elias S.G.Carotti, Juan C.De Marin and Roberto Merletti, "Compression of Surface EMG Signals with Alzebraic Code Excited Linear Prediction," http://ieeexplore.ieee.org/search/, 2006.

[8] Elias S. G. Carotti, Juan Carlos De Martin, Dario Farina and Roberto Merletti, "Linear Predictive Coding of Myoelectric Signals," *Proceedings of (ICASSP '05) International Conference on Acoustics, Speech, and Signal Processing of IEEE*. Voume 5, Mar 18-23, 2005.

[9] P.A.berger, F.A.O.Nascimento, J.C.Carmo, A.F.Rocha, and Icaro dos santos, "Algorithm for Compression of EMG signals," *Proceedings of the 25th Annual International Conference of the IEEE EMBS*, Cancun, Mexico, September 17-21, 2003.

[10] J.A Norris, K.Englehart and D.Lovely, "Steady-State and Dynamics Myoelectric Signal Compression using Embedded Zero-tree Wavelets," *proceedings of the 23rd Annual EMBS international Conference, IEEE,* Istanbul, Turky, October 25-28, 2001

[11] Leslie Cromwell, Fred j. Weibell and Erich A.pfeiffer, "Biomedical Instrumentation and Measurements," Second edition, Prentice-Hall International, Englewood Cliffs.

[12] P.Negeshwar Reddy, "Implementation and Comparative Evaluation of Speech Compression Techniques," M.Tech. Dissertation, Department of Electrical Engineering, Indian Institute of Technology, Roorkee, June 2007.

[13] A.Krishna, "Frequency domain Analysis of Speech Compression," M.Tech. Project, Department of Electrical Engineering, Indian Institute of Technology, Roorkee, September 2007.

[14] A. M. M. A. Najih, A. R. bin Ramli, V. Prakash and A. R. Syed, "Speech Compression using Discrete Wavelet Transform," *Telecommunication Technology, NCTT2003 Proceedings, 4th national conference*, pp.1-4, Jan 2003

[15] A. Chen, N. Shehad, A. Virani and E. welsh, "Discrete Wavelet Transform for Audio Compression," http://is.rice.edu/~welsh/elec431/wavelets.html

[16] M. Schindler, "Data Compression Consulting," *Practical Huffman coding*, http://www.compressconsult.com/ Huffman/.

[17] A. Graps, "An Introduction to Wavelets," *Computational Science and Engineering, IEEE,* Volume 2, Issue 2, pp. 50-61, summer 1995.

[18] M. Misiti, Y. Misiti, G. Oppenheim and J. Poggi, "Matlab Wavelet Tool Box," The Math Works Inc., 2000.

[19] J. I. Agbiya, "Discrete Wavelet Transform Techniques in Speech Processing," *Tencon Digital Signal Processing Applications Proceedings, IEEE*, pp. 514-519, Nov 1996.

[20] W. Kinsner and A. Langi, "Speech and Image Signal Compression with Wavelets," *WESCANEX93 Communications, Computers and Power in the Modern Environment, Conference Proceedings, IEEE*, pp.368-375, May 1993.

[21] Ming Yang, "Low bit rate Speech coding," *Potentials, IEEE*, Volume 23, Issue 4, pp.32-36, Oct-Nov 2004.

[22] S. W. Park, M. Gomez, and R. Khastri, "Speech Compression using Line Spectrum Pair Frequencies and Wavelet transform," *Intelligent Multimedia, Video and Speech Processing 2001. Proceedings of 2001 International Symposium*, pp. 437-440, May 2001.

[23] M. Misiti, Y. Misiti, G. Oppenheim and J. Poggi, "Matlab Wavelet Tool Box," The Math Works Inc., 2000.

[24] A. M. Kondoz, "Digital Speech," *A John Wiley and Sons, INC., Publication*, 2001.

[25] L. R. Rabiner and R. W. Schafer, "Digital Processing of Speech Signal," third edition

http://www.data-compression.com/speech.shtml

[26] http://physionet.org/physiobank/database/#neuro.

[27] E. B. Fgee, W. J. Phillips and W. Robertson, "Comparing Audio Compression Using Wavelets with Other Audio Compression Schemes," *Canadian Conference on Electrical and Computer Engineering, Proceeding of the IEEE*, Volume 2, pp. 698-701, May 1999.